Sgr A*- the galactic center black hole

The COST action "Black Holes in a Violent Universe" (MP-0905) organizes a Summer School on "Black Holes at all scales Ioannina, Greece, September 16 and 18

SEVENTH FRAMEWORK PROGRAMME

STRONGGRAVITY EU FP7-SPACE research project 312789 2013 - 2017

Andreas Eckart

I.Physikalisches Institut der Universität zu Köln

Max-Planck-Institut für Radioastronomie, Bonn

Max-Planck-Institut für Radioastronomie

Universität zu Köln

16:30-18:00 Part II: simultaneous radio NIR X-ray light curves – bremsstrahlung - synchrotron – synchrotron selfcompton mechanism - adiabatic expansion – polarized radiation from SgrA - relativistic models of the emitting regions*

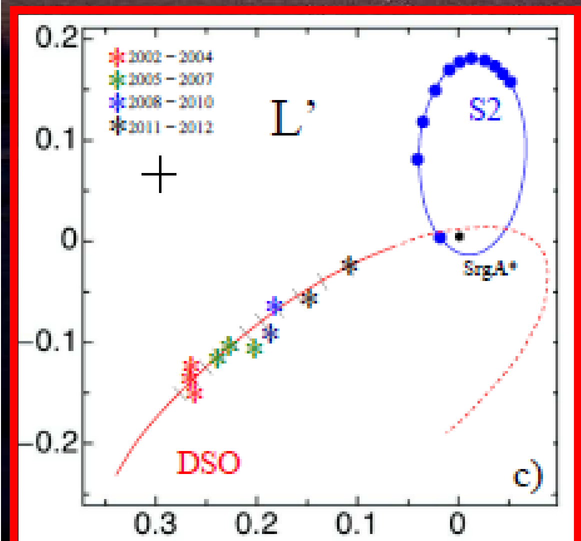

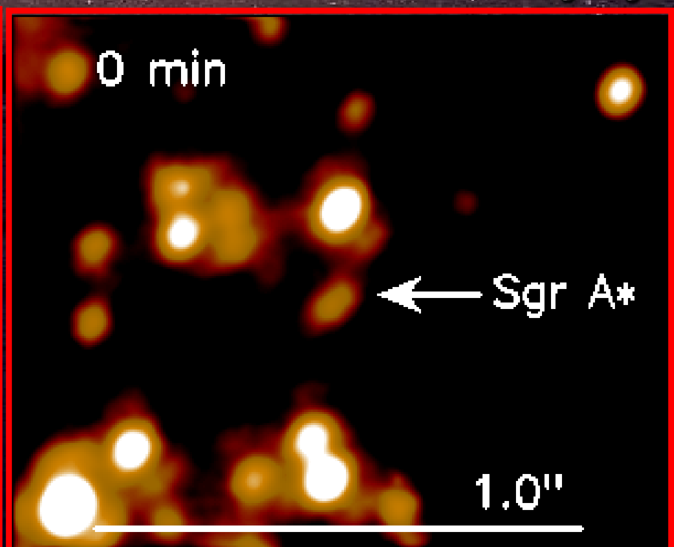

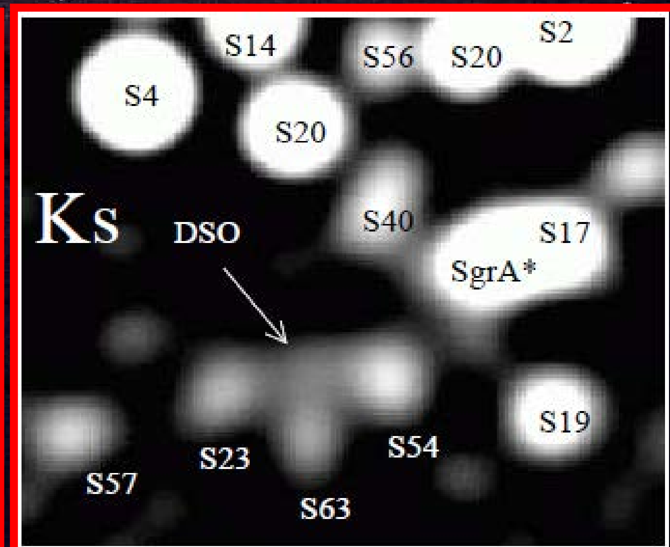

The Center of the Milky Way

Closest galactic genter at 8 kpc
High extinktion of Av=30 Ak=3
Stars can only be seen in the NIR

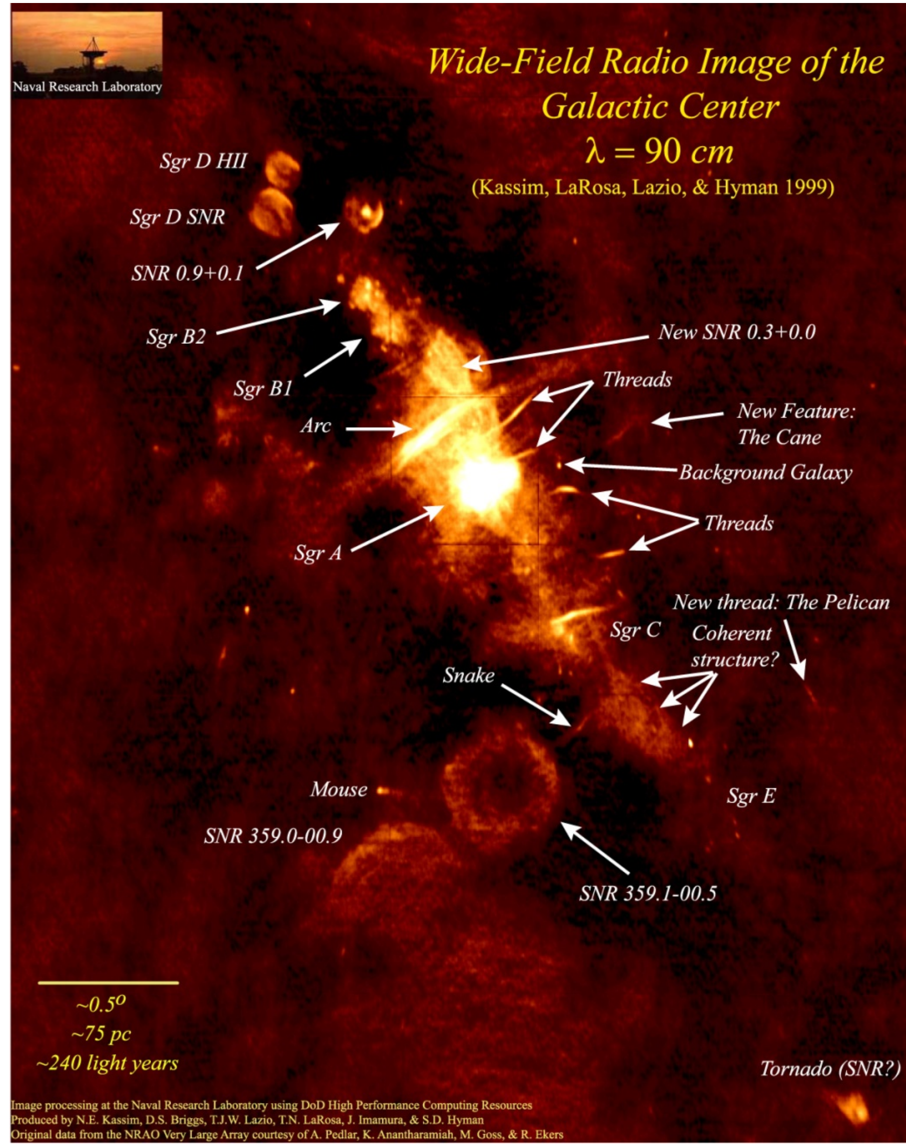

VLA 90cm

Kassim, Briggs, Lasio, LaRosa, Imamura, Hyman

Plan

- Geschichtliches und Einführung
- Bausteine eines galaktischen Kerns
- Staubquellen im Galaktischen Zentrum
- Quelle DSO/G2 auf Kollisionskurs
- Vergleich zu aktiven Kernen
- Ausblick

The first 2.2μm scans through the GC

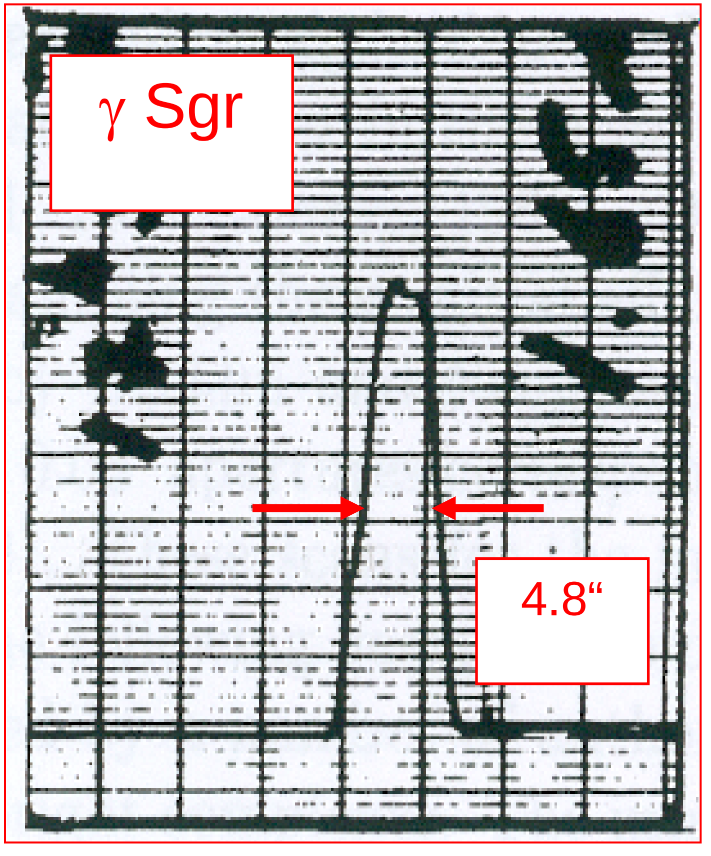

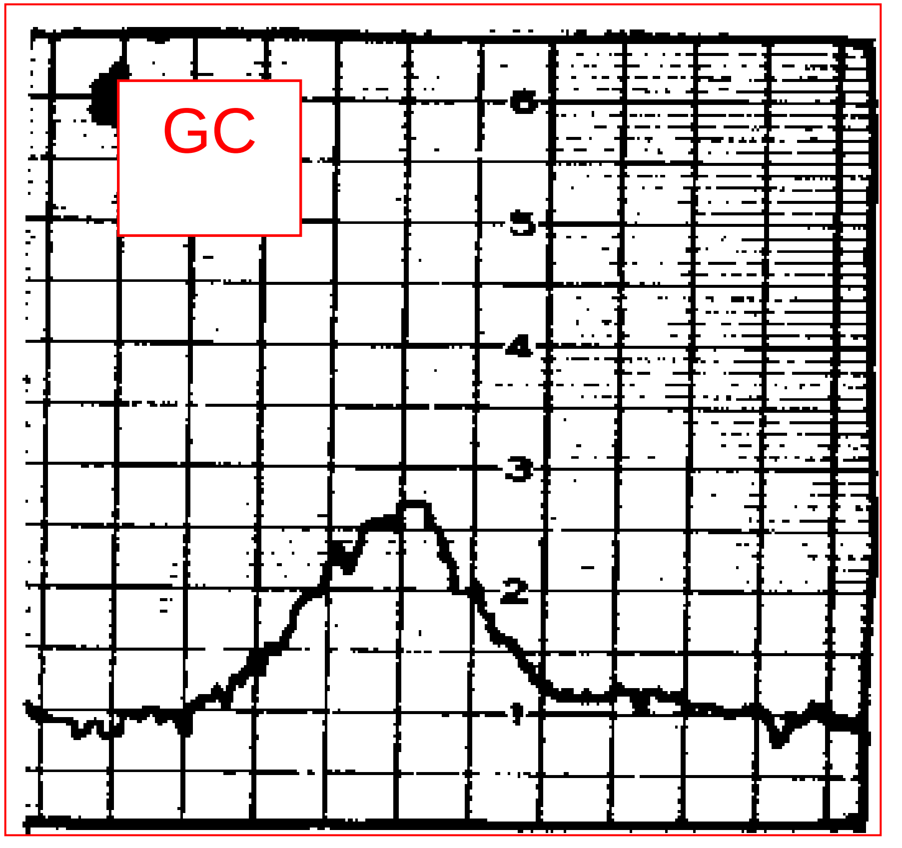

R.A. scans with a single pixel detector (Becklin & Naugebauer 1968)

The first 2.2μm scans through the GC

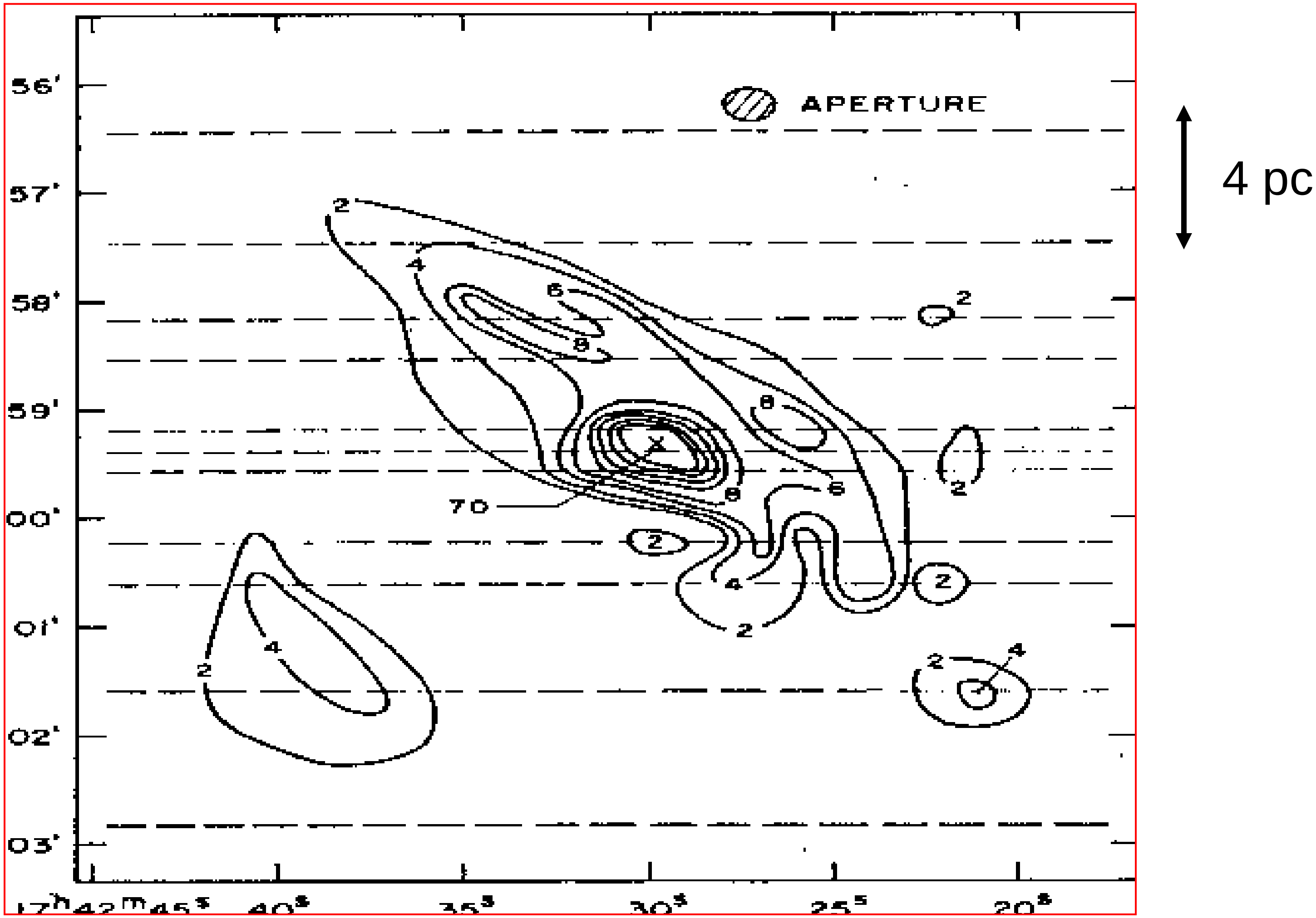

R.A. scans with a single pixel detector (Becklin & Naugebauer 1968)

The first 2.2µm scans through the GC

4 pc

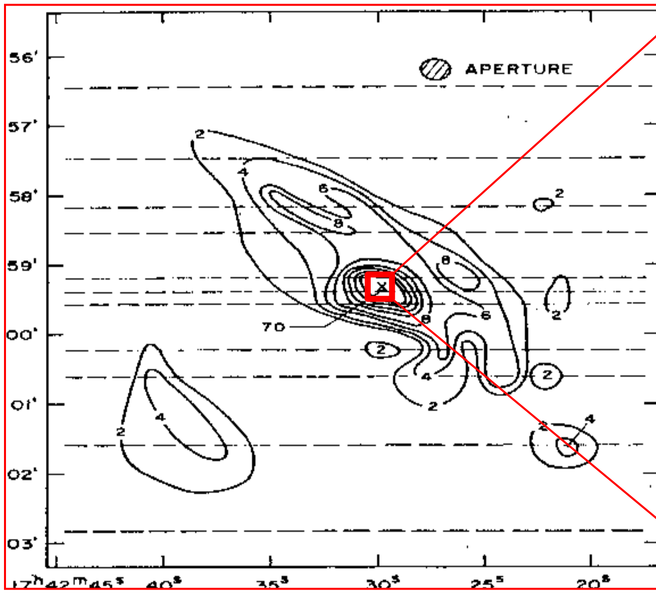

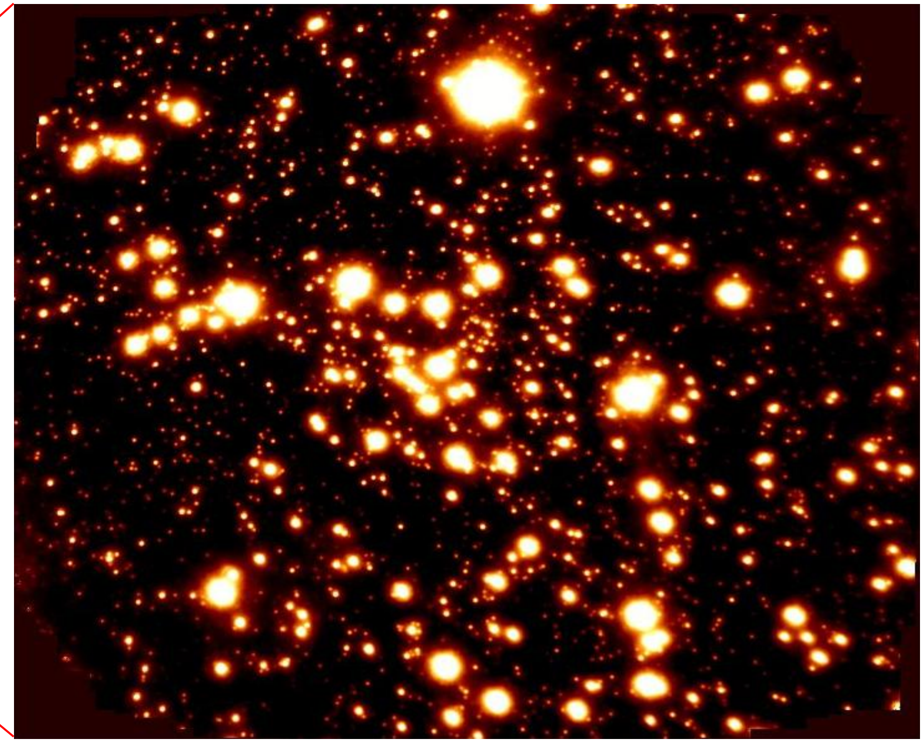

0.5 pc

(Becklin & Naugebauer 1968)

NACO AO NIR
Observations at the VLT in Chile
ince 1999
(+7 years NTT)

•Introduction

- The SMBH SgrA* and its environment

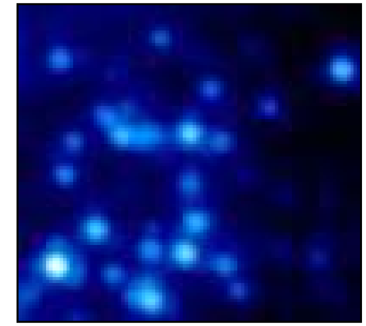

- Synchrotron and synchrotron self-Compton modeling the NIR/X-ray flares of SgrA*

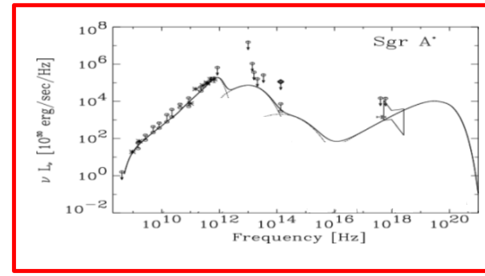

- Statistics of NIR light curves of SgrA*

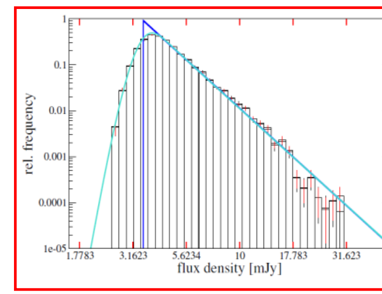

- Polarization signatures
  Relativistic disk calculations

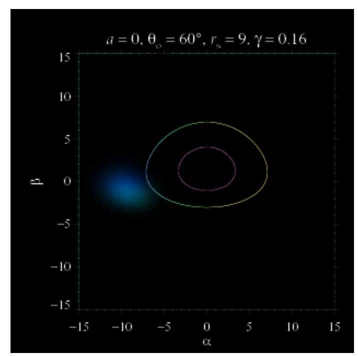

- Upcoming violent events

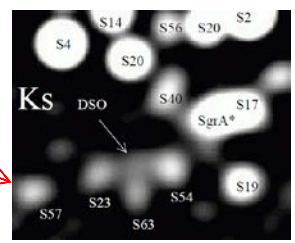

•Summary

Flares: positive flux density excursions in NIR and excursions above the quiescent state in X-ray

The Evironment of SgrA*

Orbital motion of high-velocity S-stars

On the possibility to detect relativistic and Newtonian peri-center shifts

- Granularity of scatterers
- Search for stellar probes

Synchrotron and synchrotron self-Compton modeling the NIR/X-ray flares of SgrA*

Simultaueous NIR/X-ray Flare emission 2004

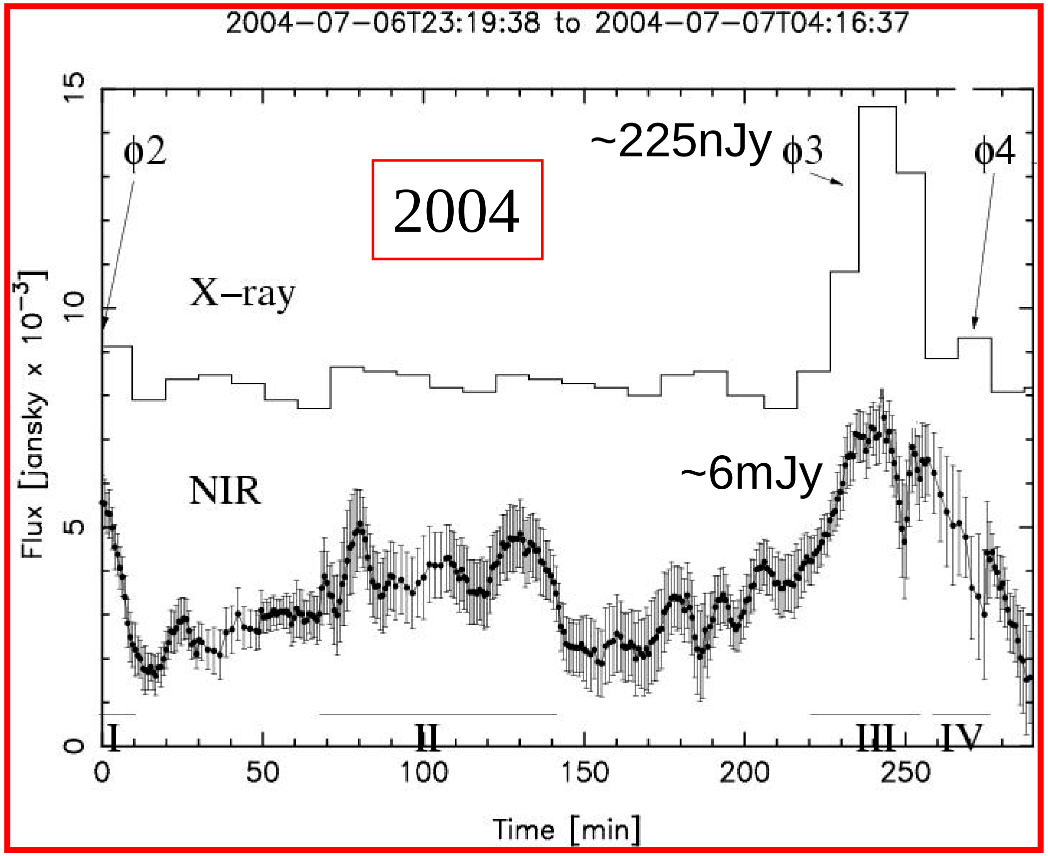

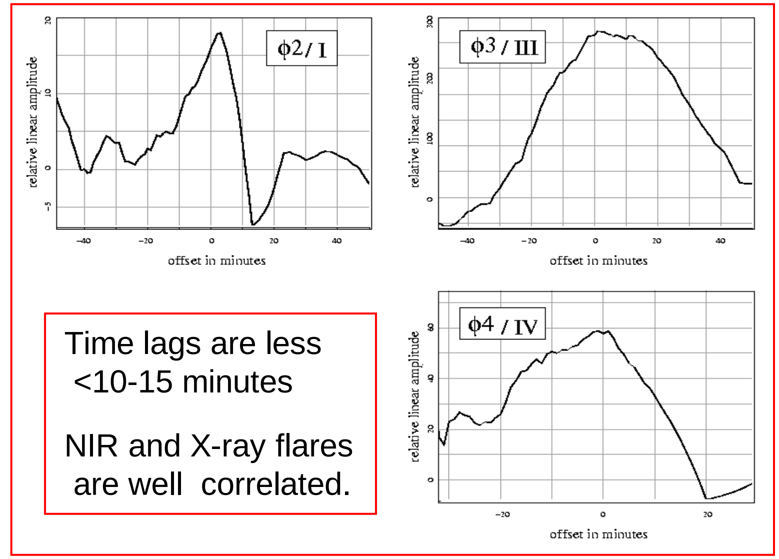

Flare emission originates from within <10mas form the position of SgrA*

First simultaneous NIR/X-ray detection
2003 data: Eckart, Baganoff, Morris, Bautz, Brandt, et al. 2004 A&A 427, 1
2004 data: Eckart, Morris, Baganoff, Bower, Marrone et al. 2006 A&A 450, 535

see also Yusef-Zadeh, et al. 2008, Marrone et al. 2008

The 15 May 2007 NIR Flare

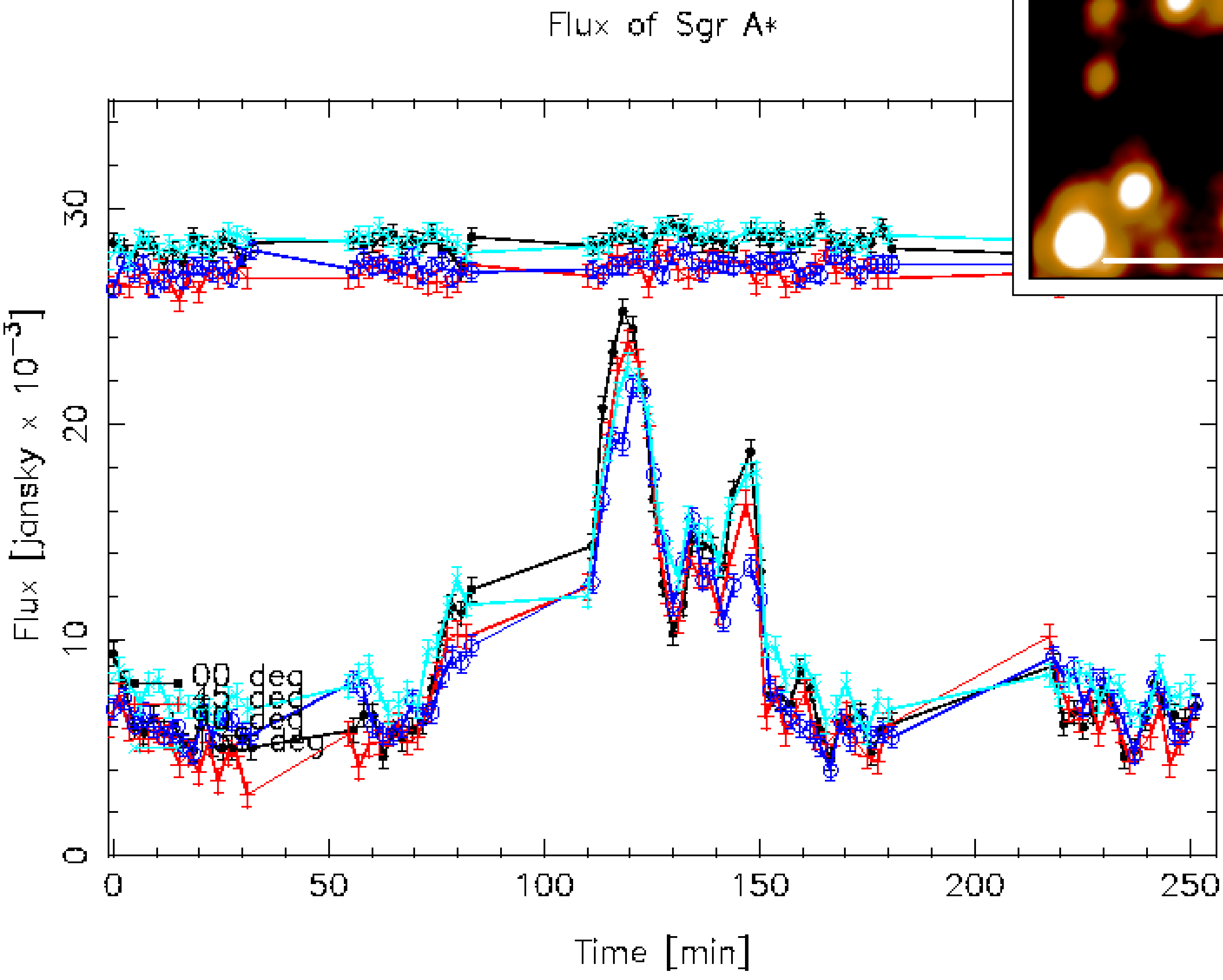

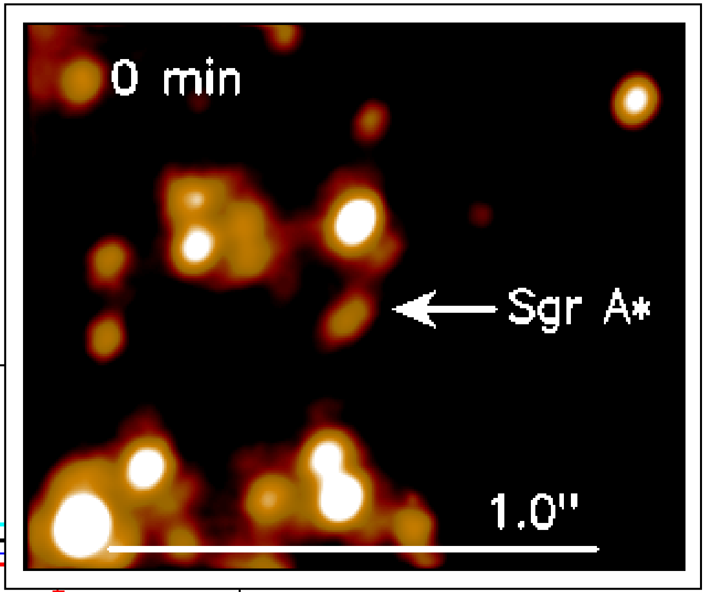

May 2007 CARMA / NIR data

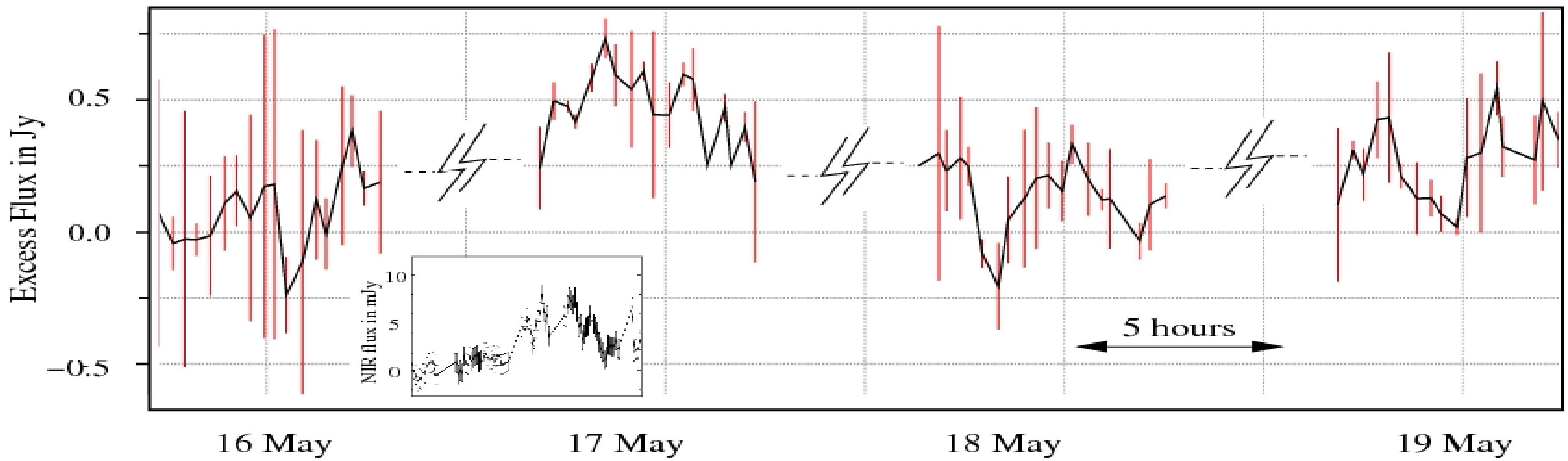

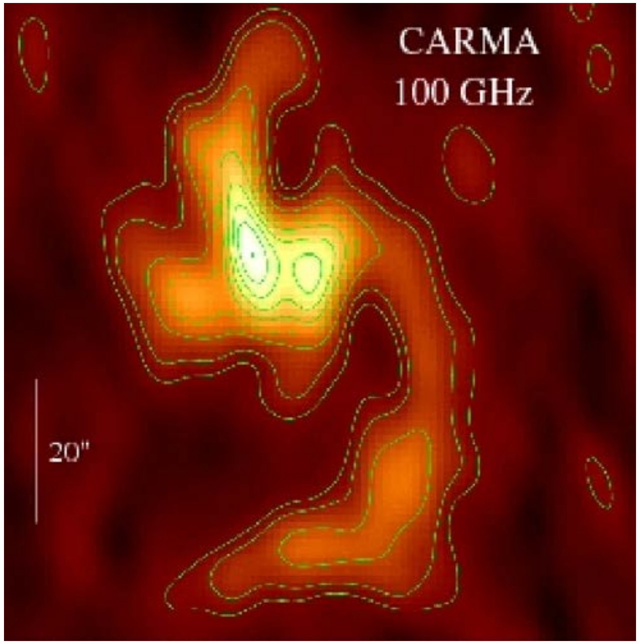

The 17 May 2007 NIR Flare

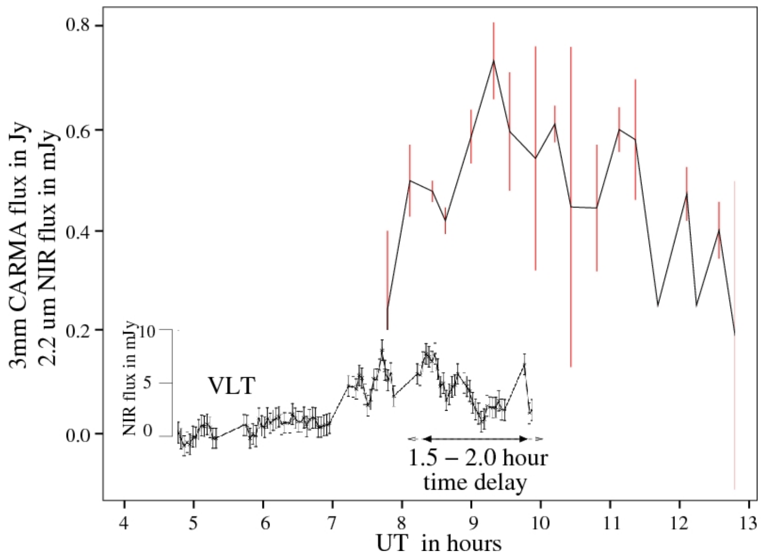

May 2007: CARMA, ATCA, IRAM 30m data on SgrA*

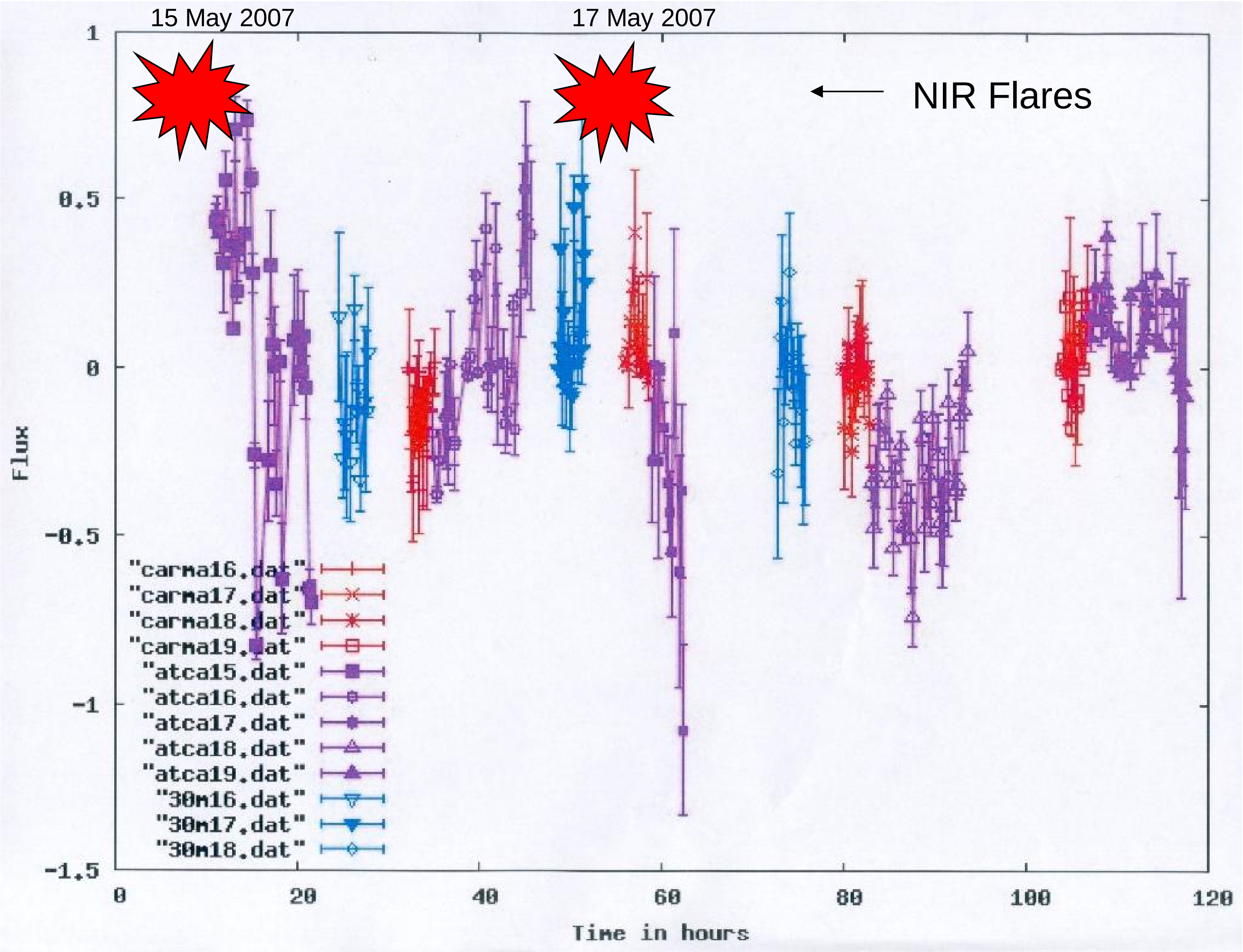

SgrA* VLT L-band flare on 3 June 2008

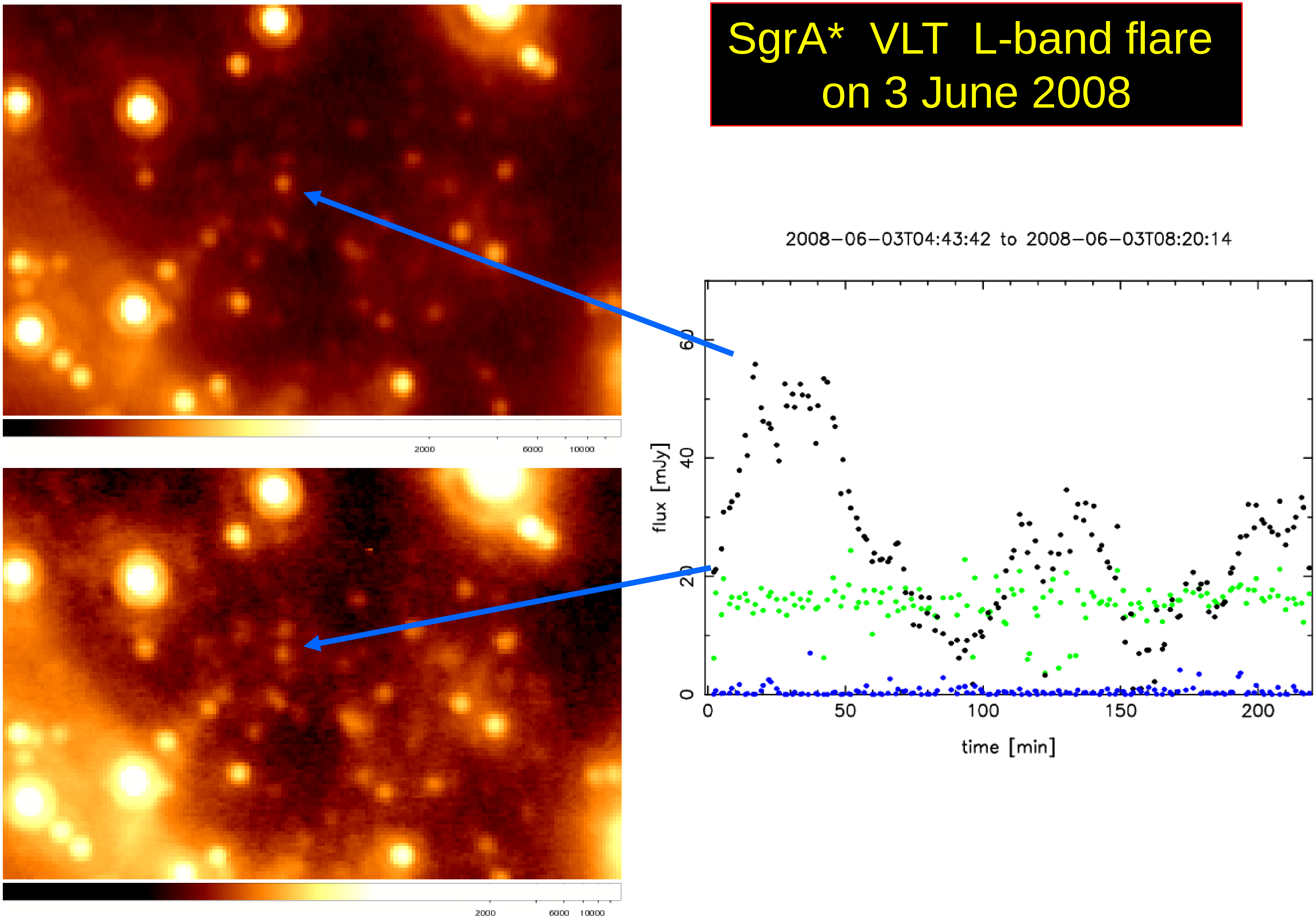

SgrA* APEX sub-mm flare on 3 June 2008

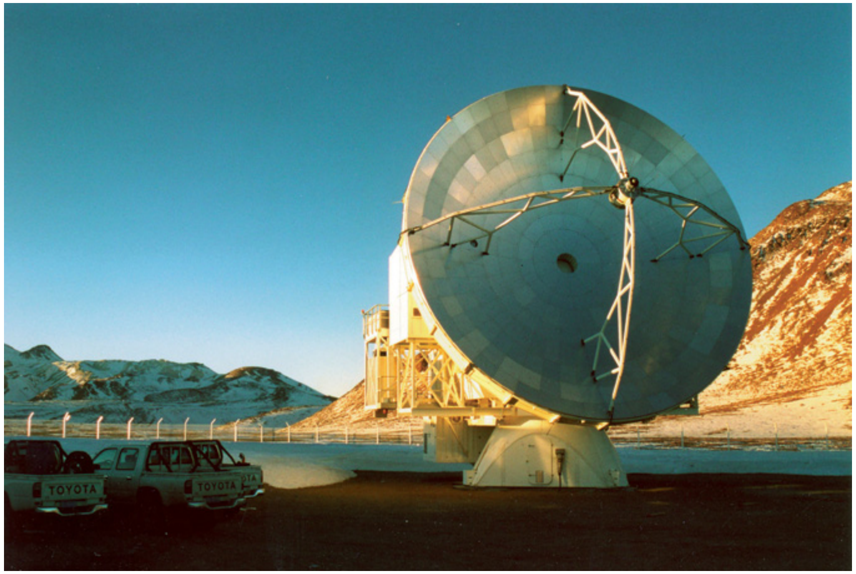

Observations

SgrA* on 3 June 2008:
VLT L-band and APEX
sub-mm measurements

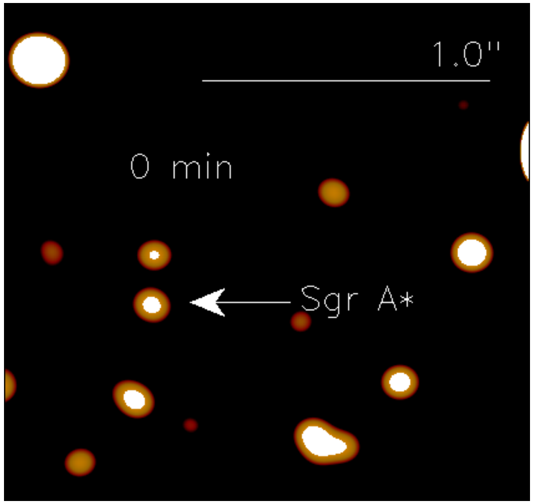

VLT 3.8um L-band

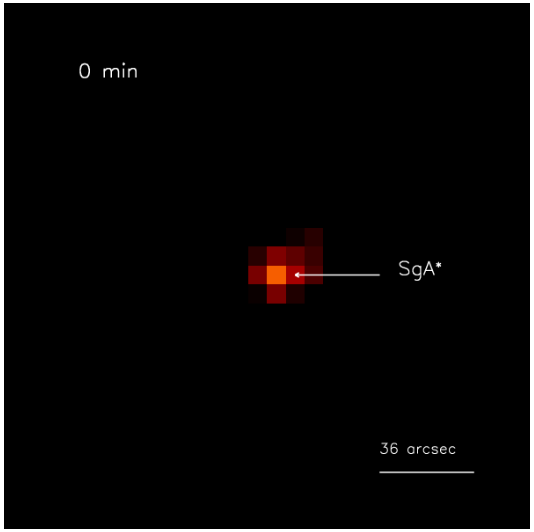

APEX 1.3 mm

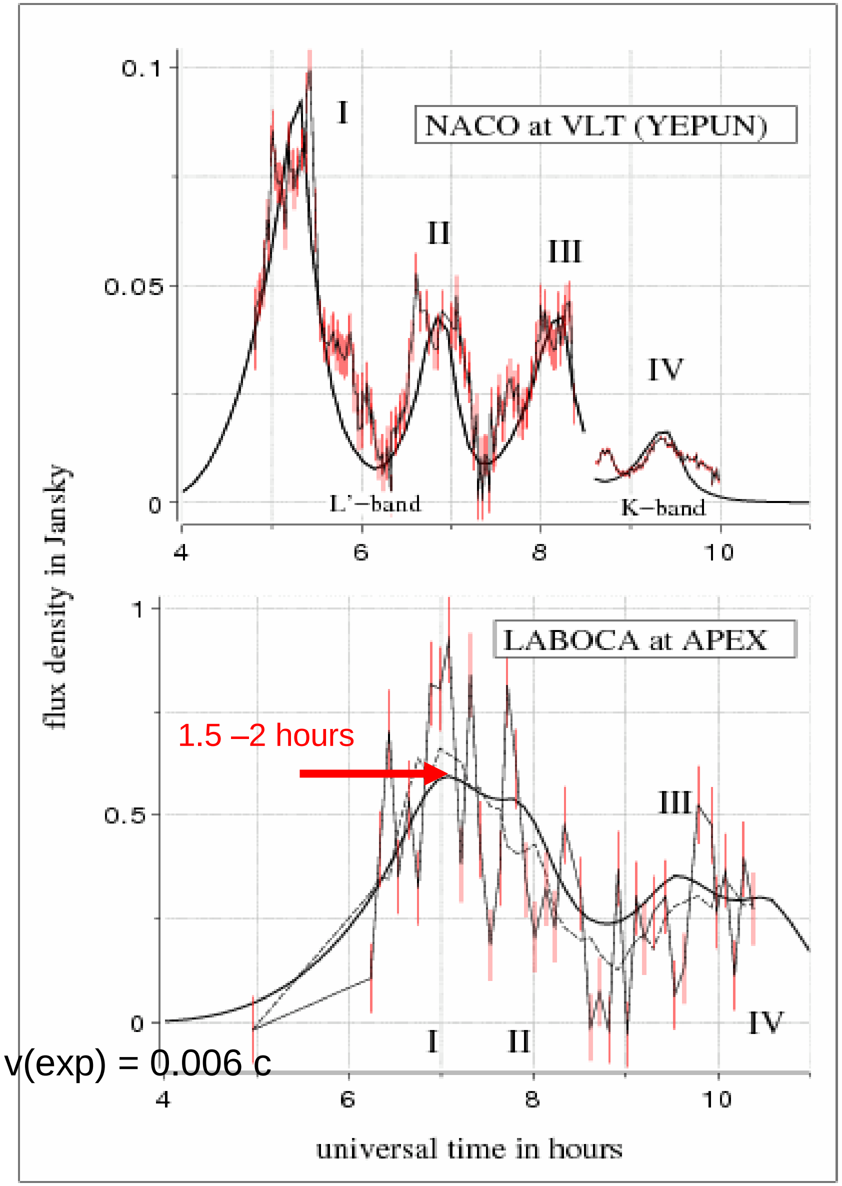

Eckart et al. 2008; A&A 492, 337
Garcia-Marin et al.2009

Flare Emission from SgrA*

Recent work on SgrA* variability

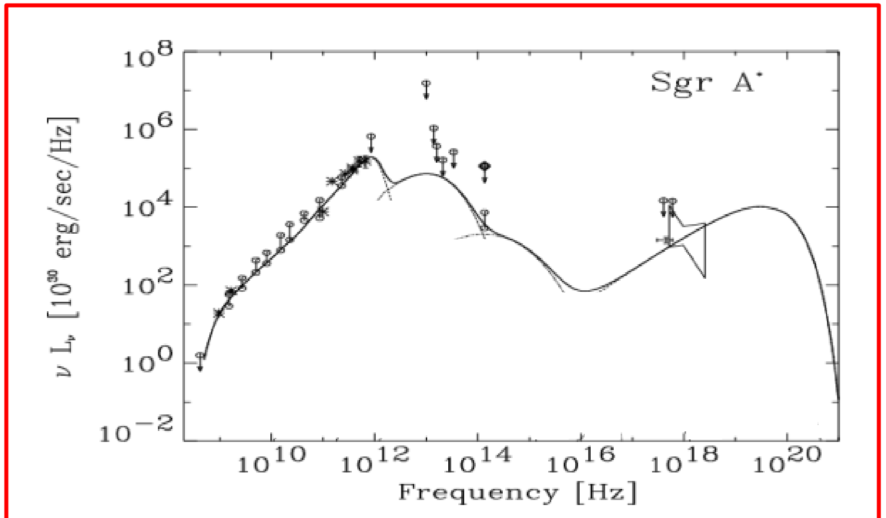

Radio/sub-mm:
Mauerhan+2005, Marrone+2006/8, Yusef-Zadeh+2006/8 and may others

X-ray:
Baganoff+2001/3, Porquet+2003/2008, Eckart+2006/8, and several others

NIR:
Genzel+2003, Ghez+2004, Eckart+2006/9, Hornstein+2007,Do+2009, and many others

Multi frequency observing programs:
Genzel, Ghez, Yusef-Zadeh, Eckart and many others

Questions:
- What are the radiation mechanisms
- (How) Are flux density variations at different wavelength connected to each other

Theory

Radiative Models of SGR A* from GRMHD Simulations

MOTION IN
OR CLOSE TO
THE MIDPLANE

relativistic effects
may become
observable here

Accretion of matter onto SgrA* results in a variable spectrum

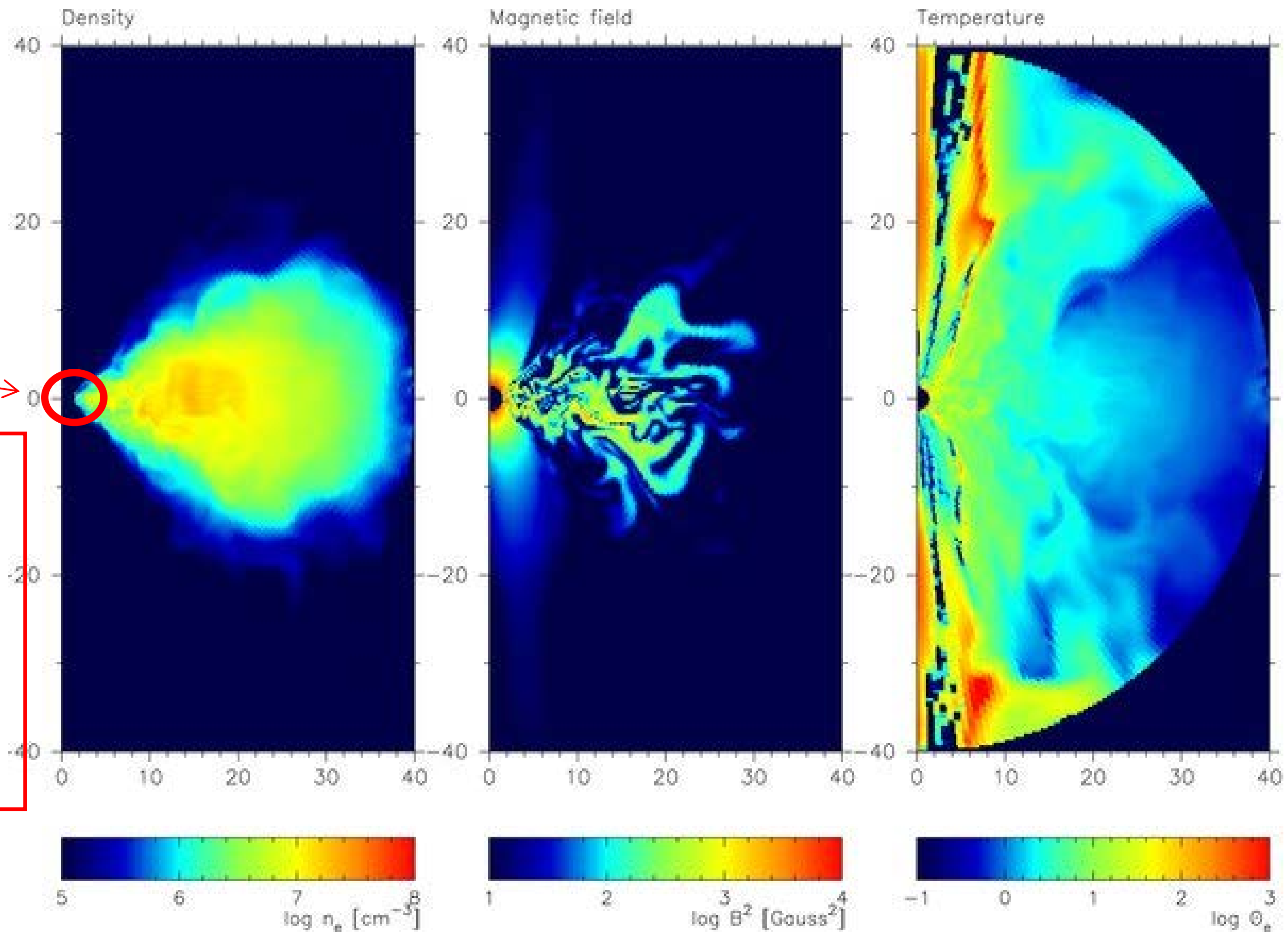

Mościbrodzka+ 2010, 2009
Dexter+ 2010

Possible flare scenarii

Possible flare models

NIR X-ray

SYN-SYN: Synchrotron-synchrotron

SYN-SSC: Synchrotron-Self-Compton

SSC-SSC: Self-Compton-self-Compton

Parametrization of the logarithmic expression

Two extreme cases:
High demands on electron acceleration or density

SYN-SYN: X-ray produced by synchrotron radiation;
<10% by SSC

$$n_e \approx 10^6 cm^{-3} \qquad \gamma_e \approx 10^{6-7}$$

SSC-SSC: X-ray produced by synchrotron self-Compton;
<10% by SYN; required density higher than average

$$n_e \geq 10^8 cm^{-3}$$

Moderate demand on density and acceleration

SYN-SSC: radio/NIR by Syncrotron and X-ray by SSC

$$n_e \approx 10^6 cm^{-3} \qquad \gamma_e \approx 10^{3-4}$$

Spectral distribution of cutoff frequencies

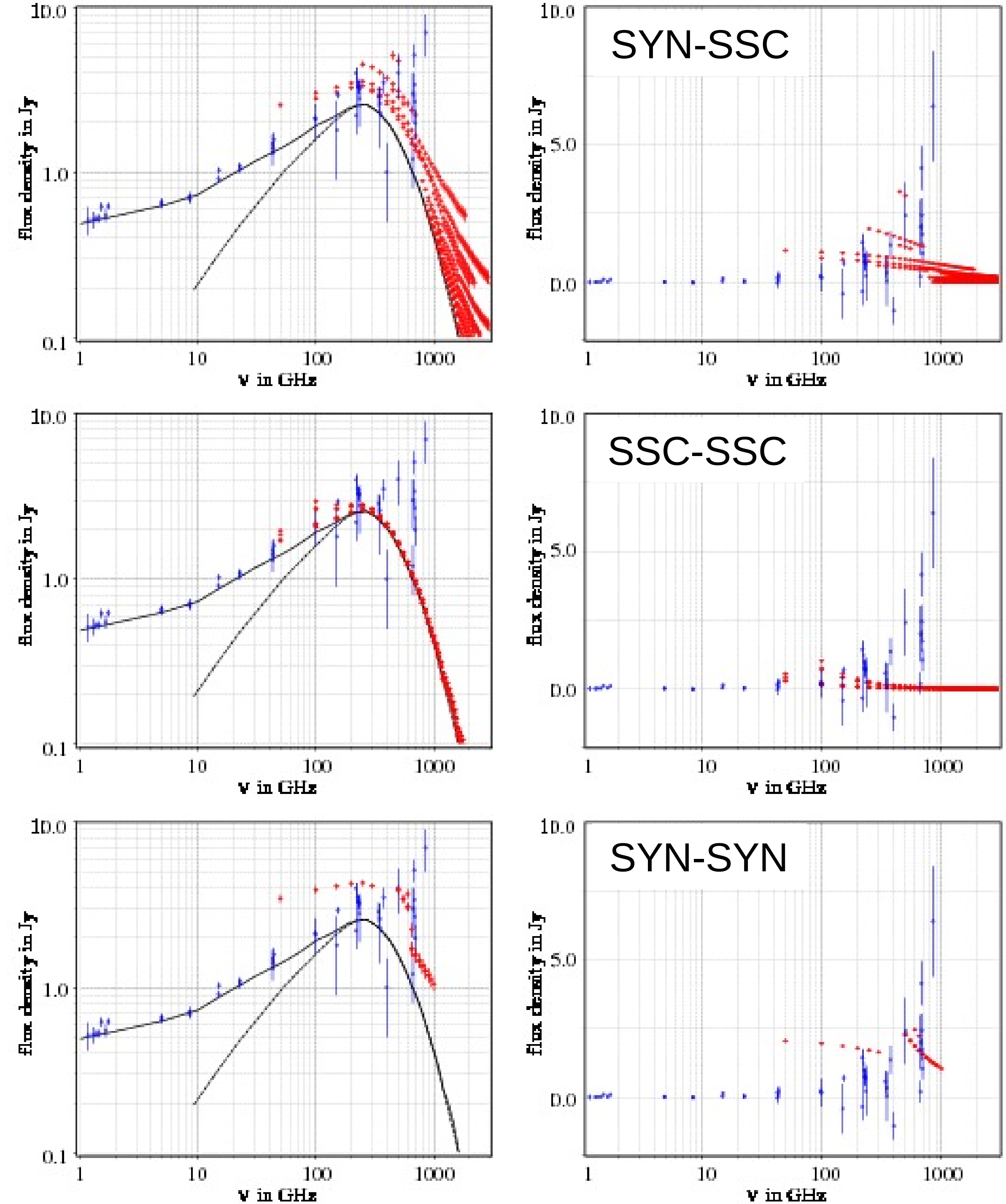

Density rather high but consistent with MHD model of mid-plane.

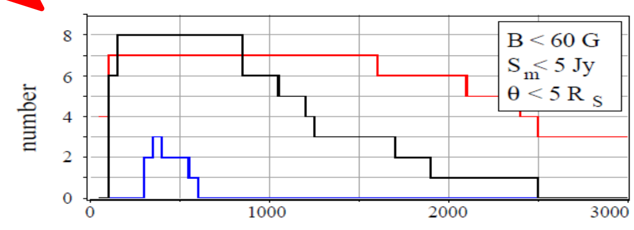

Density like the low average value in central 20Rs
but a rather rare explanation delivering generally
too high mm-fluxes

Visualization of possible flare scenarii

$$S_m = \kappa_1 \nu^{-\alpha}$$

$$\theta = \kappa_2 \nu_m^{\zeta_1}$$

$$B = \hat{\rho} \nu_m^{\zeta_2}$$

$$N_0 = \kappa_3 \nu_m^{\zeta_3}$$

relativistic electron density

$$\rho = mc^2 \int_{\gamma_1}^{\gamma_2} N(\gamma) d\gamma = N_0 \frac{(mc^2)^{-2\alpha}}{2\alpha} (\gamma_1^{-2\alpha} - \gamma_2^{-2\alpha})$$

$$N(\gamma) = N_0 E(\gamma)^{2\alpha+1}$$

All important quantities can be written as powers of the turnover frequency.

All constants are functions of observables (spectral index and fluxes) or parameters

Eckart et al. 2012

Synchrotron Modeling

Rapid variability time scales (< 1hour) imply a non-thermal radiation mechanism:

$$S_{X,ssc} = d(\alpha)\ln(\frac{\nu_2}{\nu_m})\theta^{-2(2\alpha+3)}\nu_m^{-(3\alpha+5)}S_m^{2(\alpha+2)}E_X^{-\alpha}\delta^{-2(\alpha+2)},$$

$$B = 10^{-5}b(\alpha)\theta^4\nu_m^5 S_m^{-2}\delta,$$

$$N_0 = n(\alpha)D_{Gpc}^{-1}\theta^{-(4\alpha+7)}\nu_m^{-(4\alpha+5)}S_m^{2\alpha+3}\delta^{-2(\alpha+2)},$$

Marscher 1983, 2009

Radiative Models of SGR A* from GRMHD Simulations

In the mid-plane the vertical particle distribution is well described by a Gaussian, with a dimensionless scale height of about 0.1-0.3 ($1\ \sigma$).

DENSITIES CLOSE TO THE MIDPLANE WILL BE HIGHER THAN AVERAGE

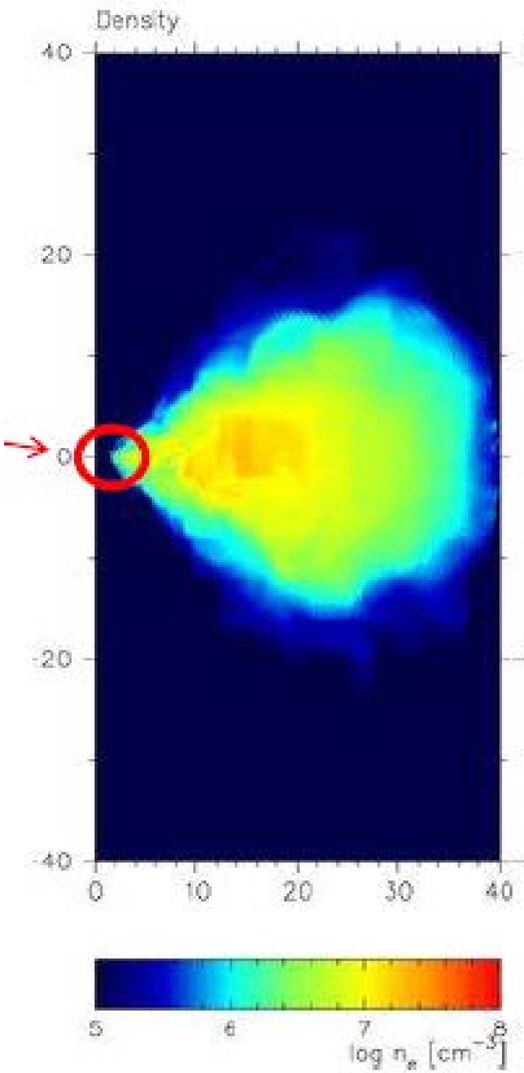

However, the thickness (and hence the mid-plane density) is mostly determined by the initial conditions and energy evolution methods used in the simulations rather than by the physics of the accretion flow.

Visualization of possible flare scenarii

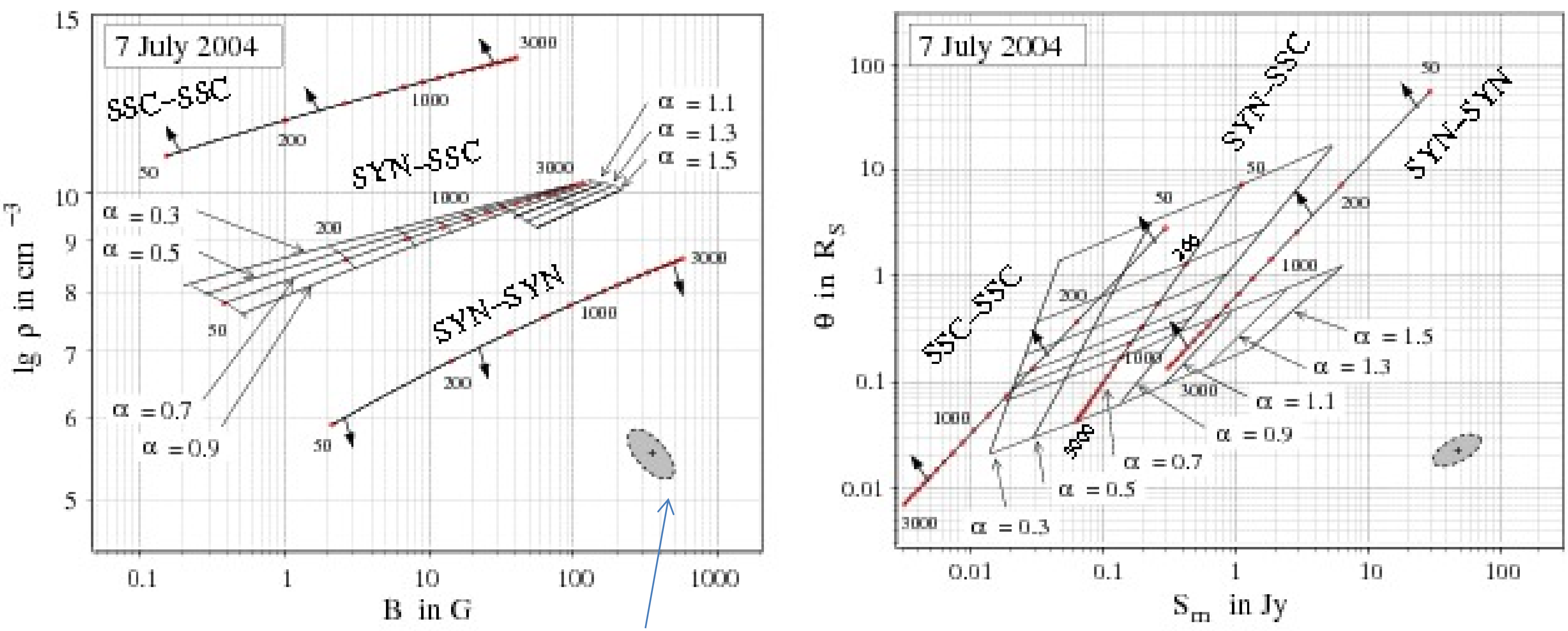

parameterized by case spectral index and turnover frequency νm.

Uncertainties due to measurement uncertaintuies

Solutions obey MIR flux limits (Schödel+ 2010,11) and: If SYN dominates less than 10% of the radiation should be due to SSC and vice versa.
Arrows point into directions of even more stringent constrains.

Eckart et al. 2012

Distribution of likely cutoff frequencies

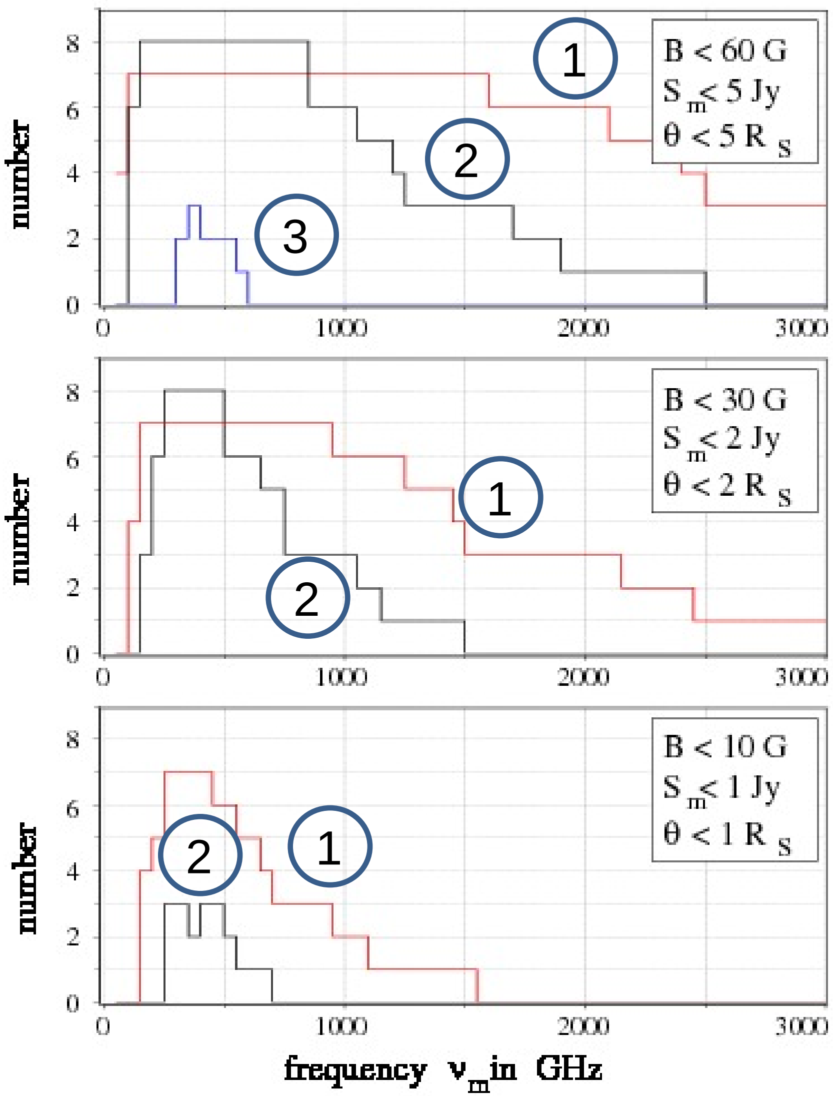

1 SSC-SSC $\alpha = \alpha_{\text{NIR/X-ray}}$

2 SYN-SSC $\alpha = -0.7$

3 SYN-SYN $\alpha = \alpha_{\text{NIR/X-ray}}$

Maximum range of turnover frequencies from extrapolation of NIR and radio spectra:

~50 GHz to 3000 GHz

Only a few cases can be explained Through SYN-SYN solutions; SYN-SSC and SSC-SSC are The most robust solutions

Eckart et al. 2012

Visualization of possible flare scenarii for the 8 simultaneous flares

Density versus magnetic field

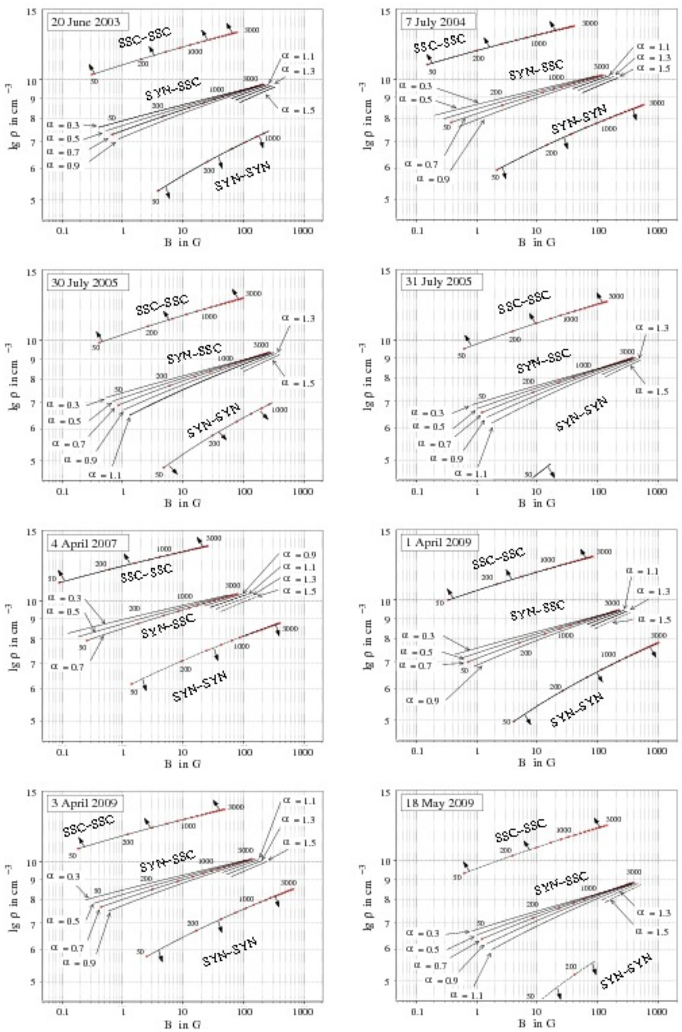

Source size versus peak flux

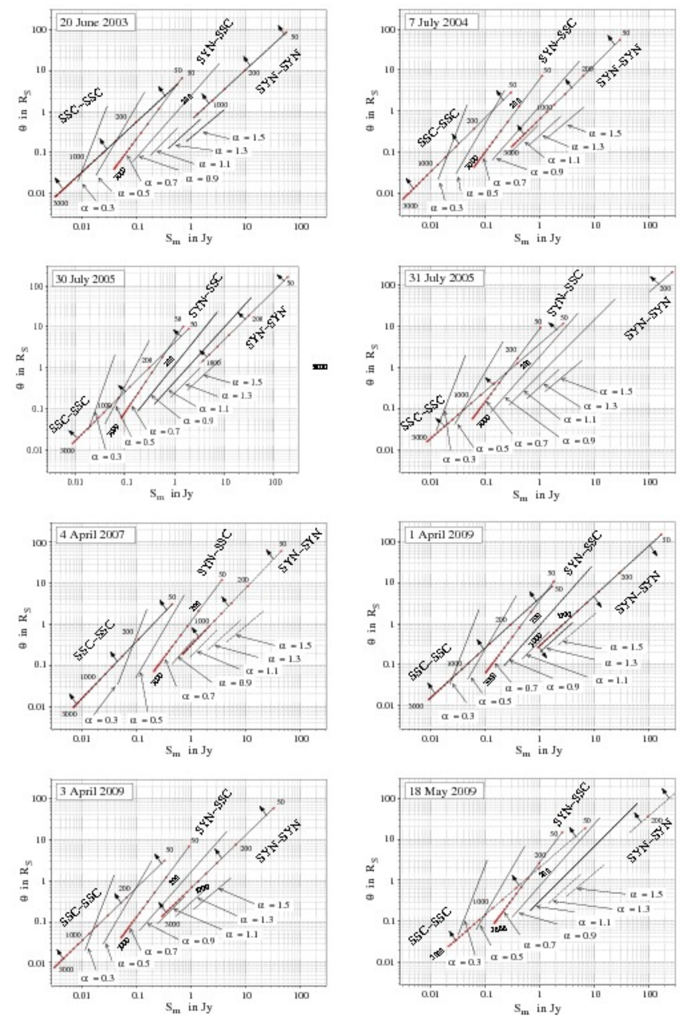

Eckart et al. 2012

Spectral distribution of cutoff frequencies

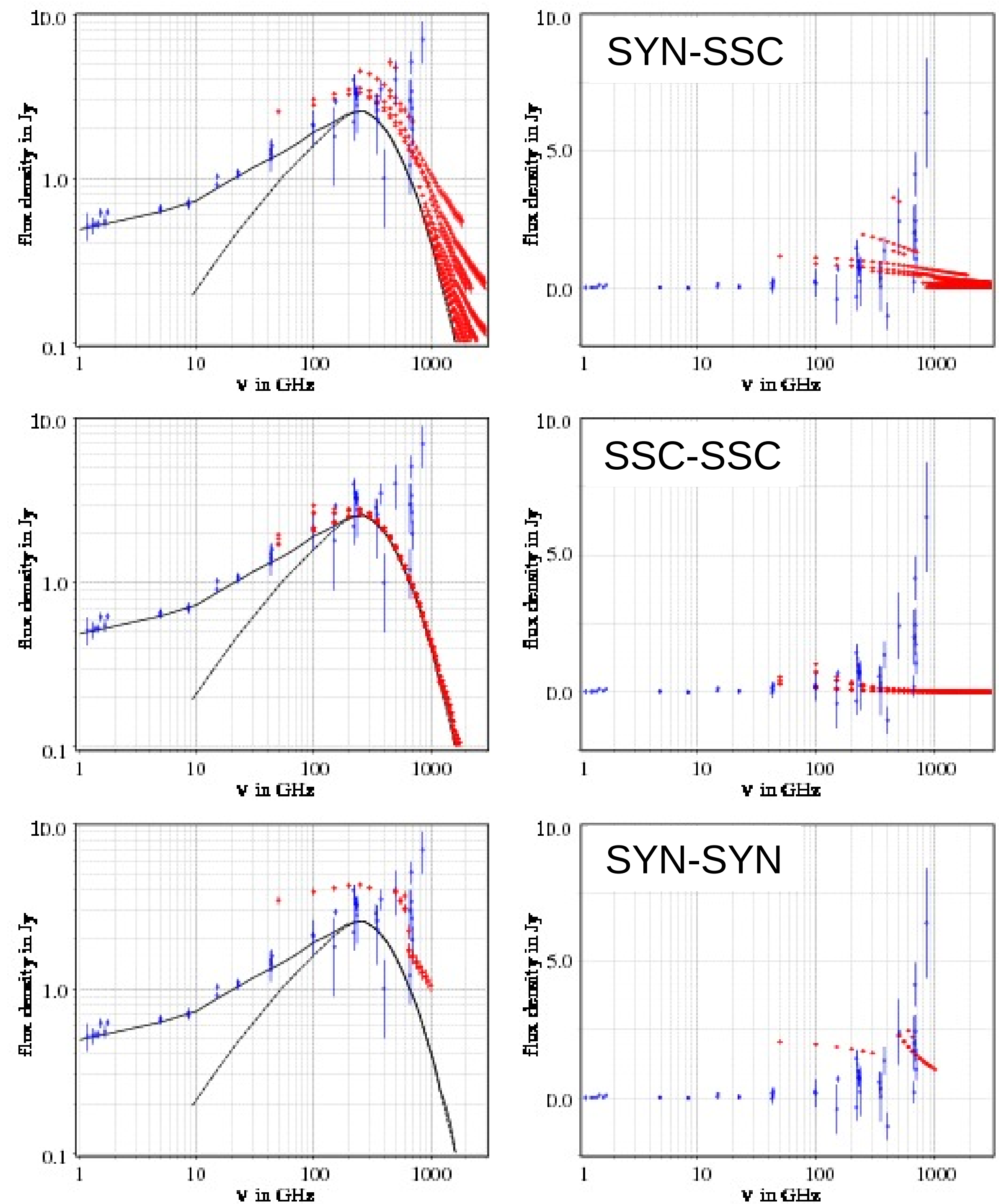

Our SYN-SYN, SSC-SSC and SYN-SSC flare modeling superimposed on top of (sub-)mm data and the a lower envelope as given by the sub-mm bump models by Dexter+2010

Flux density data as compiled by Falcke+1998 and others.

Left: spectrum
Right: only SYN/SSC variable spectrum with sub-mm bump model subtracted.

Eckart et al. 2012

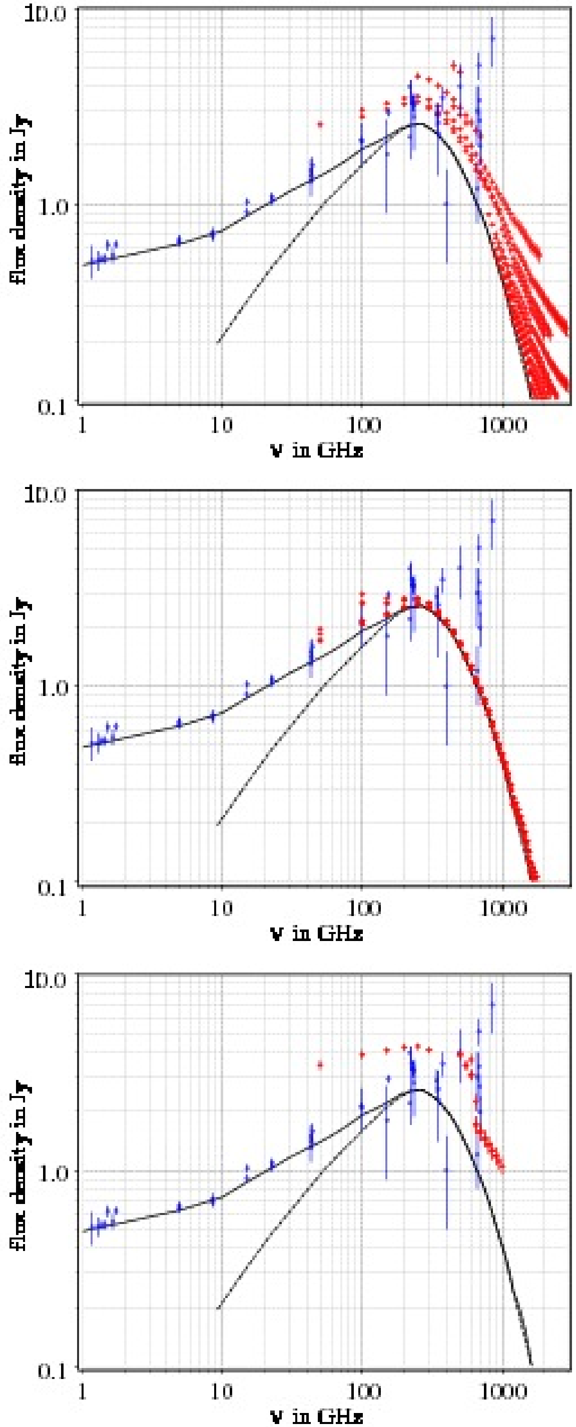

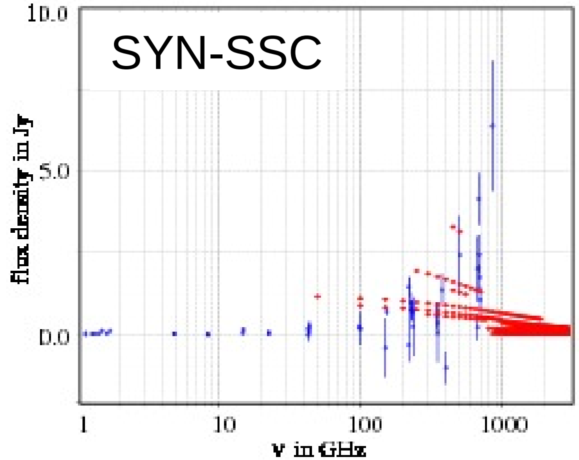

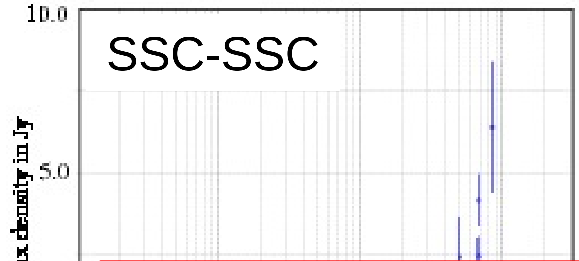

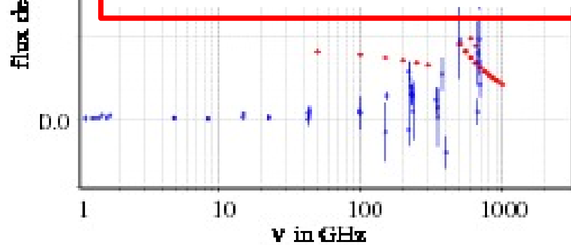

Spectral distribution of cutoff frequencies

Upper limits on B, Sm and ρ constrain the spectrum of cutoff frequencies nm
i.e. the shape of the variability spectrum of SgrA*.

case	$B[G]$	$S_m[Jy]$	$\theta\ [R_S]$	$\log \rho[cm^{-3}]$	χ^2
SYN-SSC	90	5	5	9.5	2.6
SSC-SSC	90	5	5	9.5	7.2
SYN-SYN	130	8	2	6.8	3.6

Table 5. Restricted parameters from modeling the frequency dependent variable flux density of SgrA* for the SYN-SSC, SSC-SSC, and SYN-SYN case. We list the upper limits for B, S_m, and θ as well as the lower limit for the density ρ and the χ^2 values of the model.

Eckart et al. 2012

Collisionless Shocks

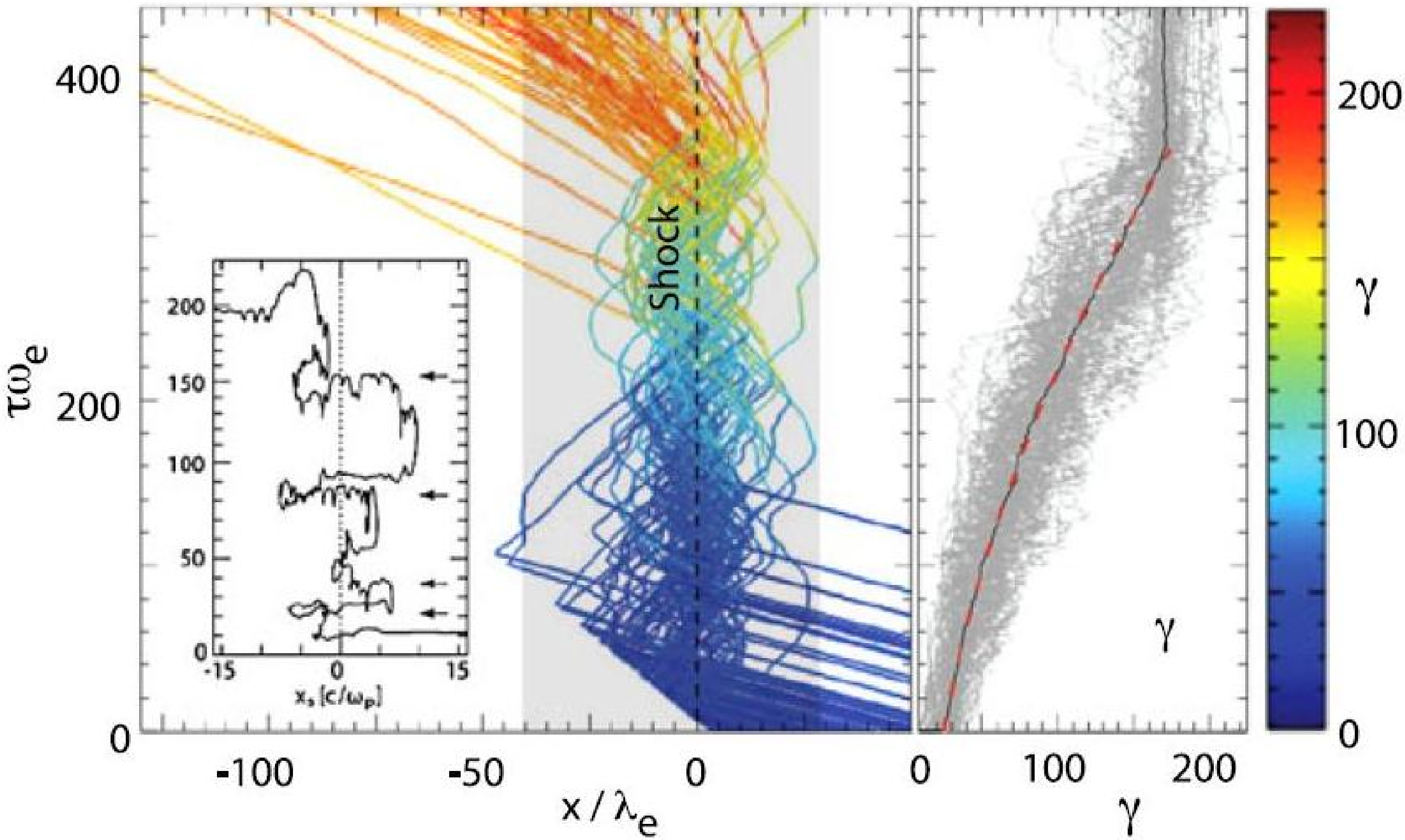

Left: Time-evolution of the orbits of the 80 most energetic ions in a non-magnetized relativistic shock simulation with $\Gamma = 20$. The particles are coming from the upstream flow, are back-scattered and accelerated in the magnetic turbulence in the shock transition, staying within the distance of an ion inertial length $\lambda i \approx 50\lambda e$.

Bykov & Treumann, 2011, Astr. Astro. Rev. 19, 42

Radiative Models of SGR A* from GRMHD Simulations

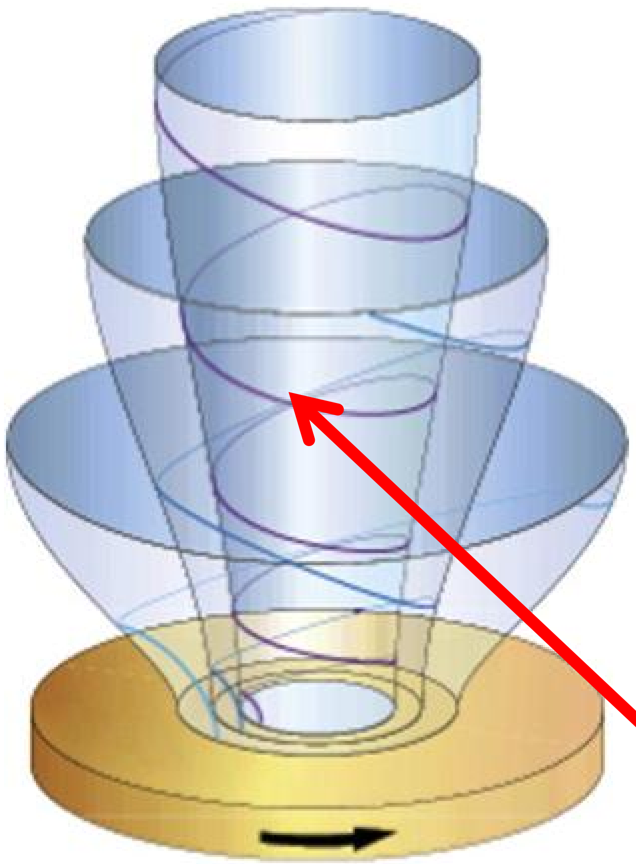

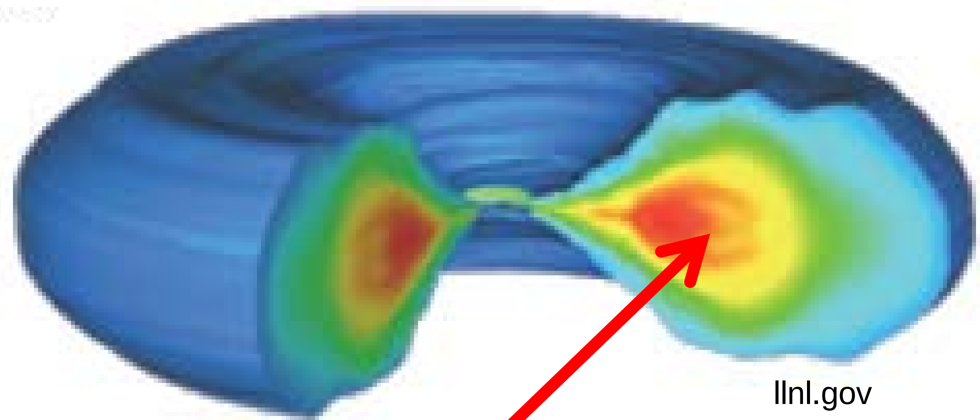

llnl.gov

Jonathan Ferreira, Remi Deguiran,
High Energy Density Physics
Volume 9, Issue 1, March 2013, Pages 67–74

Possible locations of electron accelerating collisionles shocks in the immediate vicinity of SgrA*.

Acceleration of Electrons in Shocks

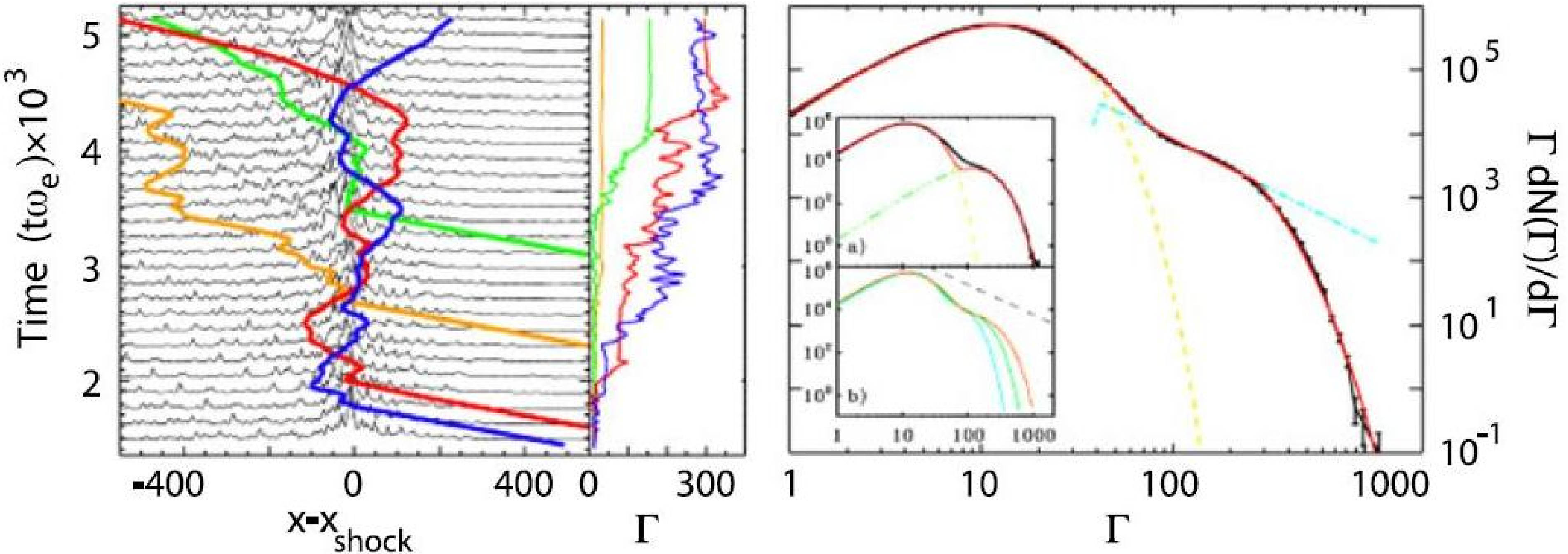

Left: The paths of four selected particles out of the non-thermal tail of the downstream particle distribution drawn on top of the magnetic field as function of time. The particles manage to pass the shock ramp being reflected and accelerated. *Right*: The particle spectrum downstream in a $100\lambda e$ wide slice at downstream distance $500\lambda e$. Maxwellian fits are shown, and a power-law fit to the flat region is indicated.

Bykov & Treumann, 2011, Astr. Astro. Rev. 19, 42

Variability in the SYN-SSC case

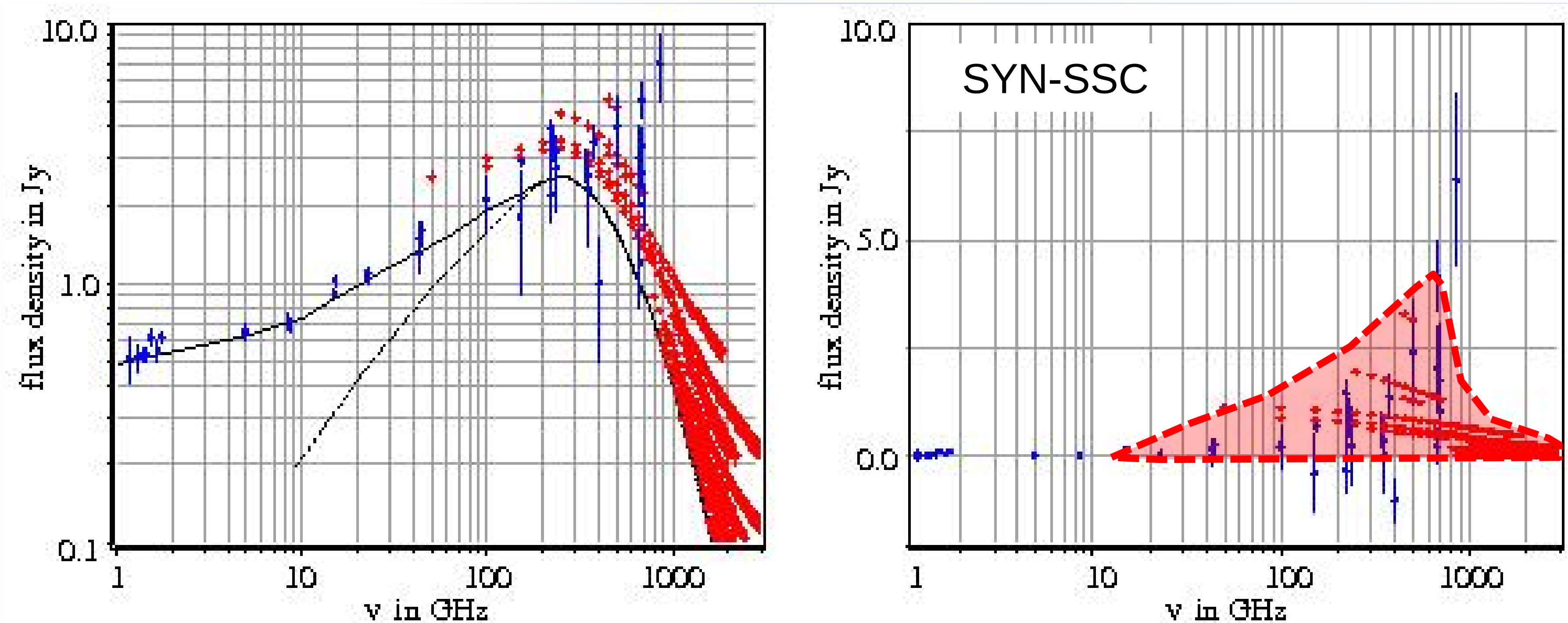

$$n_e \approx 10^6\, cm^{-3}$$

$$\gamma_e \approx 10^{3-4}$$

SYN-SSC: Density moderate
consistent with MHD model of mid-plane
Moderate demand on electron acceleration

Eckart et al. 2012

Indication for Adiabatic Expansion of Synchrotron Source Components:
The 7 July 2004 Flare

Adiabatic expansion in SgrA*:

Zhao et al. 2004,
Eckart et al. 2006,
→ Yusef-Zadeh et al. 2008,
→ Marrone et al. 2008

Synchrotron Self-Compton Sources

$$S_\nu \propto \nu^{-\alpha}$$

$$N(E) \propto E^{-p}$$

$$p = 1 + 2\alpha$$

$$\gamma_e = (1-\beta_e^2)^{-1/2}$$

$$\Gamma_{bulk} = (1-\beta_{bulk}^2)^{-1/2}$$

$$\delta = \Gamma^{-1}(1-\beta_{bulk}\cos\phi)^{-1}$$

$$B \sim \theta^4 \nu_m^5 S_m^{-2}$$

upper frequency cutoff of scattered spectrum

$$\nu_2 = 2.8\times10^6 B\gamma_2$$

synchrotron cooling time scale

$$t_s \sim 3\times10^7 \nu_9^{-0.5} B^{-3/2}$$

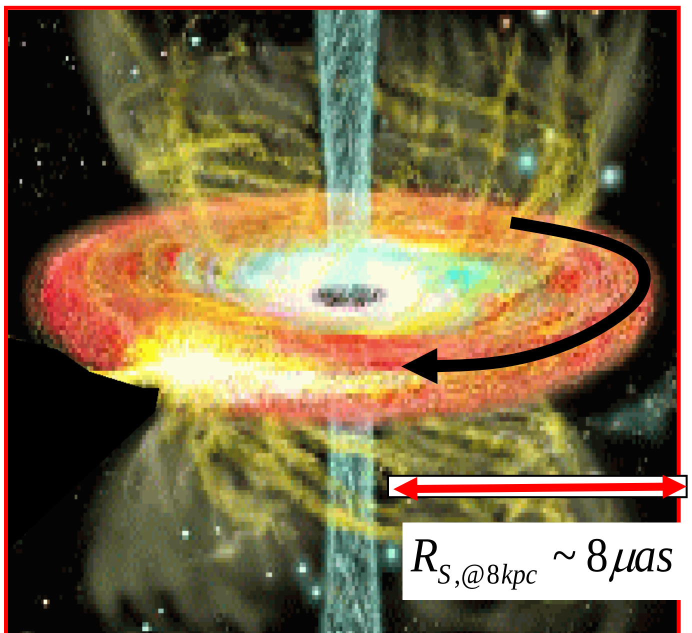

SSC model

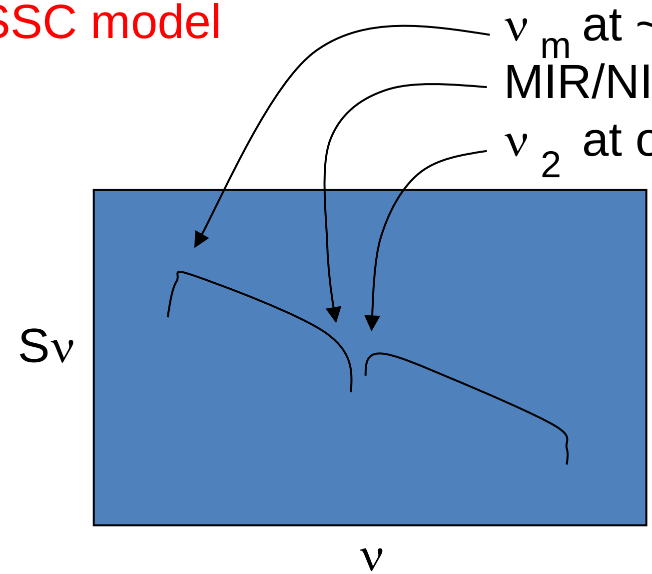

$$\boxed{\gamma_e \sim 10^3}$$

$$\Gamma = 1.2 - 2.0$$

$$\delta = 1.3 - 2.0$$

$$(\phi = 10^o - 45^o)$$

$$B \approx 50G$$

SSC disk modeling of individual flares: 2004

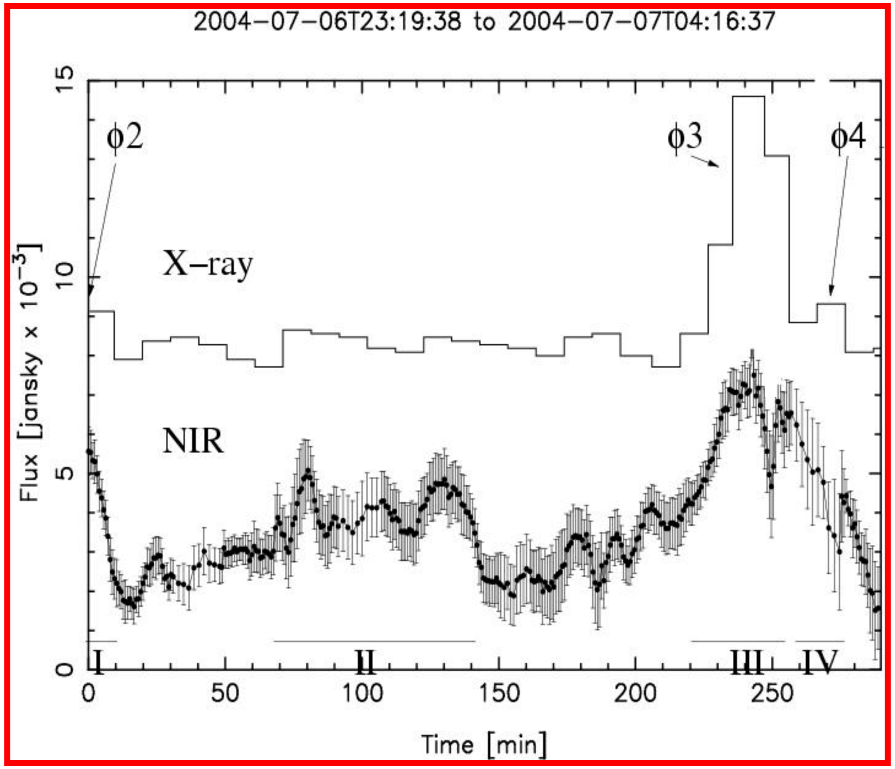

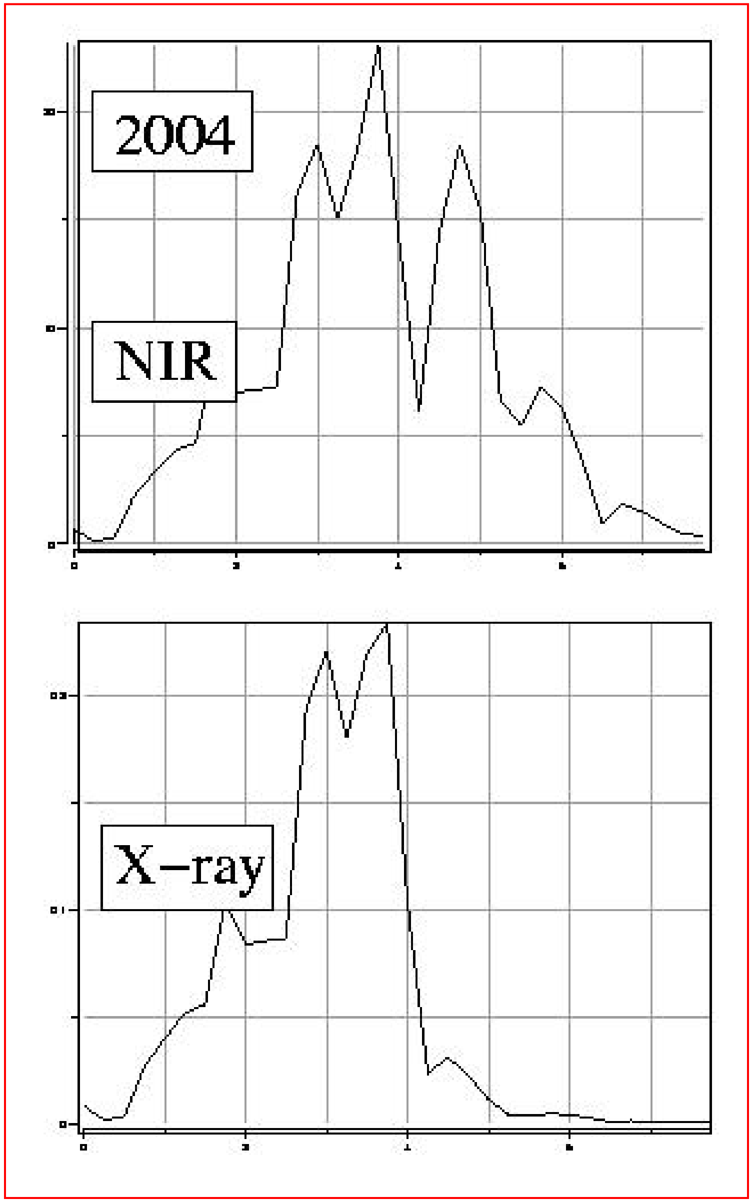

2 flare phases $\phi 3$ $\phi 4$

Adiabatic Expansion of Synchrotron Sources

$$S_\nu \propto \nu^{-\alpha}$$

$$N(E) \propto E^{-p}$$

$$p = 1 + 2\alpha$$

$$\tau_\nu = \tau_0 \left(\frac{\nu}{\nu_0}\right)^{-(p+4)/2} \left(\frac{R}{R_0}\right)^{-(2p+3)}$$

$$e^{\tau_0} - (2p/3+1)\tau_0 - 1 = 0$$

$$S_\nu = S_0 \left(\frac{\nu}{\nu_0}\right)^{5/2} \left(\frac{R}{R_0}\right)^{-(2p+3)} \frac{1-\exp(-\tau_\nu)}{1-\exp(-\tau_0)}$$

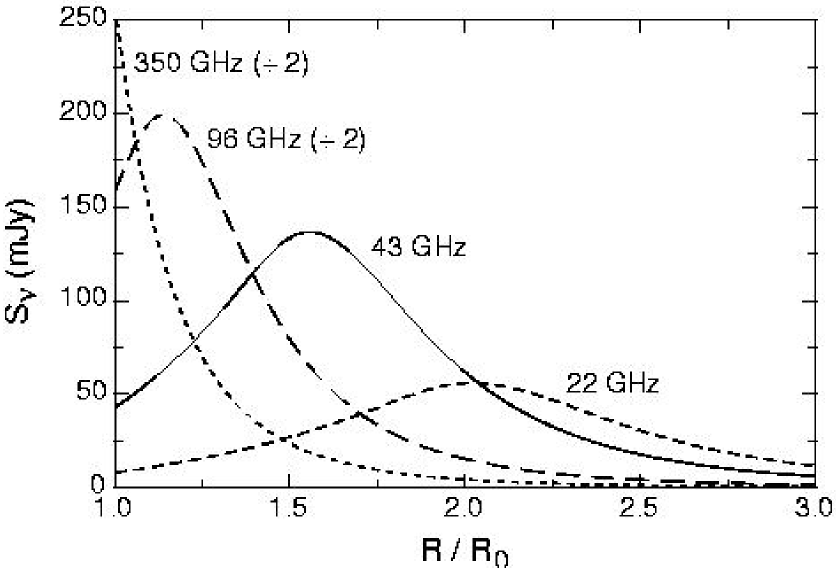

$$S(\nu_2) = S(\nu_1)\left[\nu_1 / \nu_2\right]^{-(7p+3)/(4p+6)}$$

linear transformation to light curves

$$R - R_0 = v_{\exp}(t - t_0)$$

The Effect of Different Expansion Velocities

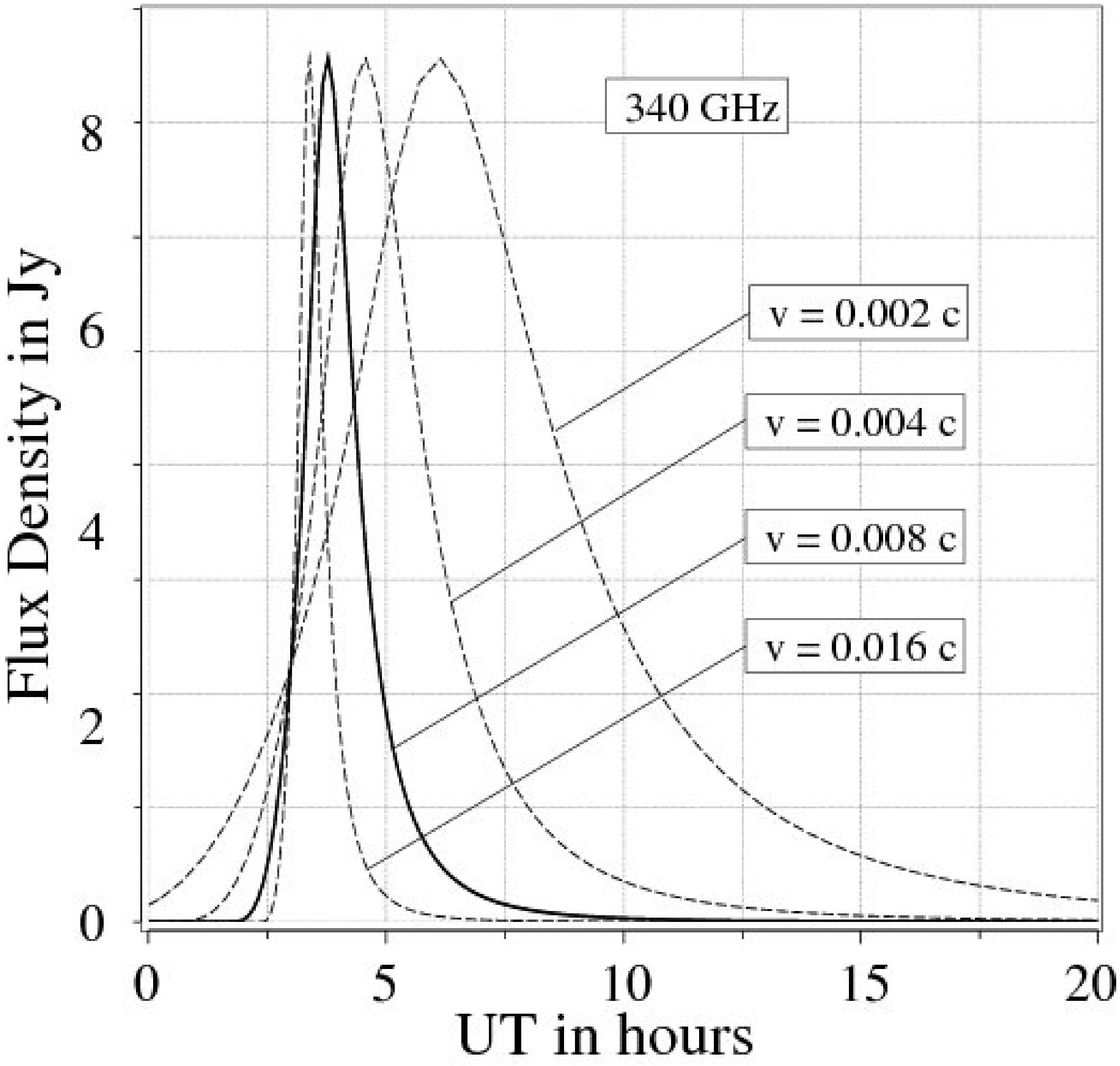

We find 0.008c
as a suitable
expansion velocity!

consistent with
Yusef-Zadeh's values
of 0.003-0.1 c

SgrA*: Emission from a disk with a short jet

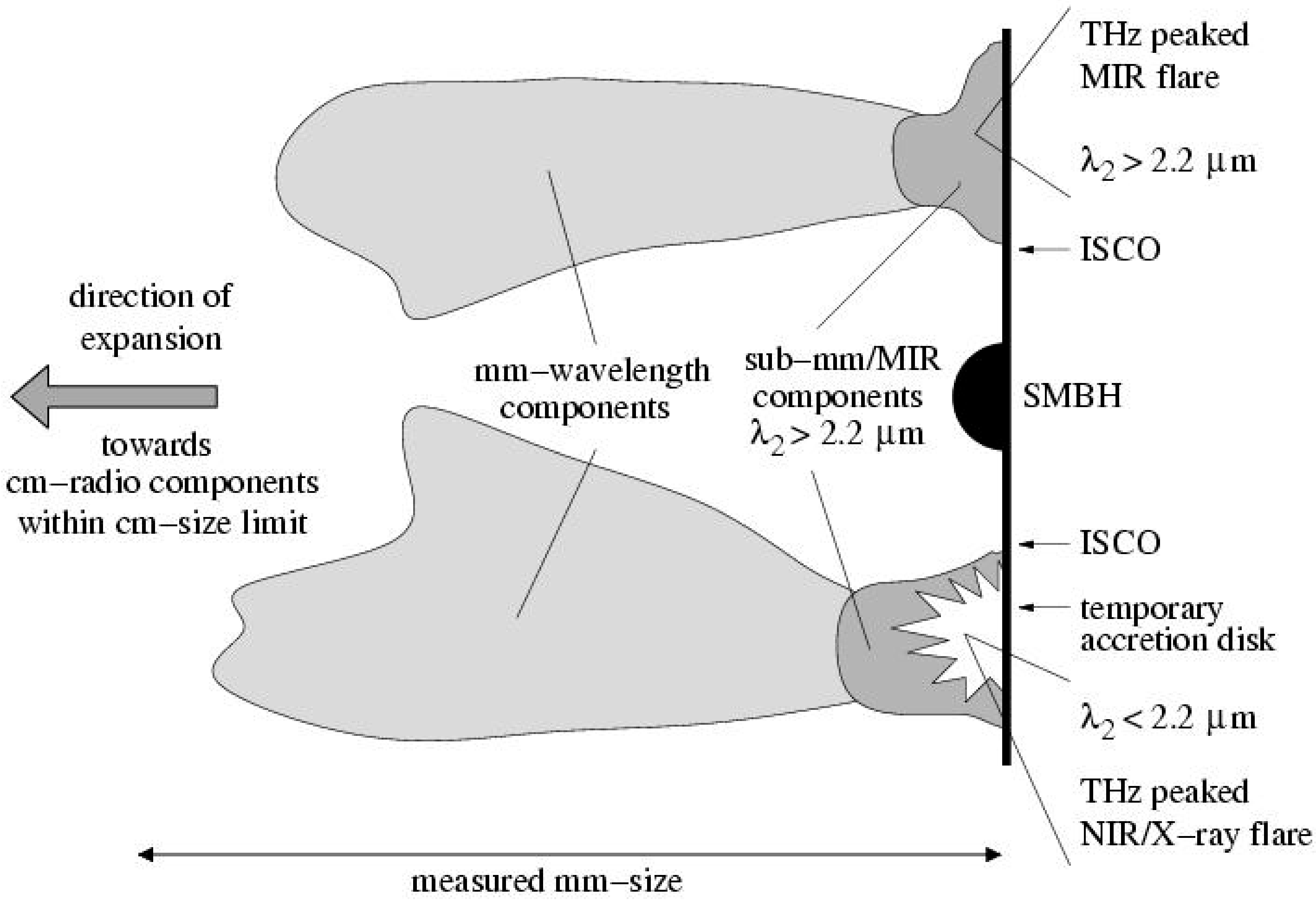

Statistics of NIR light curves of SgrA*

Synchrotron radiation is responsible for flux density variations in the NIR – which can be studied there best – without confusion due to fluxes from the larger scale accretion stream.

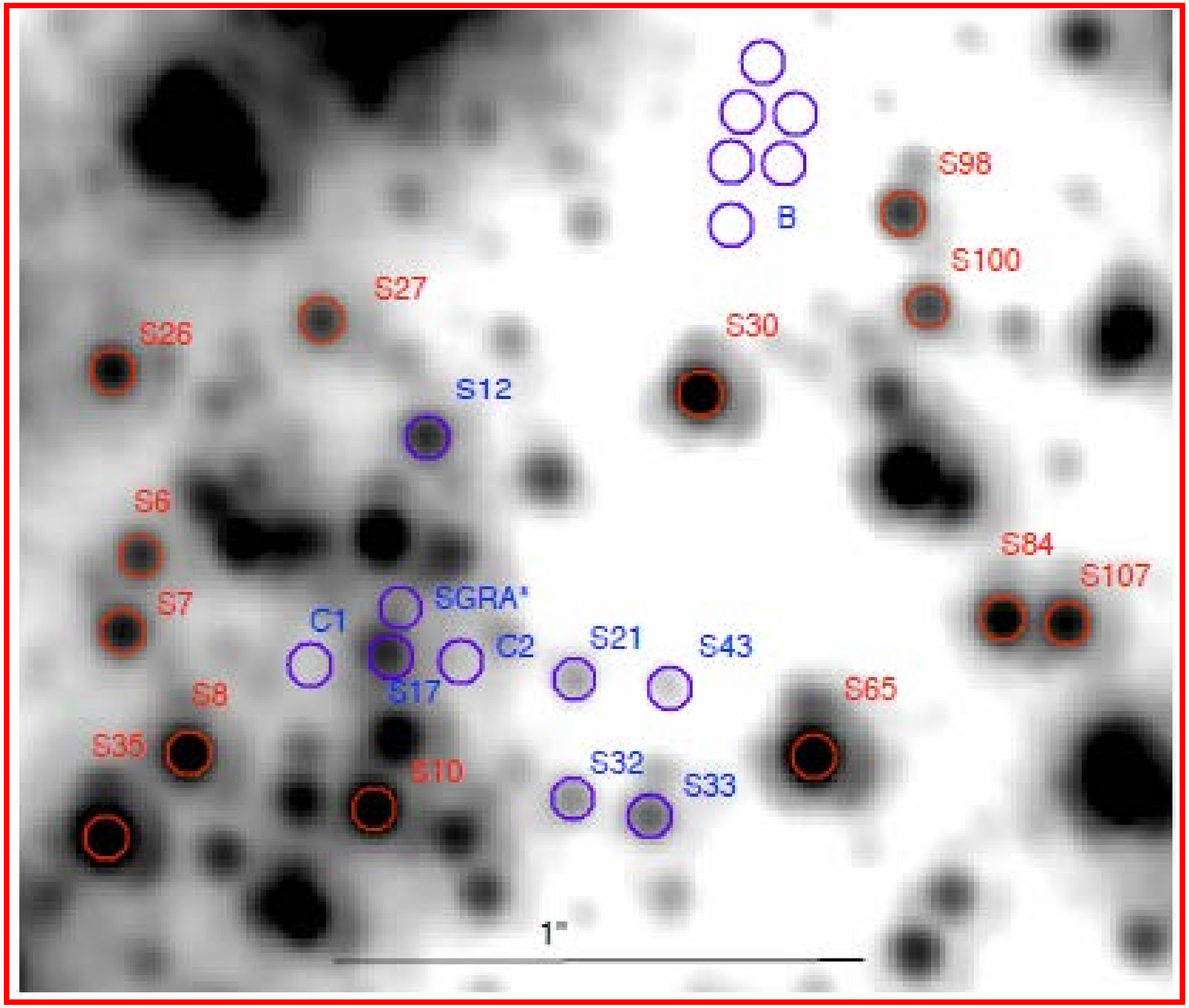

Measurements at 2 μm

Apertures on
(1) SgrA*.
(2) reference stars,
(3) and off-positions

Ks-band mosaic from 2004 September 30. The red circles mark the constant stars (Rafelski et al. 2007) which have been used as calibrators, blue the position of photometric measurements of Sgr A*, comparison stars and comparison apertures for background estimation (Witzel et al. 2012).

Witzel et al. 2012

NIR light curve of SgrA* over 7 years

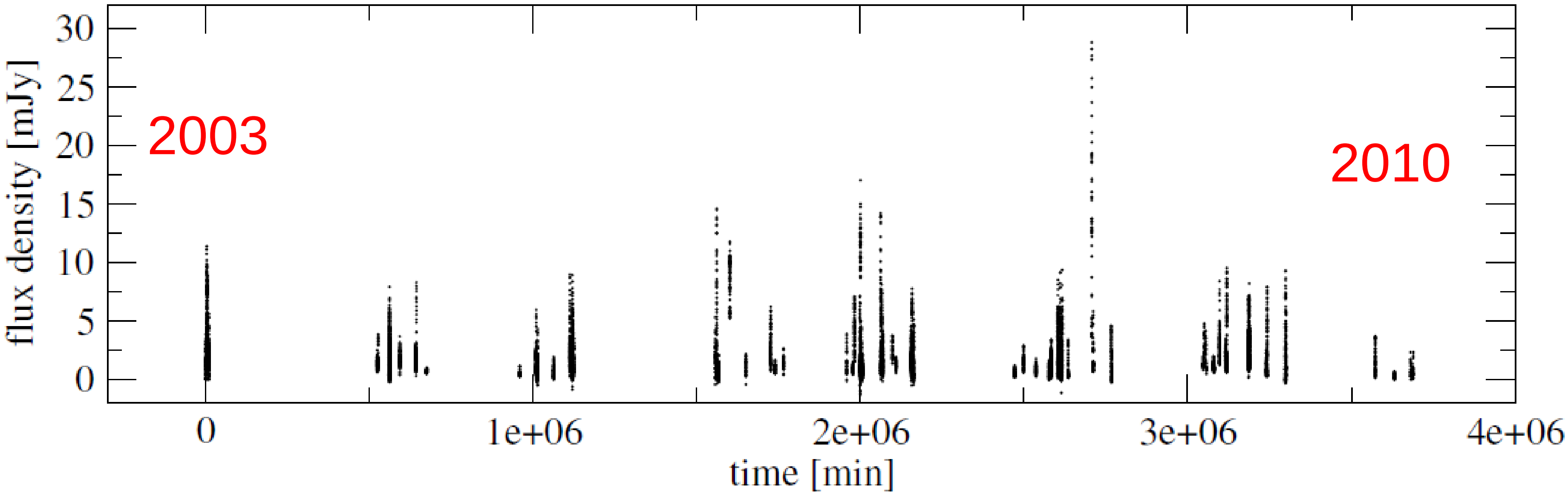

Light curve of Sgr A*. Here no time gaps have been removed, the data is shown in its true time coverage. A comparison of both plots shows: only about 0:4% of the 7 years have been covered by observations.

Witzel et al. 2012

Modeling light curves

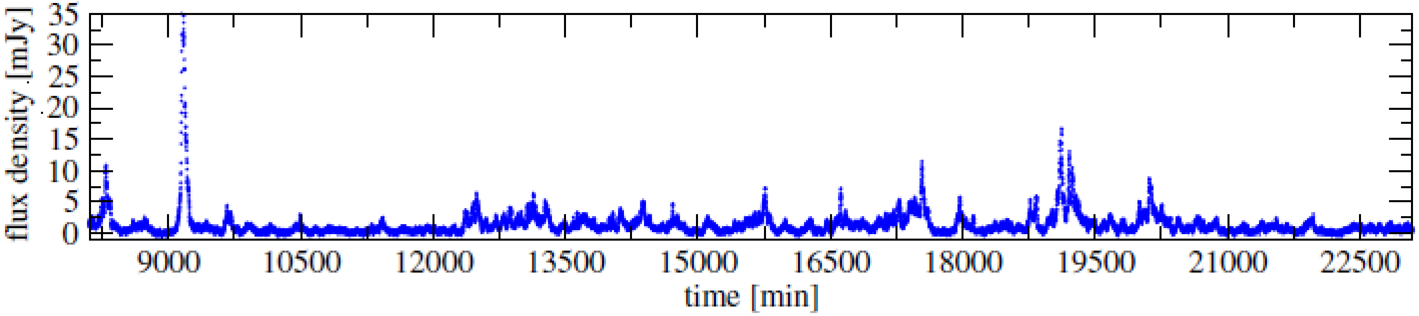

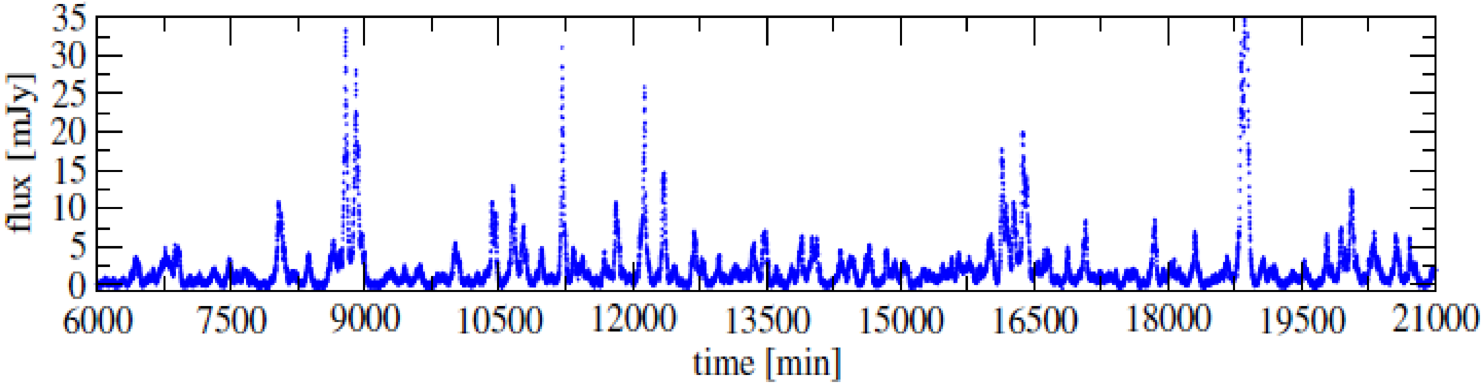

Using a Gaussion random process (Timmer & König 1995) Witzel et al. (2012) found a transformation that allows us to reproduce the observed light curves that show only positive flux density deviations and are asymmetric with respect to their mean value.

a) Shows a curve reproduced from the best double and b) the best single broken PSD.

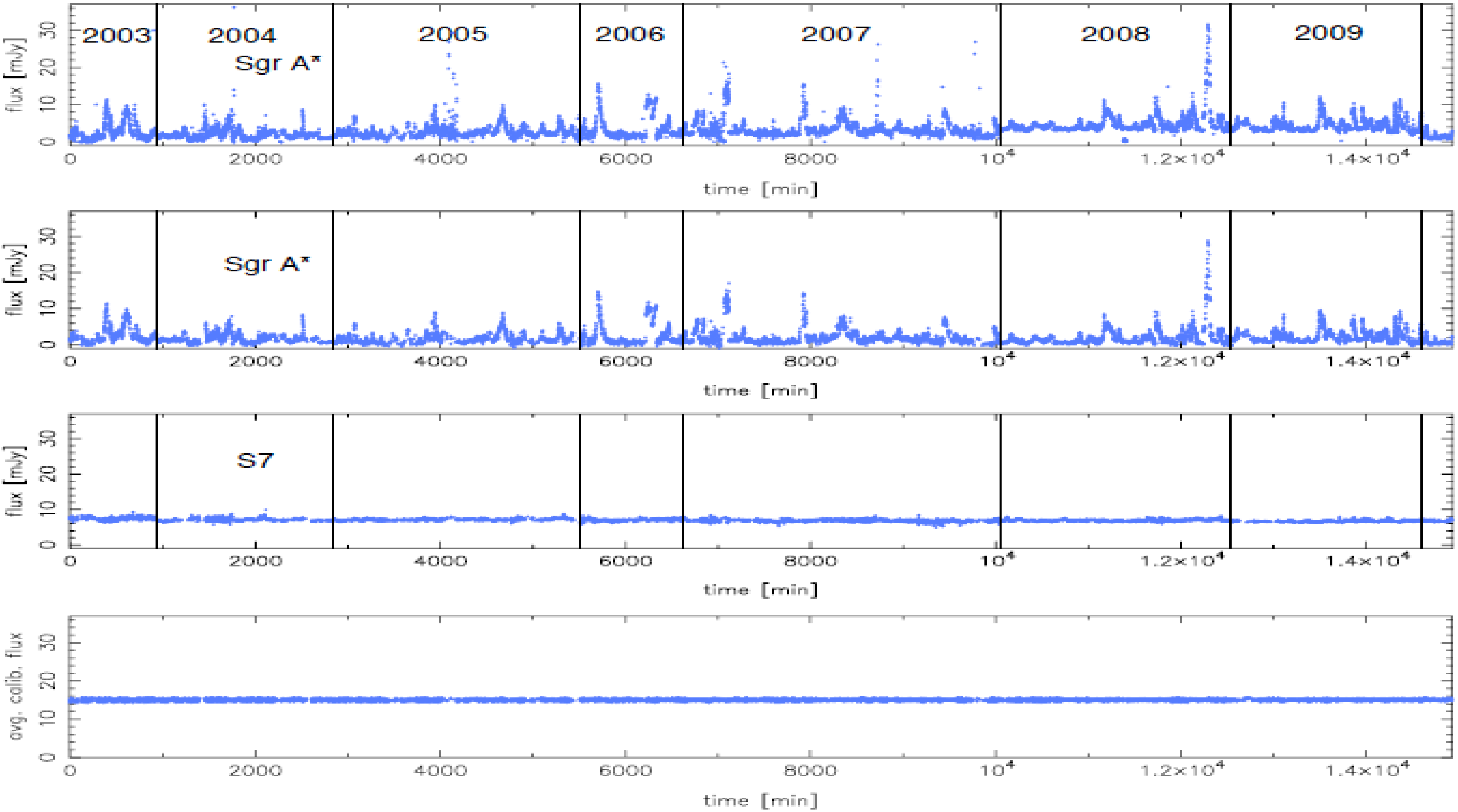

The concatenated light curve of Sgr A* and S7, time gaps longer than 30 minutes removed. - **Top:** Result of aperture photometry before quality cut, the **next** panel the same data after quality cut. **Third** panel: Light curve of the nearby calibrator S 7. **Bottom:** Average ratio between the measured flux of each calibrator and its reference value, scaled with a factor of 15.

Witzel et al. 2012

Simulation flux density histograms

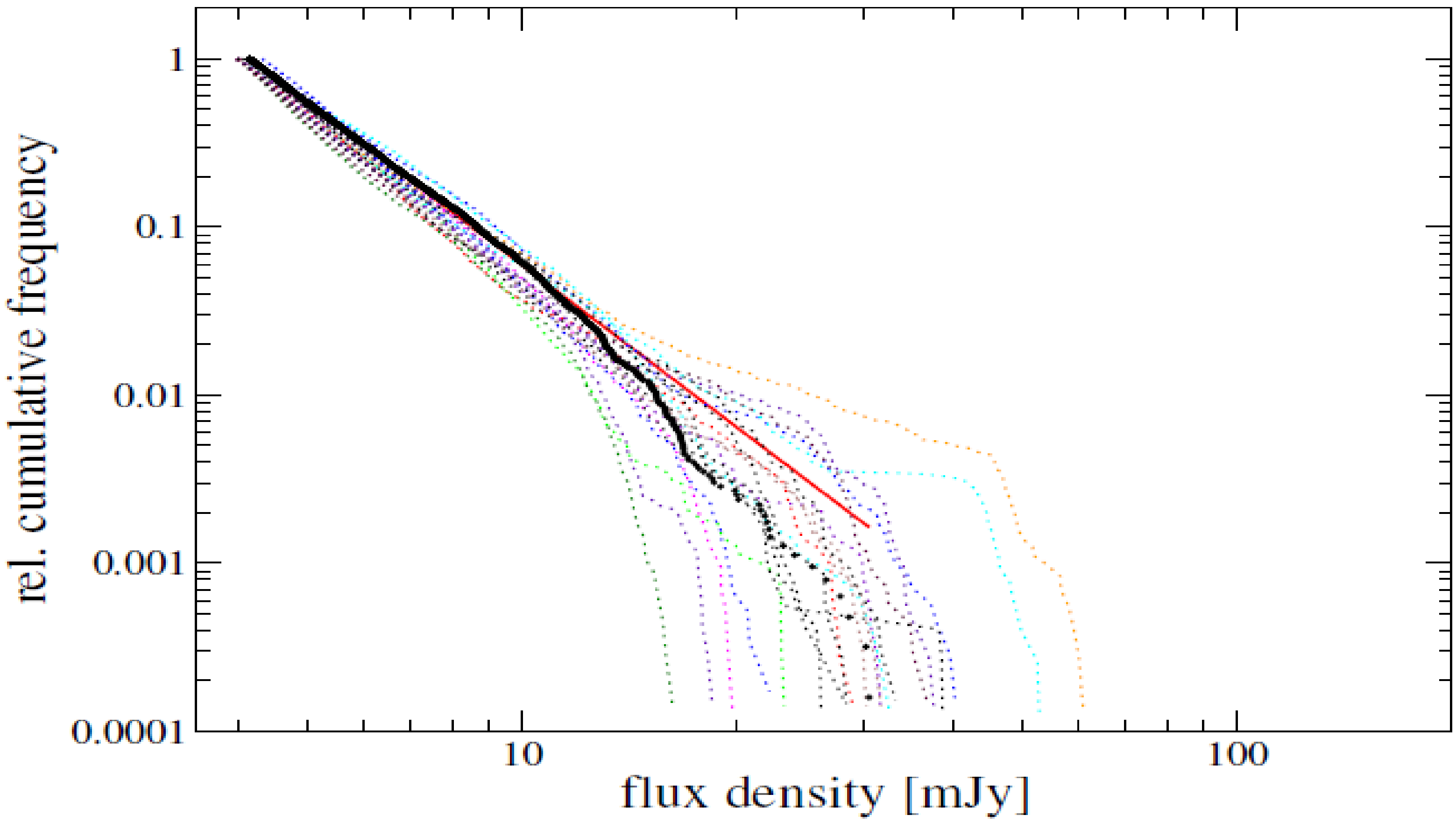

Witzel et al. 2012

The observed histogram (black) of flux densities and 20 randomly selected sets of time correlated power-law surrogate data (colored dashed lines). The best diagram is shown as a continuous red line.

Flux density histogram for SgrA*

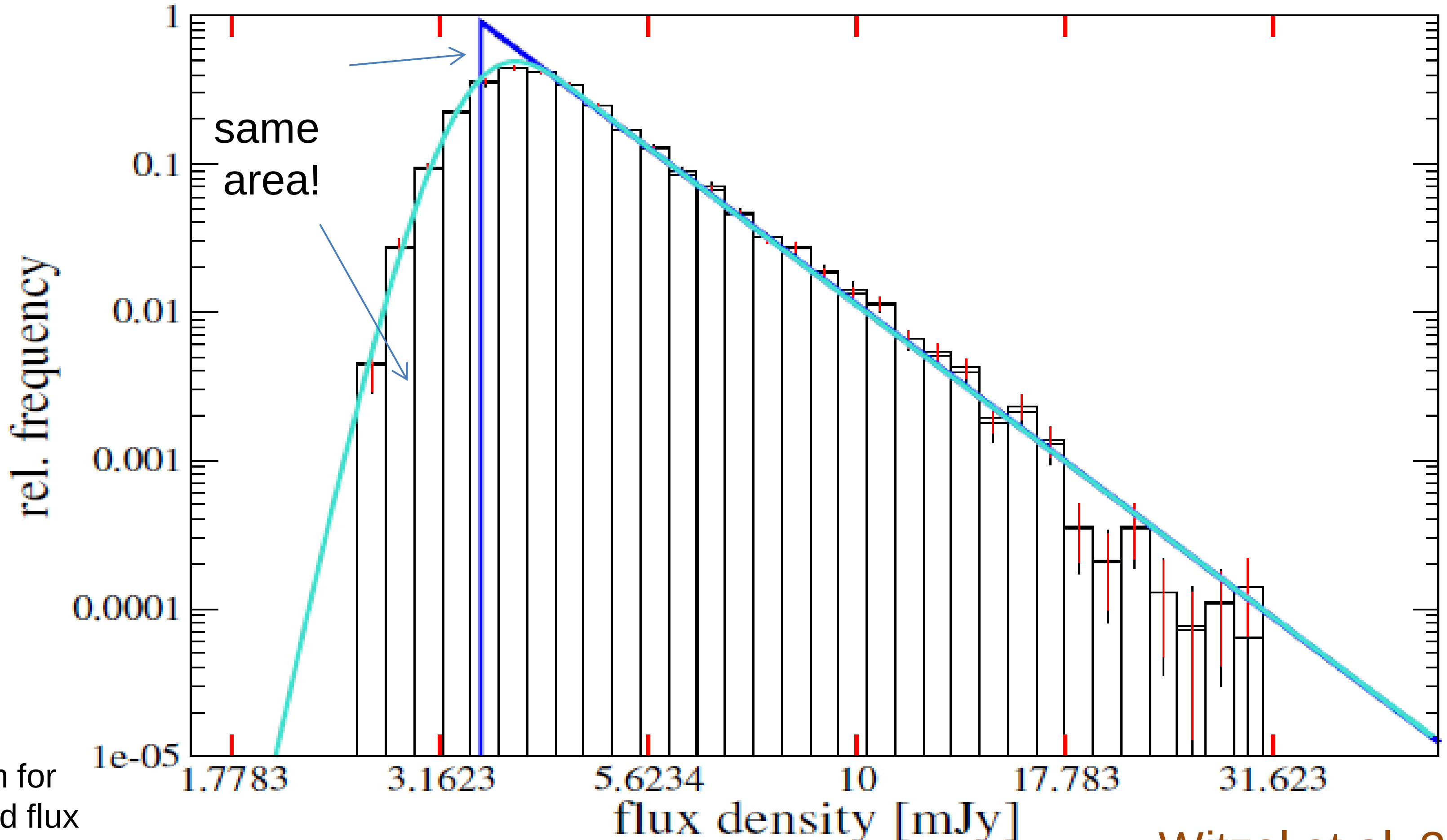

Diagram for polarized flux in work

Witzel et al. 2012

The brown line shows the extrapolation of the best power-law fit, the cyan line the power-law convolved with a Gaussian distribution with 0.32 mJy width.

The statistics allows to explain the event 400 years ago that results in the observed X-ray light echo

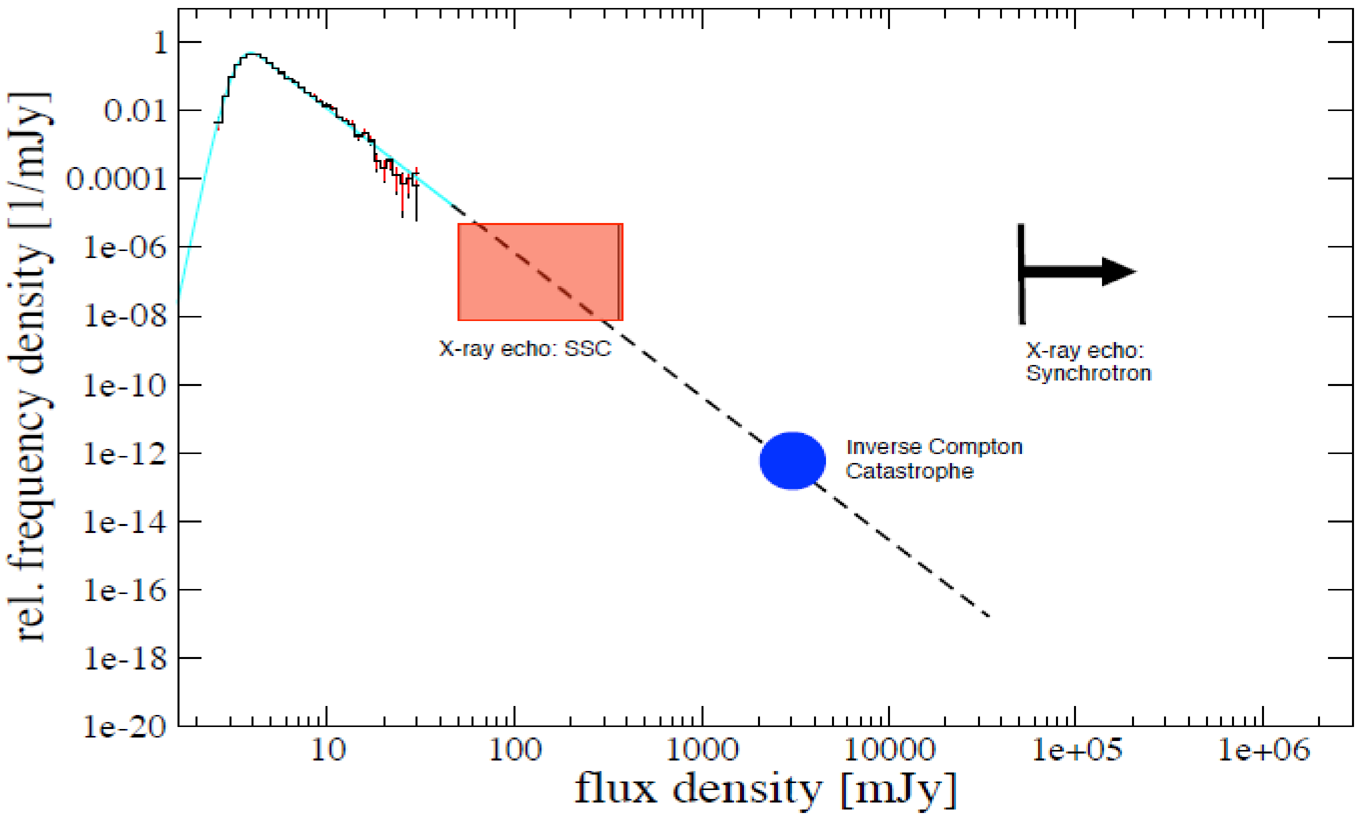

Fluorescent back-scatter from molecular clouds surrounding the GC:

Revnivtsev et al. 2004, Sunyaev & Churazov 1998, Terrier et al. 2010

and

Witzel et al. 2012

Illustration of a flux density histogram extrapolated from the statistics of the observed variability. The expected maximum flux density given by the inverse Compton catastrophe and a estimation of its uncertainty is shown as the magenta circle, the SSC infrared flux density for a bright X-ray outburst as expected from the observed X-ray echo is depicted as the red rectangular.

Structure function of the SgrA*

Total intensity only;
Physical modeling of
polarization data
possible and necessary.

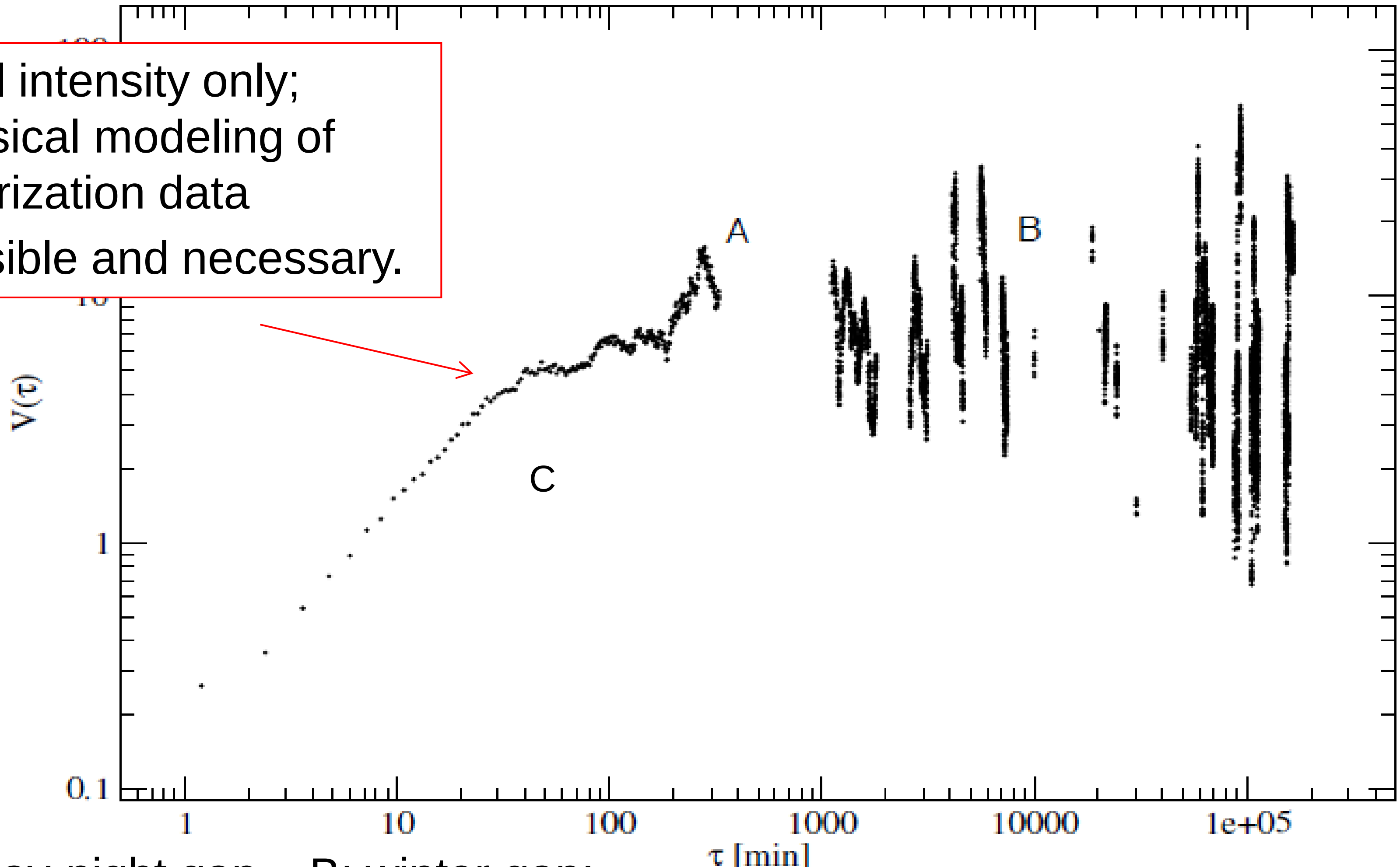

A: day-night gap,   B: winter gap;
C: still influenced by window function;
time binning 1.2 min.

Witzel et al. 2012

QPOs in SgrA* Flare Emission

A total of about 10 flares shows significant sub-structure:

sub-flares

e.g. Meyer et al. 2005

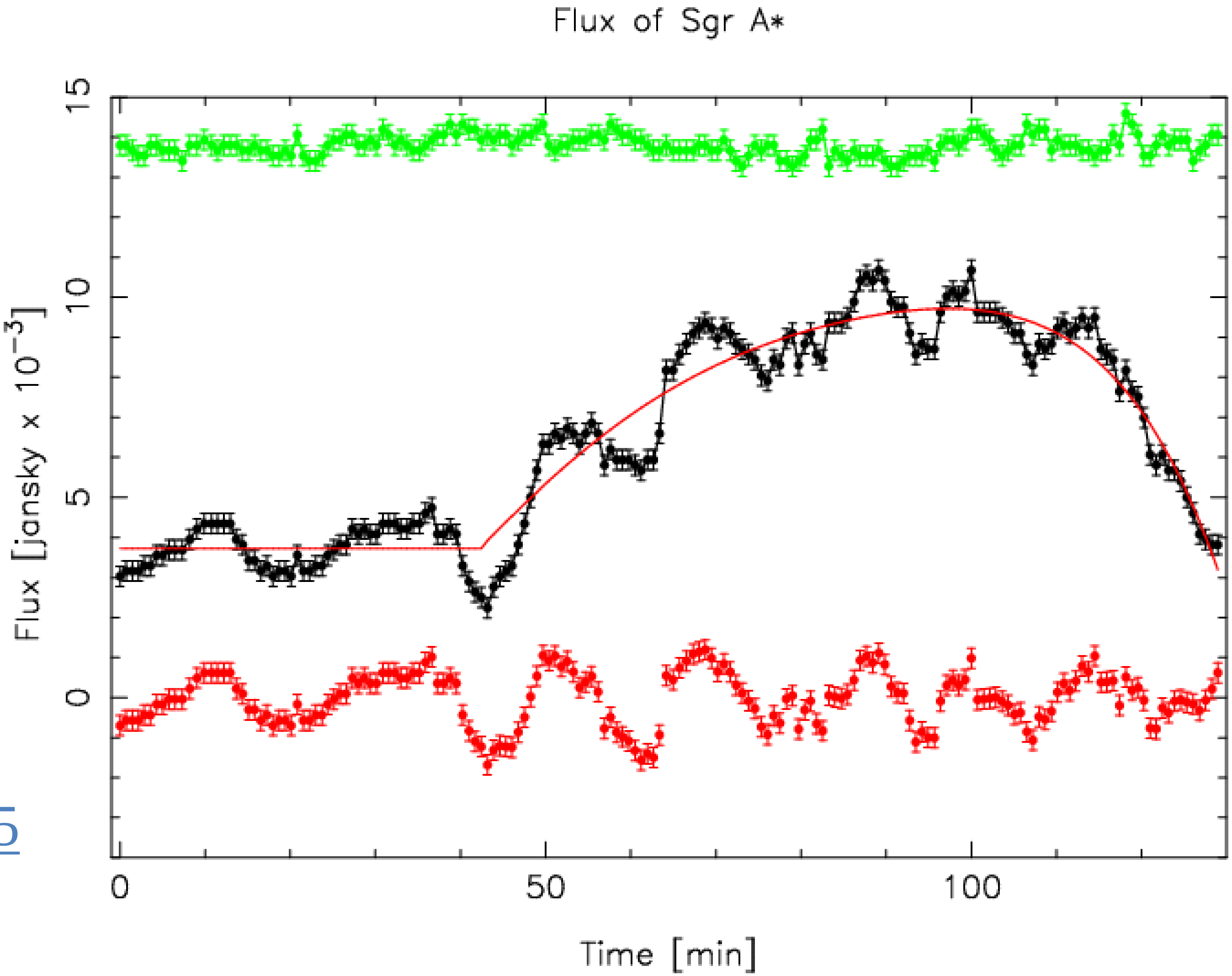

SgrA* VLT/APEX flare on 3 June 2008: NIR data-model: sub-flare structure

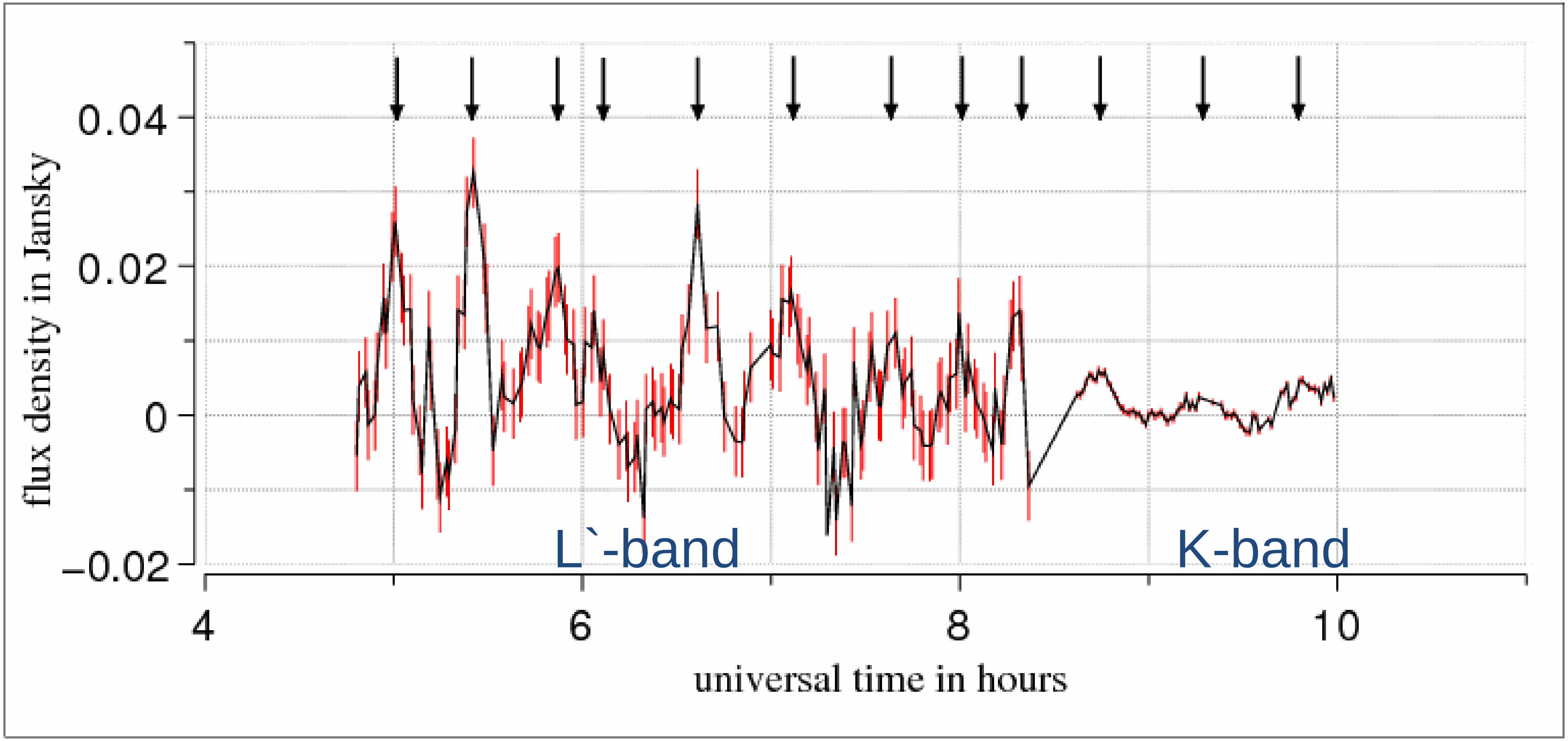

mean time difference between sub-flares: 25+-5 minutes

A ~1 h X-ray periodicity in an active galaxy RE J1034+396

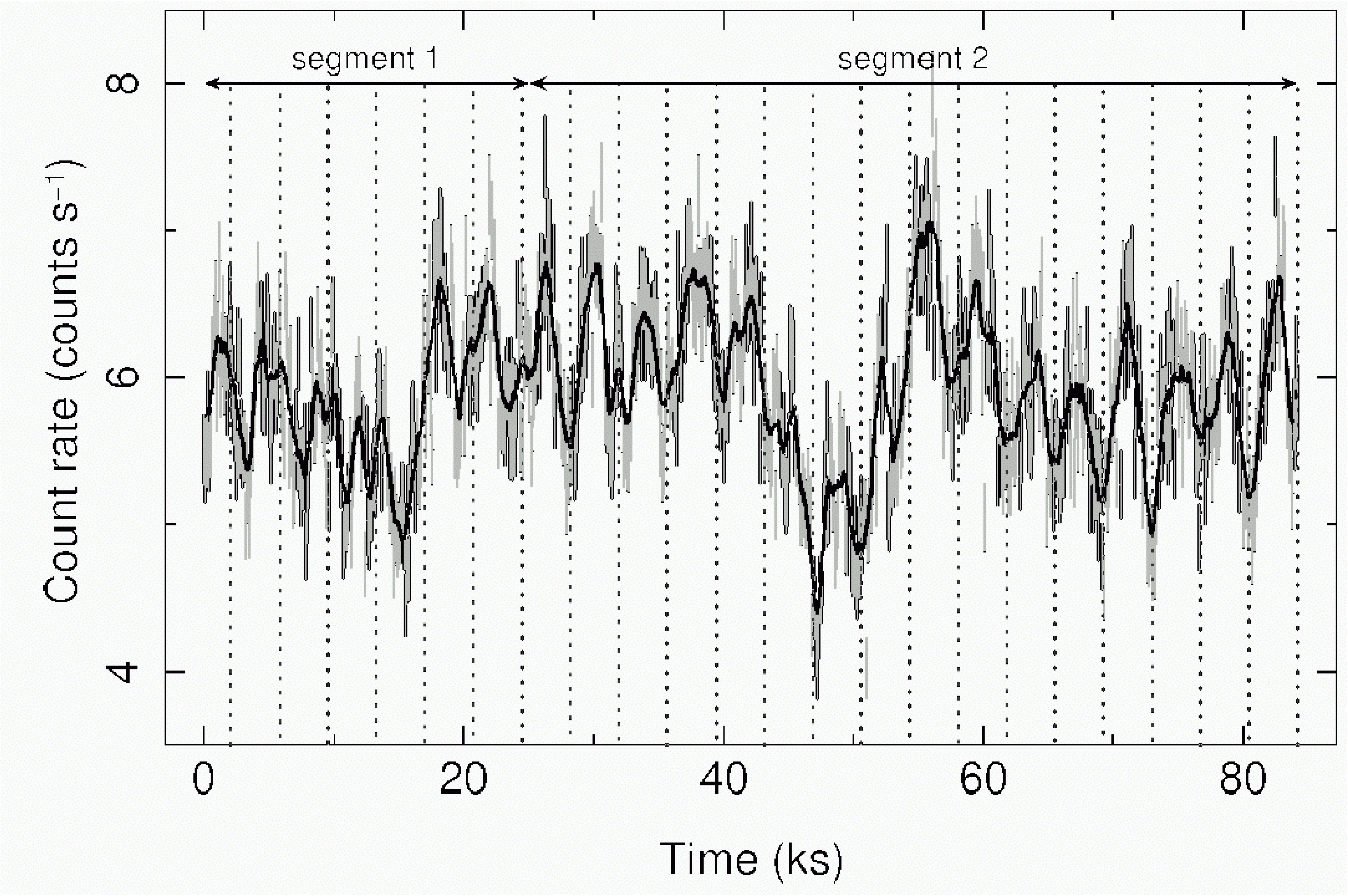

Gierlinski et al. 2008

Polarization Signatures

Modeling of individual events
Relativistic Disk calculations

NIR Polarized Flux Density from SgrA*

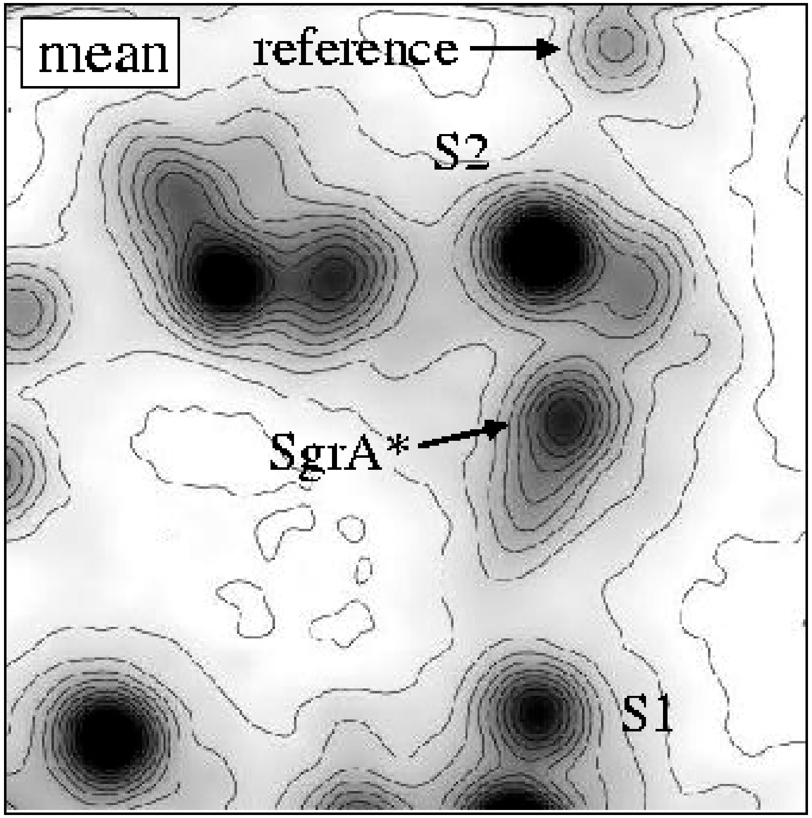

mean flux at 0 and 90 degree

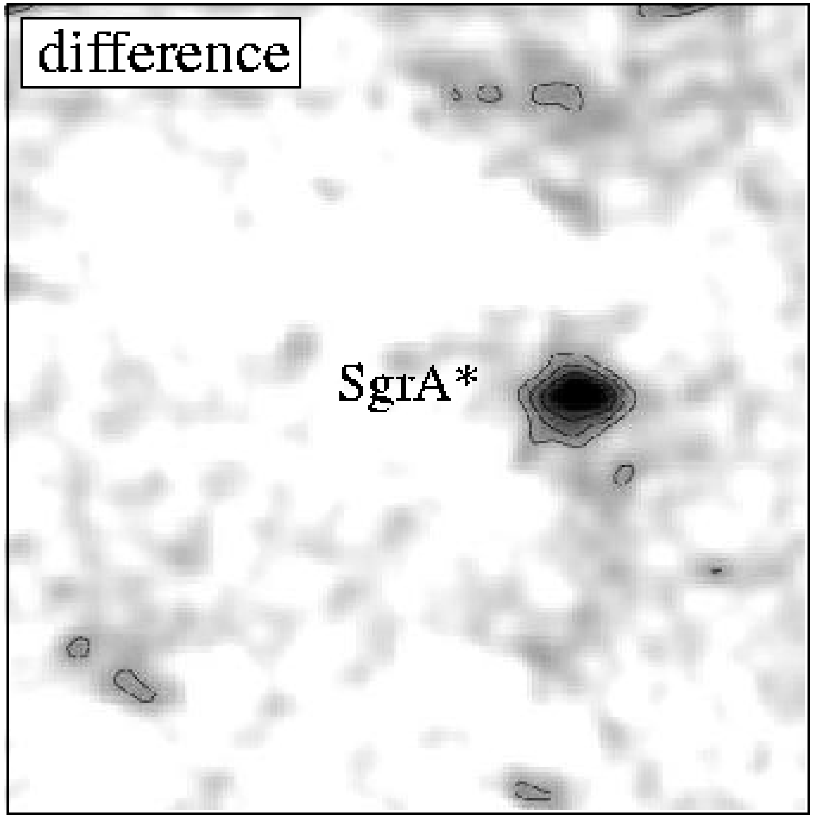

differential flux between 90 and 0 degree

July 2005: VLT NACO Wollaston prism plus $\lambda/2$ retarder wave-plate

Eckart, Schödel, et al. 2006, 455

NIR Polarized Flux Density from SgrA*

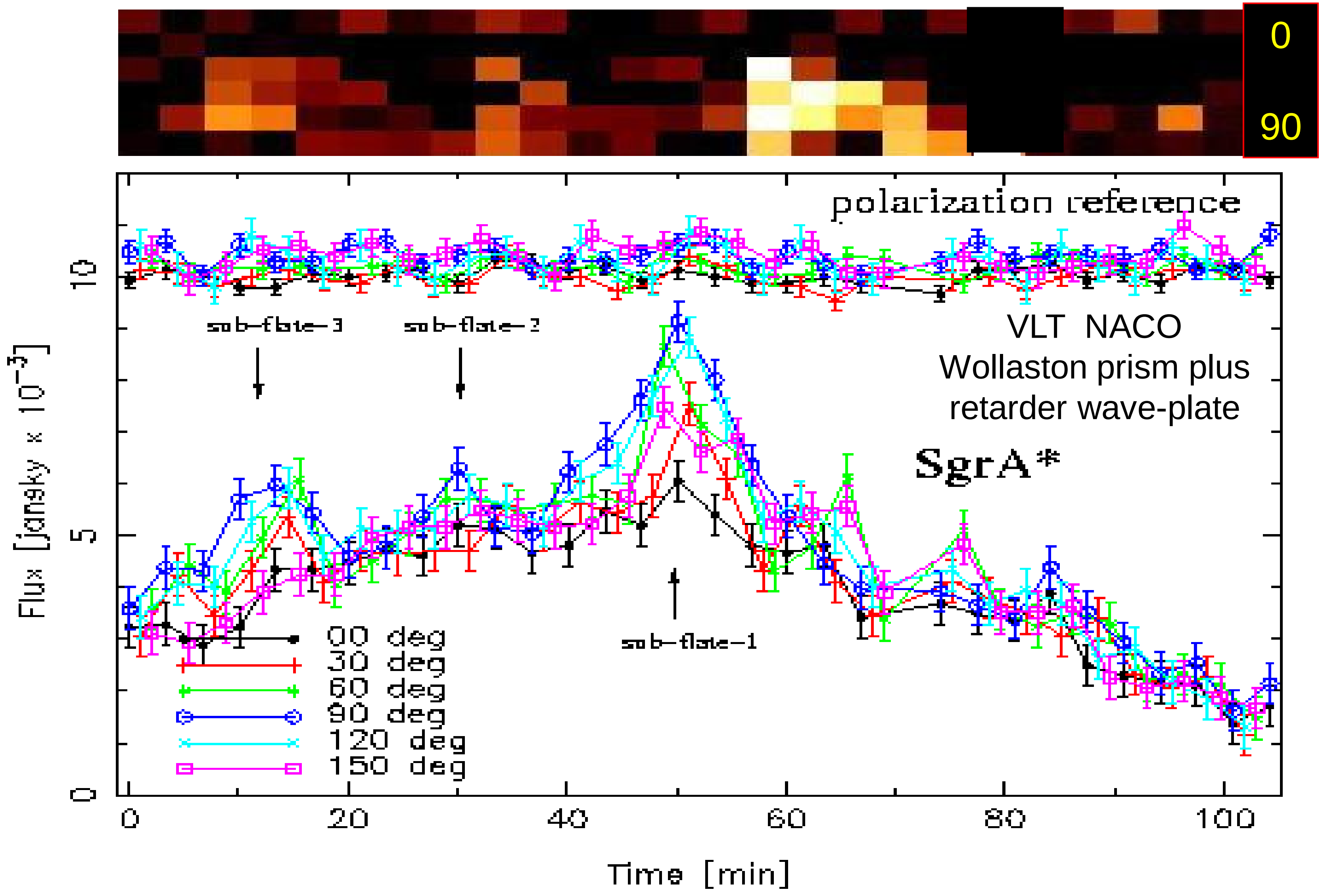

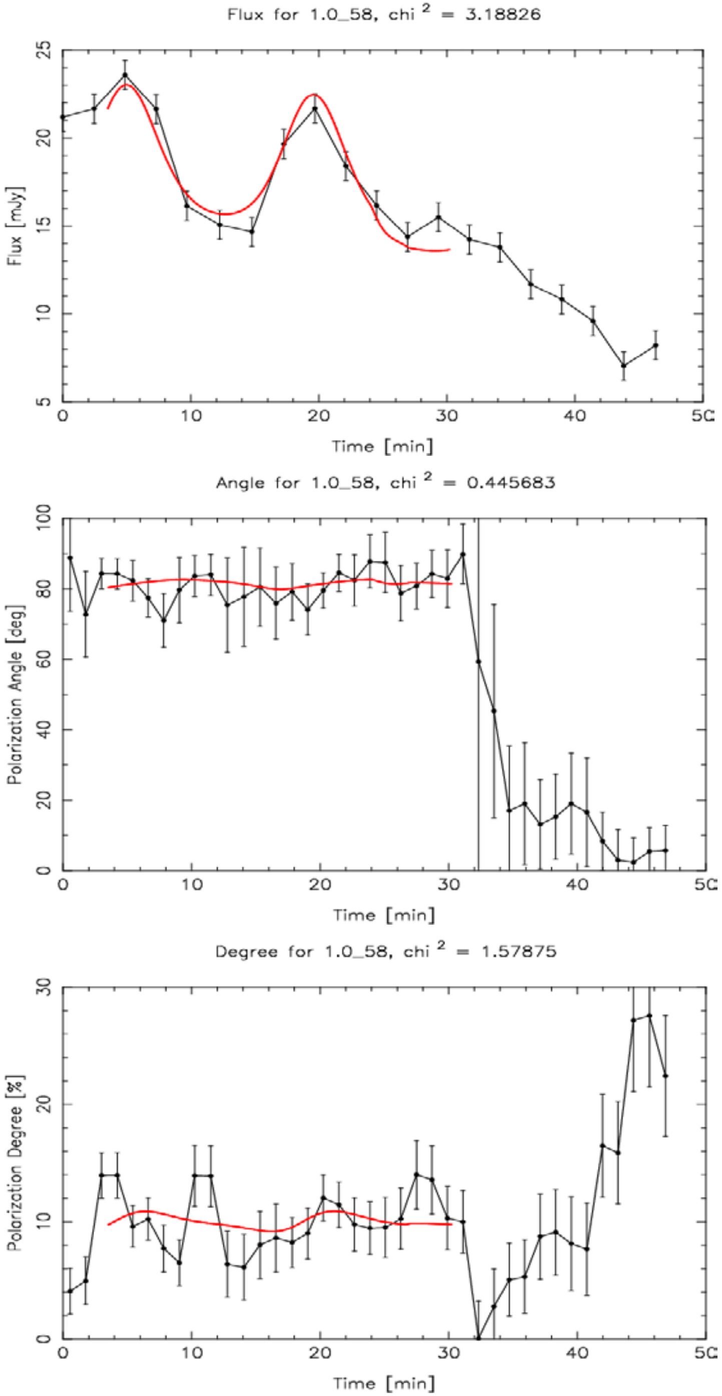

Hot Spot Model

E-vector perp. to disk

i=58, a/M~1.0, ϕ= 80
Spot close to 4.0 Rg

Precision of NIR Polarization measurements

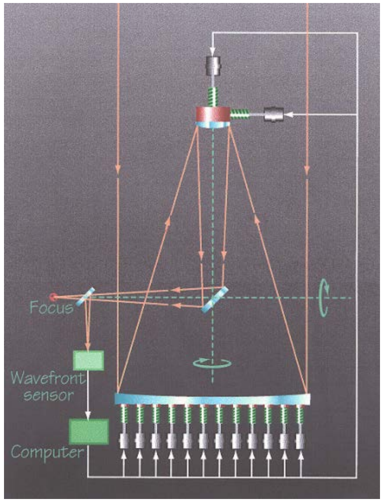

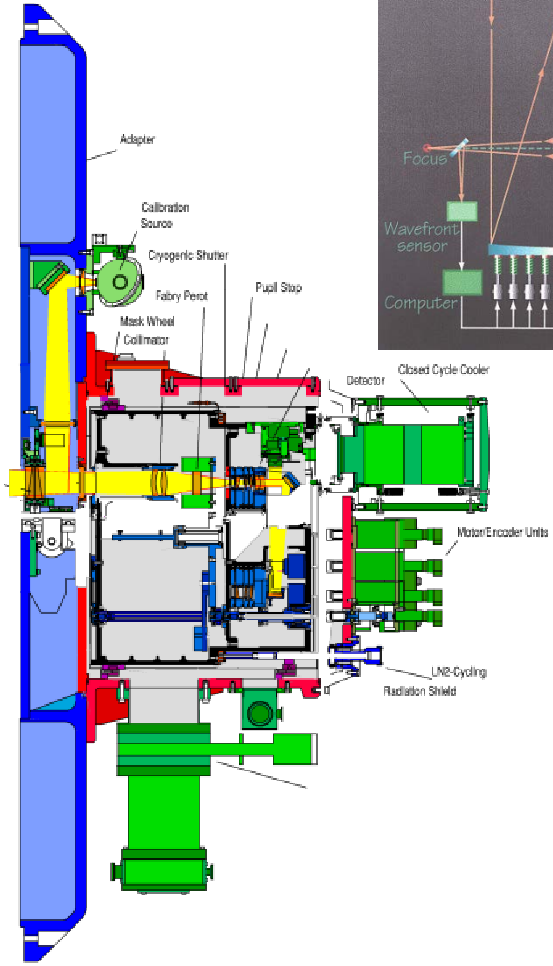

Instrument calibrated to ~1%
Current limit due to systematics ~3-4%

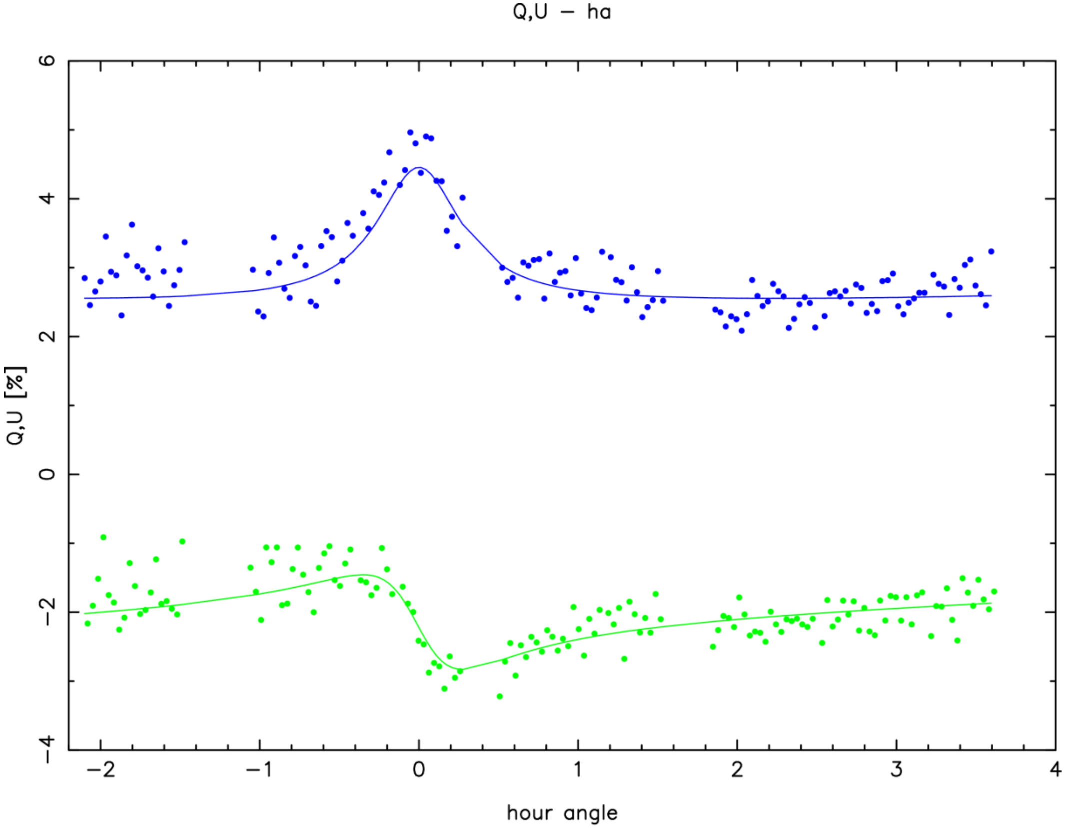

Witzel, G., et al. 2010 sumitted.

Geometry of Model

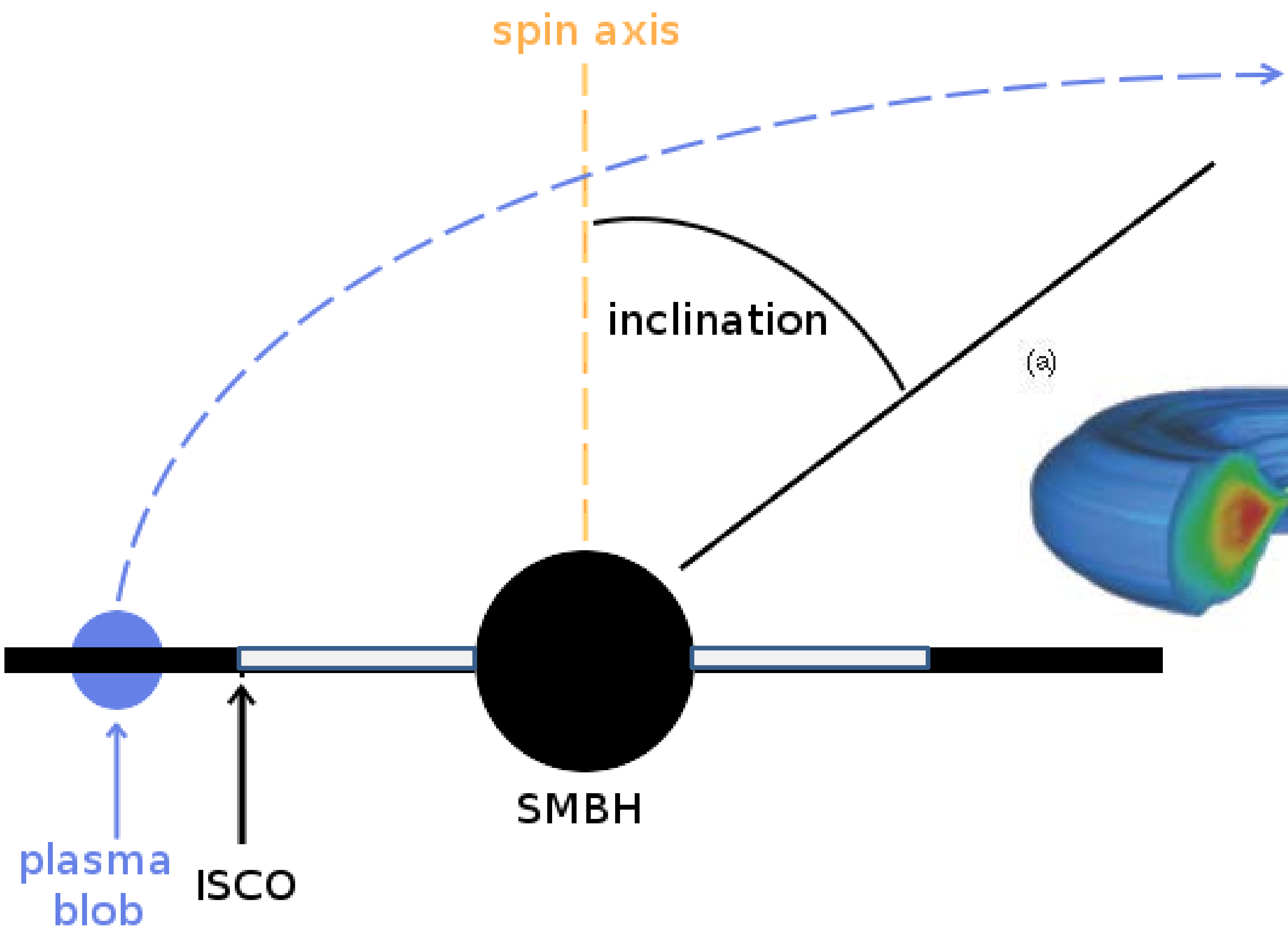

llnl.gov

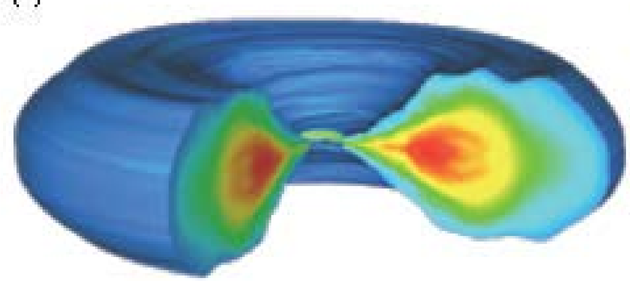

Karssen 2012

The NIR Flares show sub-structure: Sub-flares

- •typical flare length: 100 min FWZI
- •intra-flare variability with 3-5 maxima
- •interpreted as quasi-periodicity due orbital motion of a synchrotron emitting spot in orbit around SgrA*
- •in case of a multi-spot scenario the spot lifetime can be of the order or the orbital period or even less (Schnittman et al. 2005, 2006, Eckart et al. 2008)

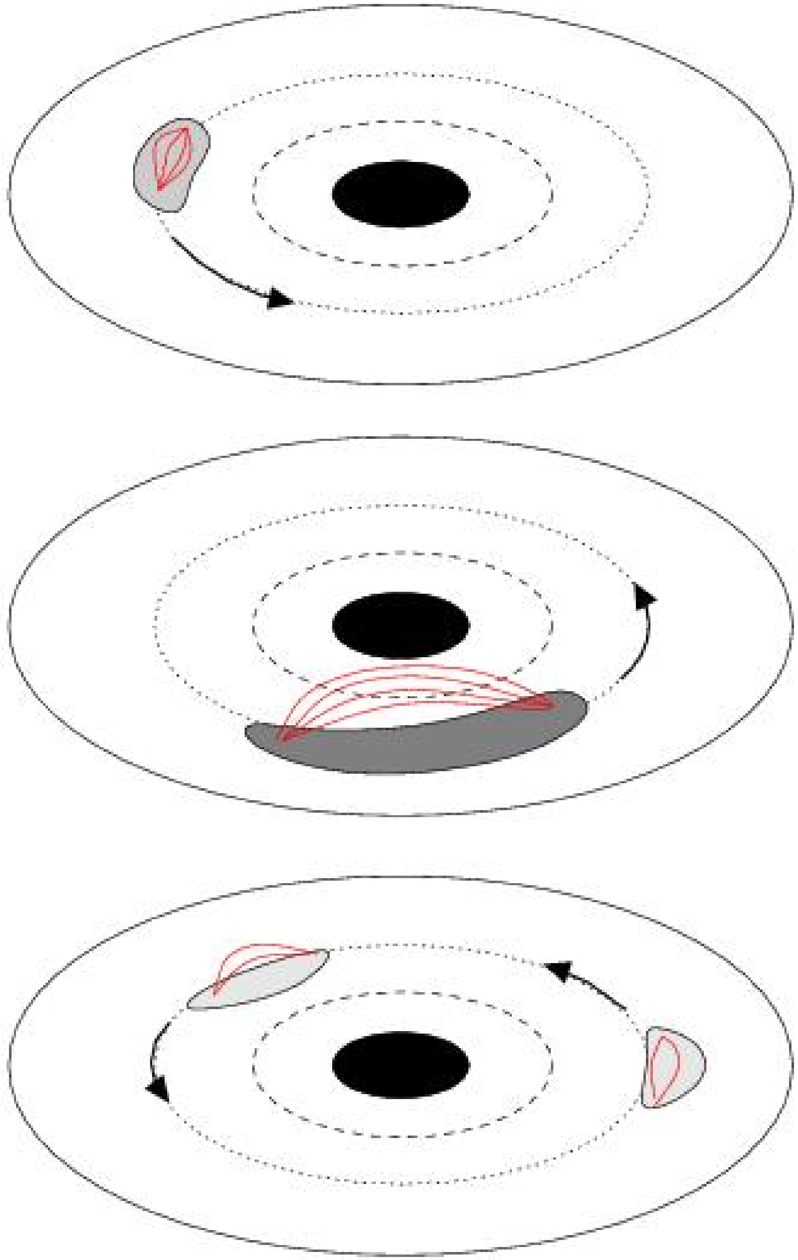

Yuan et al. 2009, Balbus & Hawley 1998, Balbus 2003

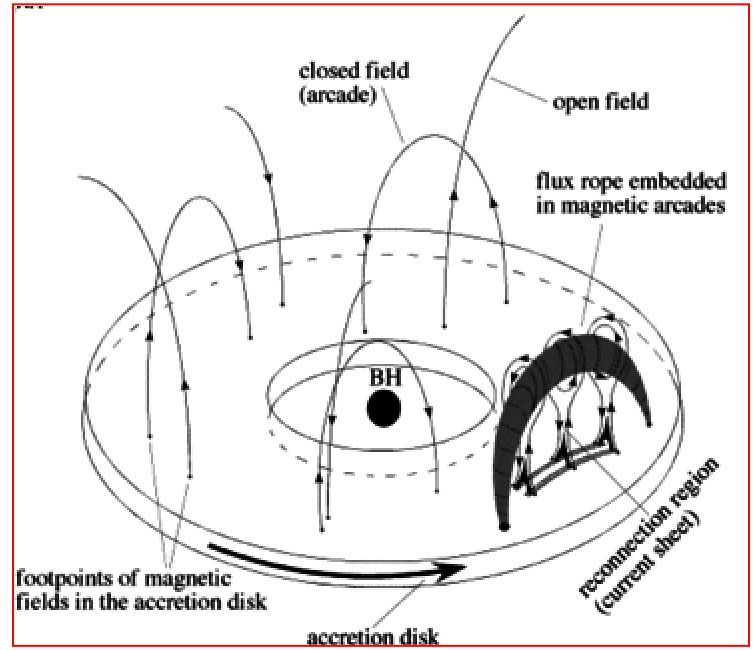

Yuan et al. 2009

Adiabatic Expansion of Source Components in the Temporary Accretion Disk of SgrA*

Black Hole
Last stable orbit
reference orbit
magnetic field lines
outer edge of disk

Eckart et al. 2008, ESO Messenger
Eckart et al. 2009, A&A 500, 935

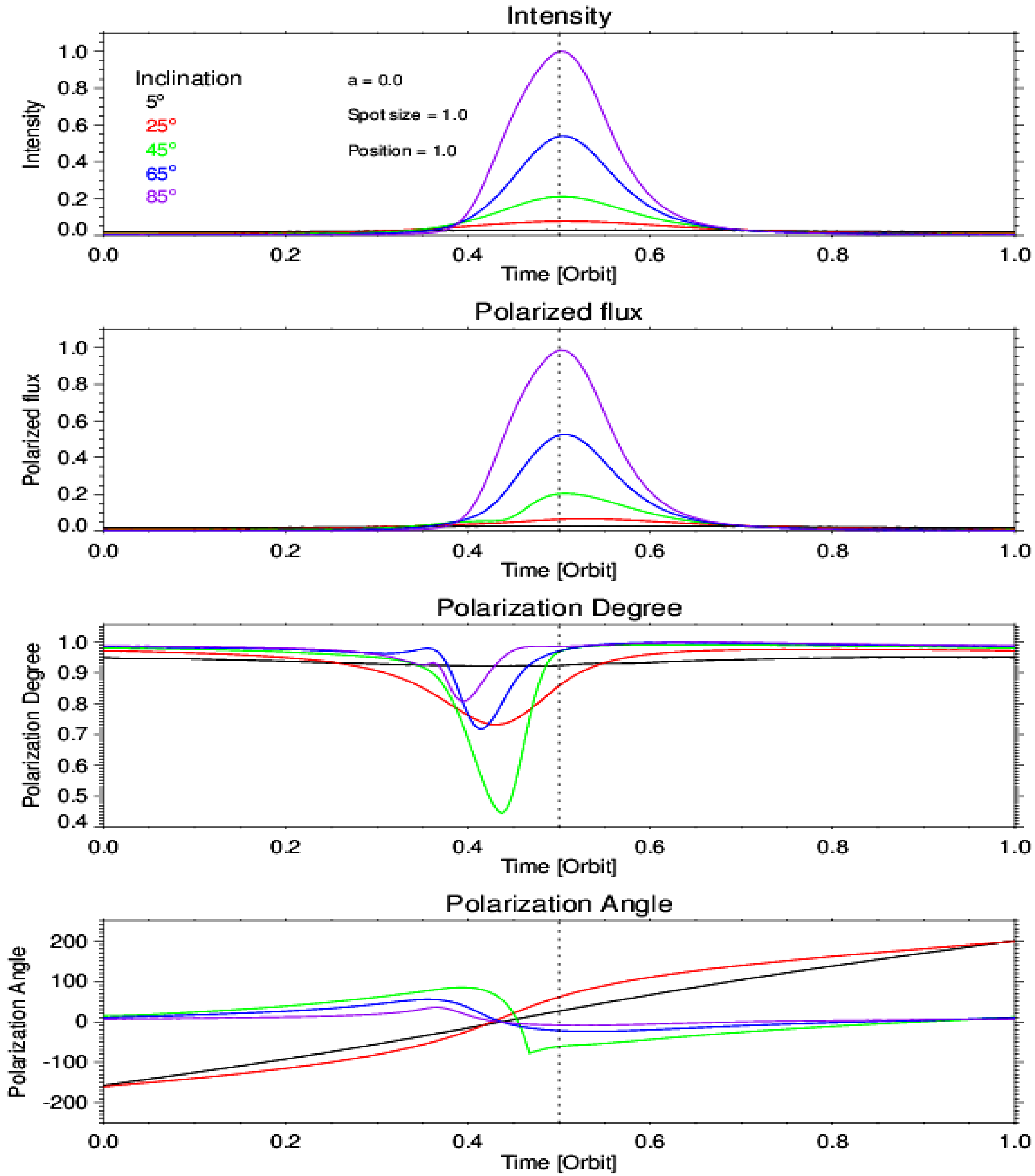

Vertical field case

a0.0-incl45-vert.mp4

Inclination: 45°

Karssen 2012

S. Karssen
M. Valencia-S.
M. Bursa,
M. Dovciak,
V. Karas
A. Eckart

NIR Polarized Flux Density from SgrA*

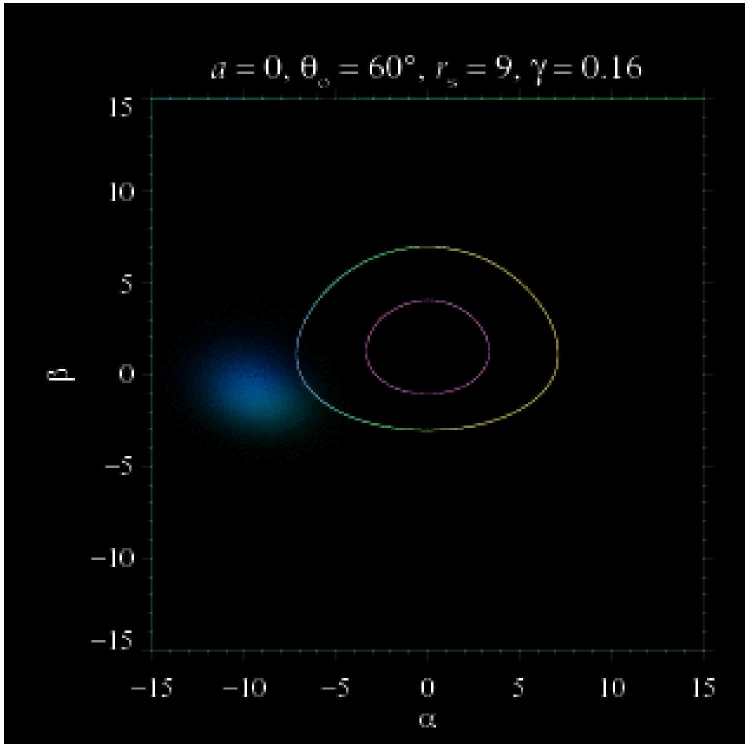

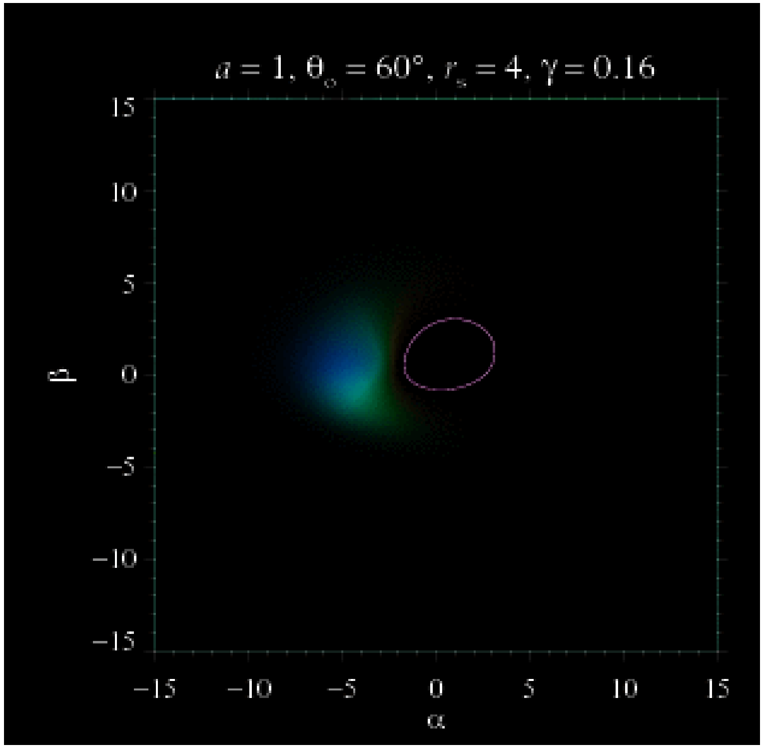

Dovciak, Karas & Yaqoob 2004, ApJS 153, 205
Dovciak et al. 2006

Goldston, Quataert & Igumenshchev 2005, ApJ 621, 785

see also Broderick & Loeb 2005 astro-ph/0509237
Broderick & Loeb 2005 astro-ph/0506433

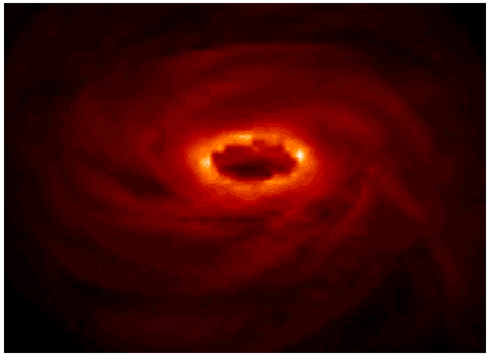

~4min prograde
~30min static
~60min retrograde
for 3.6x10**6Msol

Blandford , 2002 in Lighthouses of the Universe
Hirose, Krolik, De Villiers, Hawley 2004, ApJ 606, 1083

What Magnetic Fields Can Do

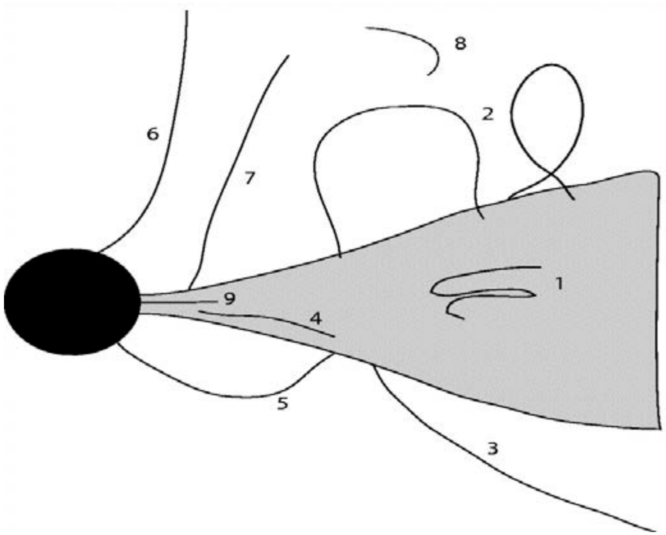

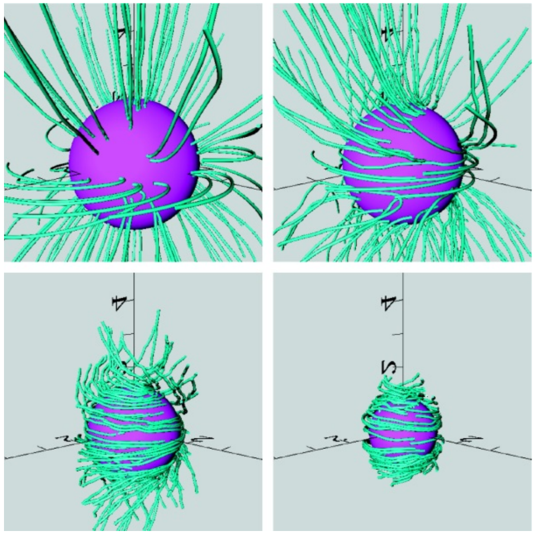

Case I: E-vector perp. to disk; sun spot like

Case II: toroidal B-field

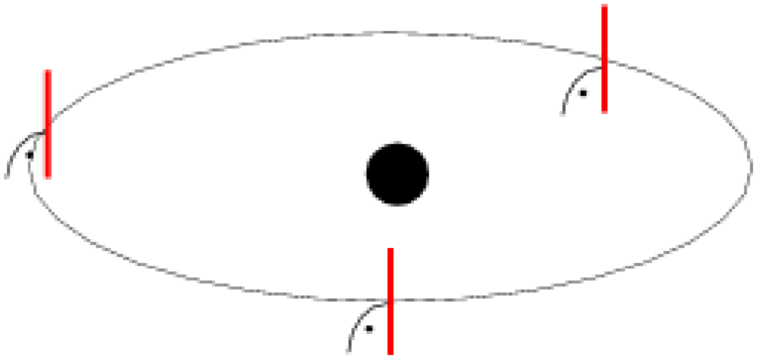

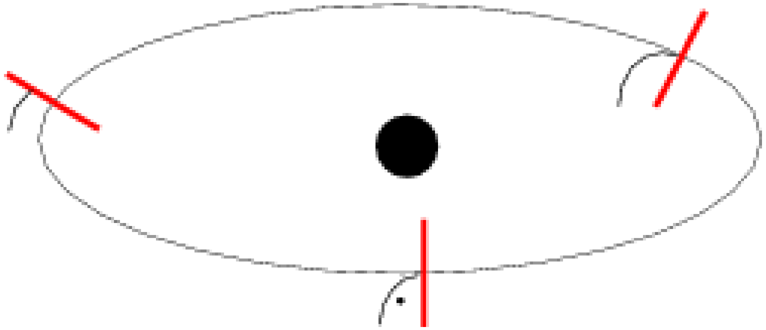

Dovciak, Karas & Yaqoob 2004, ApJS 153, 205

The 15 May 2007 NIR Flare

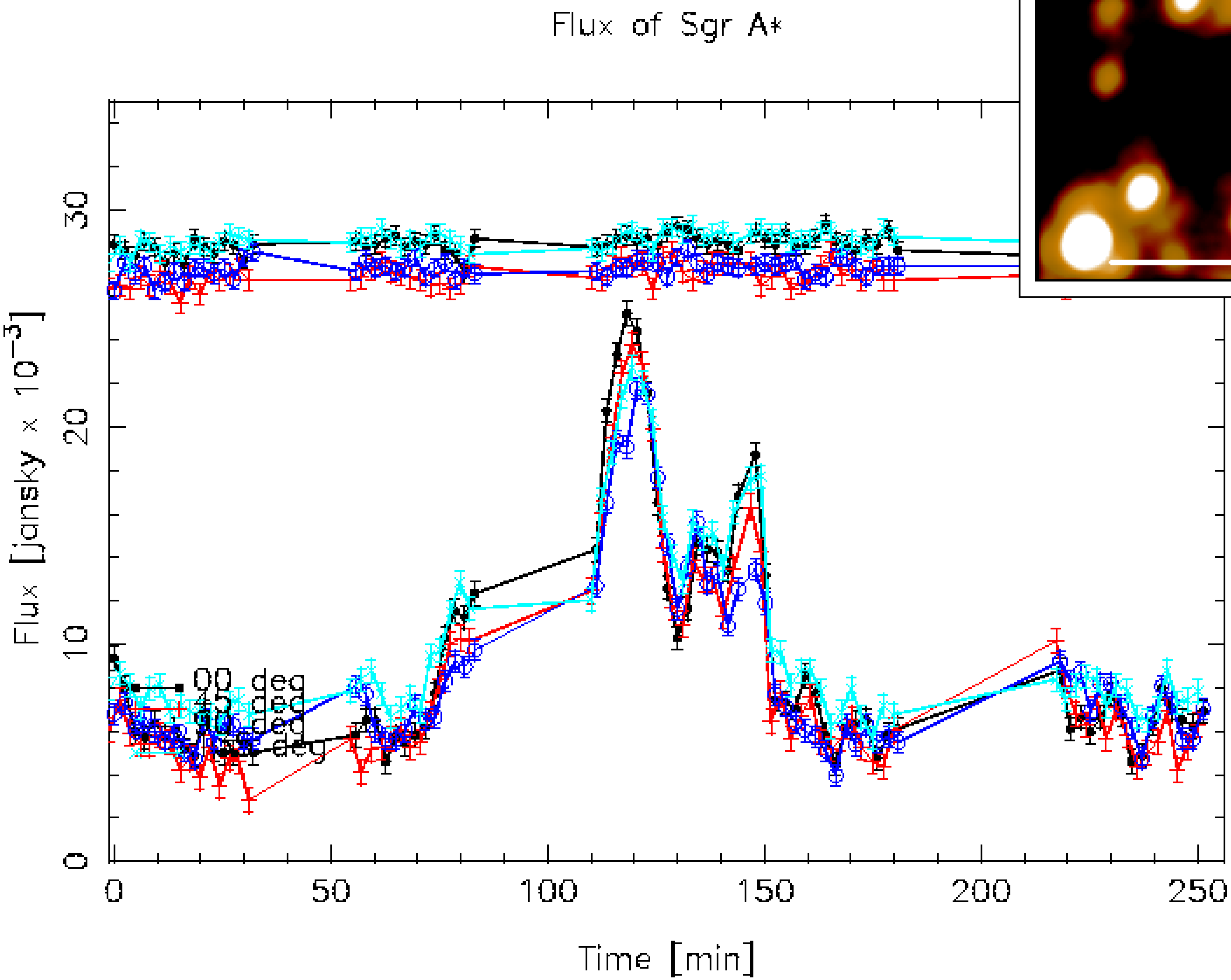

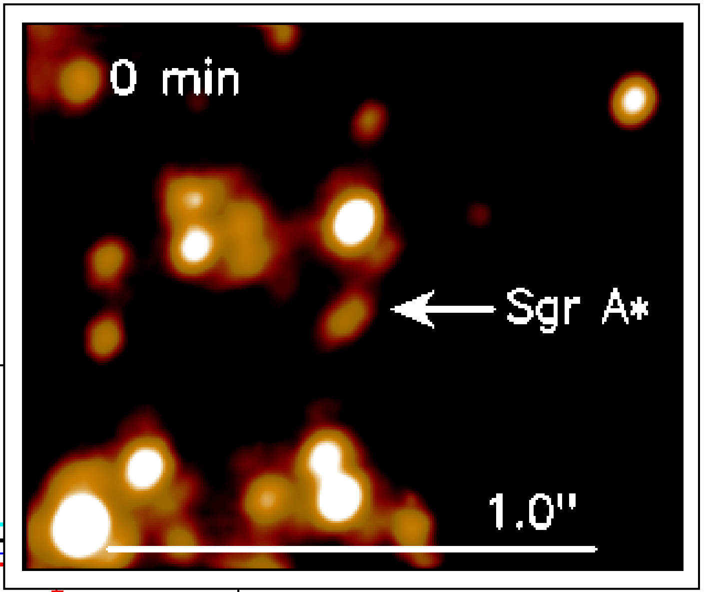

SgrA*: Observational evidence for disk phenomena

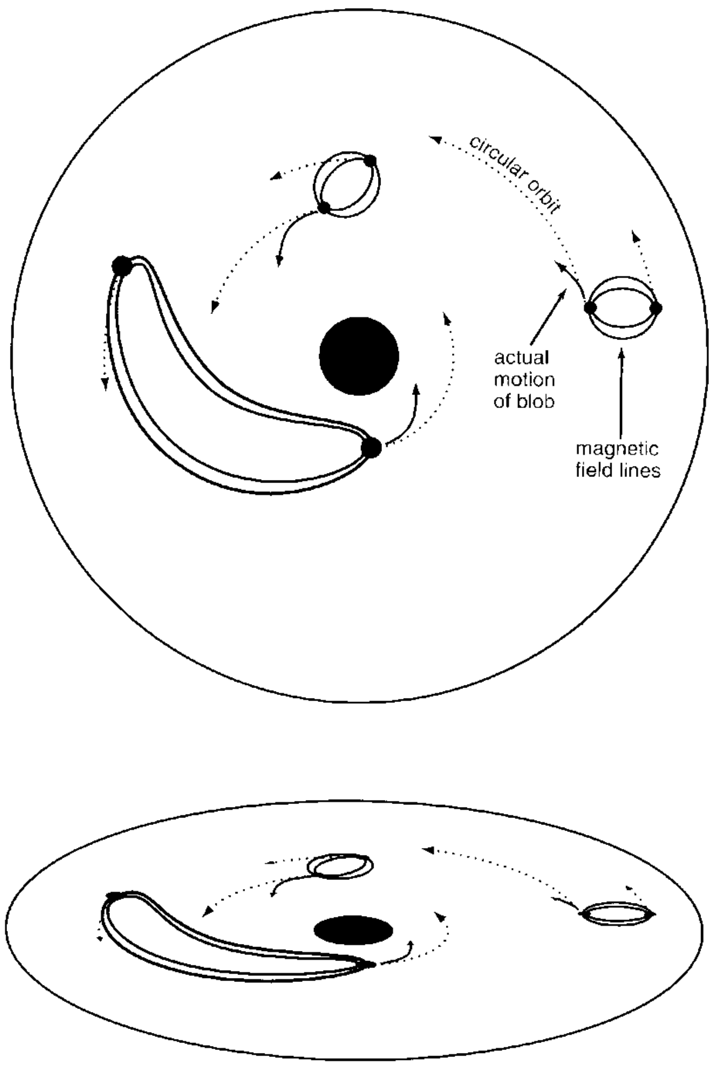

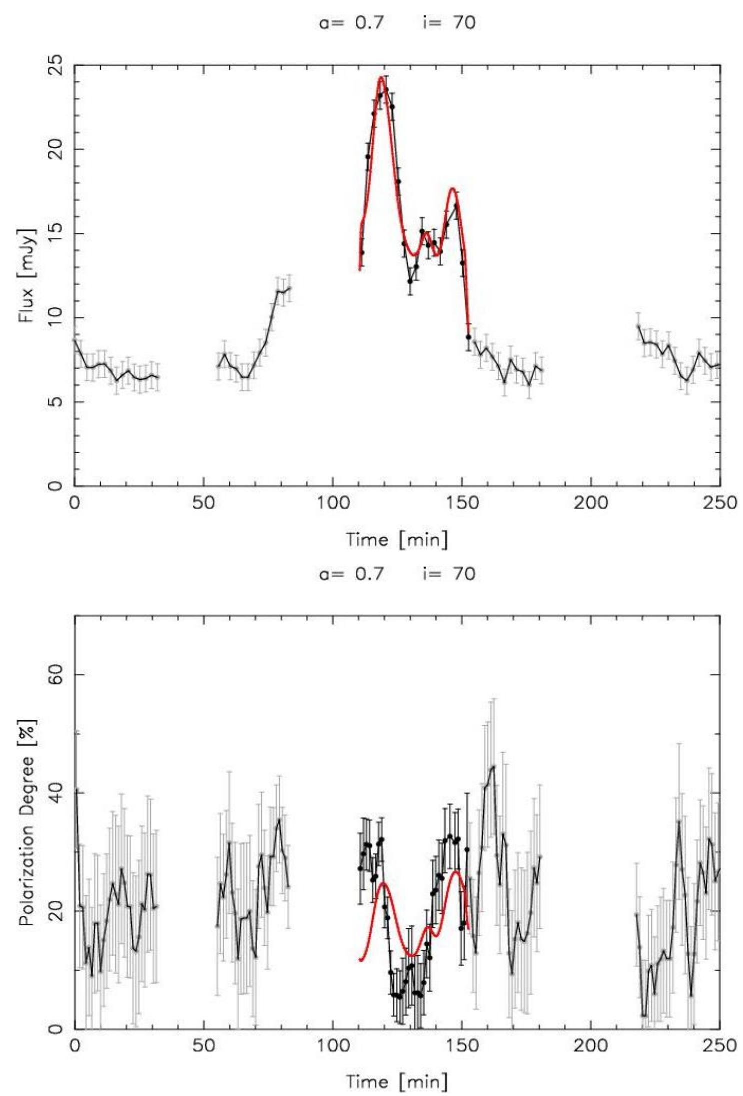

Pattern recognition against polarized red noise

30 July 2005

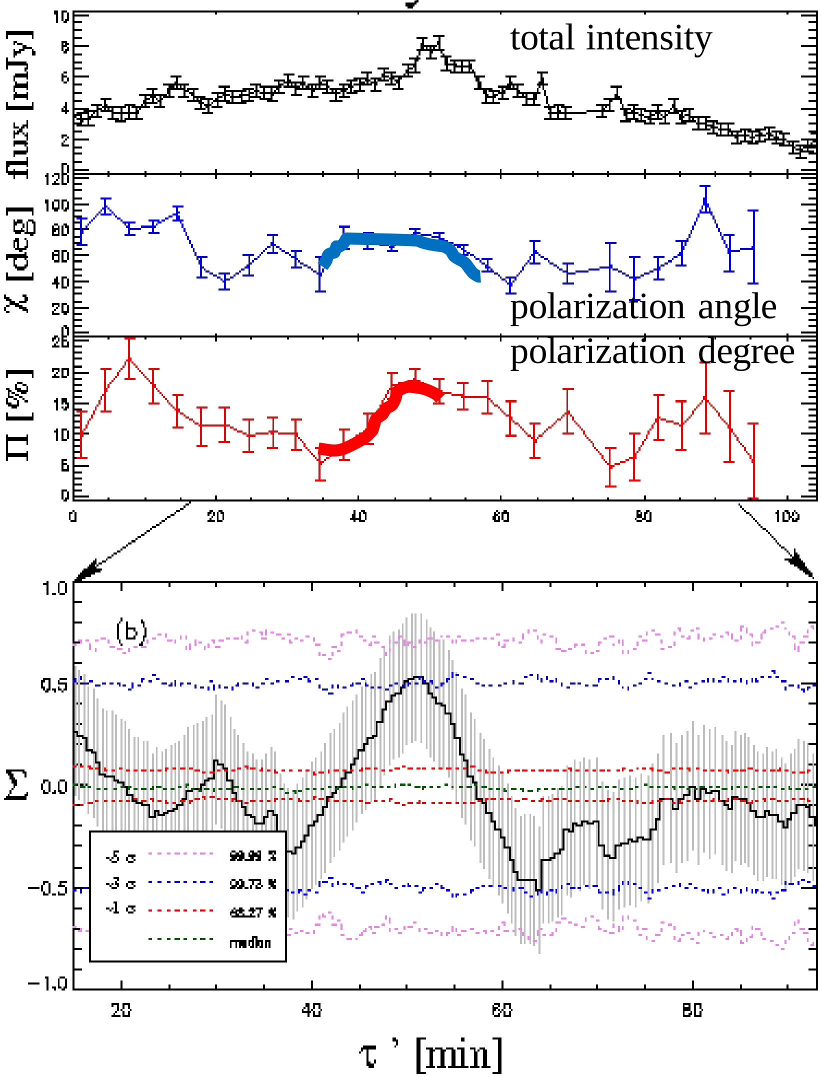

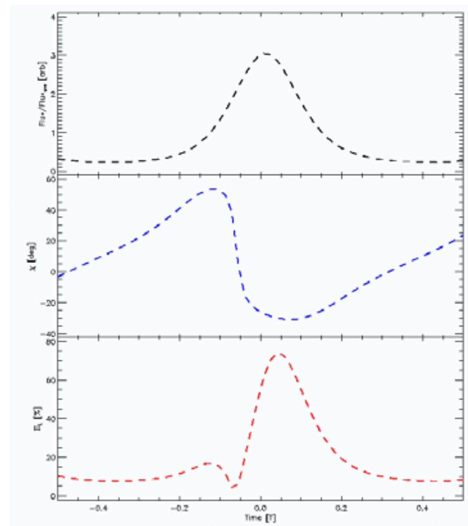

Indication of relativistically orbiting matter!

5σ

3σ

1σ

mean

randomly polarized red noise

Zamaninasab et al. 2009

Pattern of a spot orbiting at the ISCO

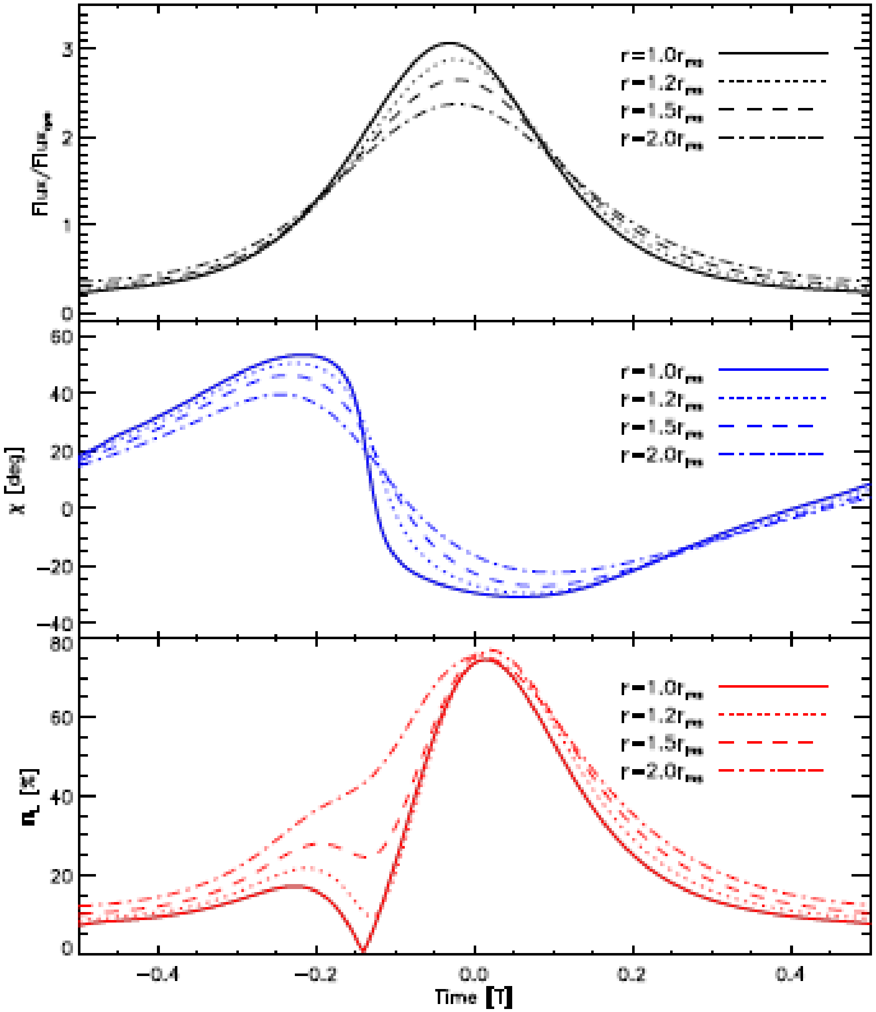

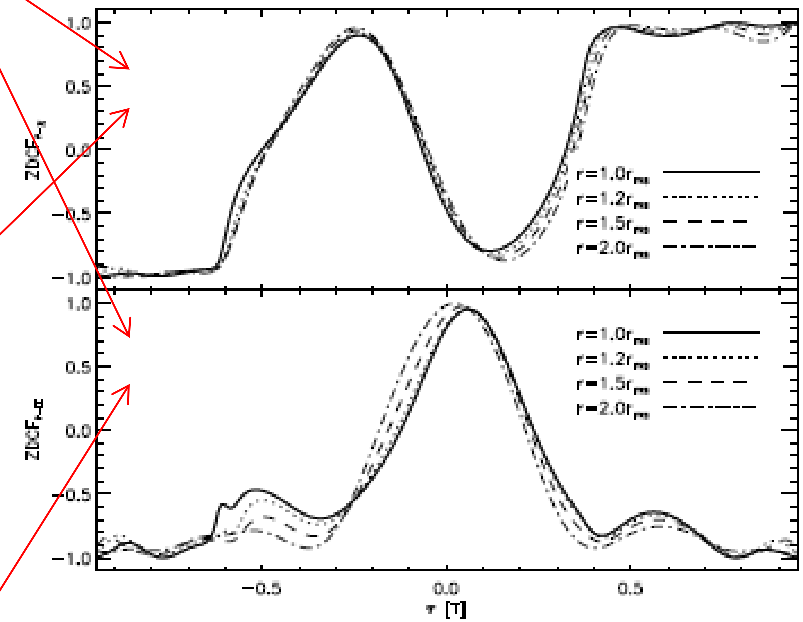

Cross-correlations

Indication of relativistically orbiting matter!

Zamaninasab et al. 2009

Spot evolution in a differentially rotating disk

face on view
i=0; a=0.5

at times after
1/4T, 3/4T,
5/4T and 7/4T
(left to right).

different degrees of spot shearing

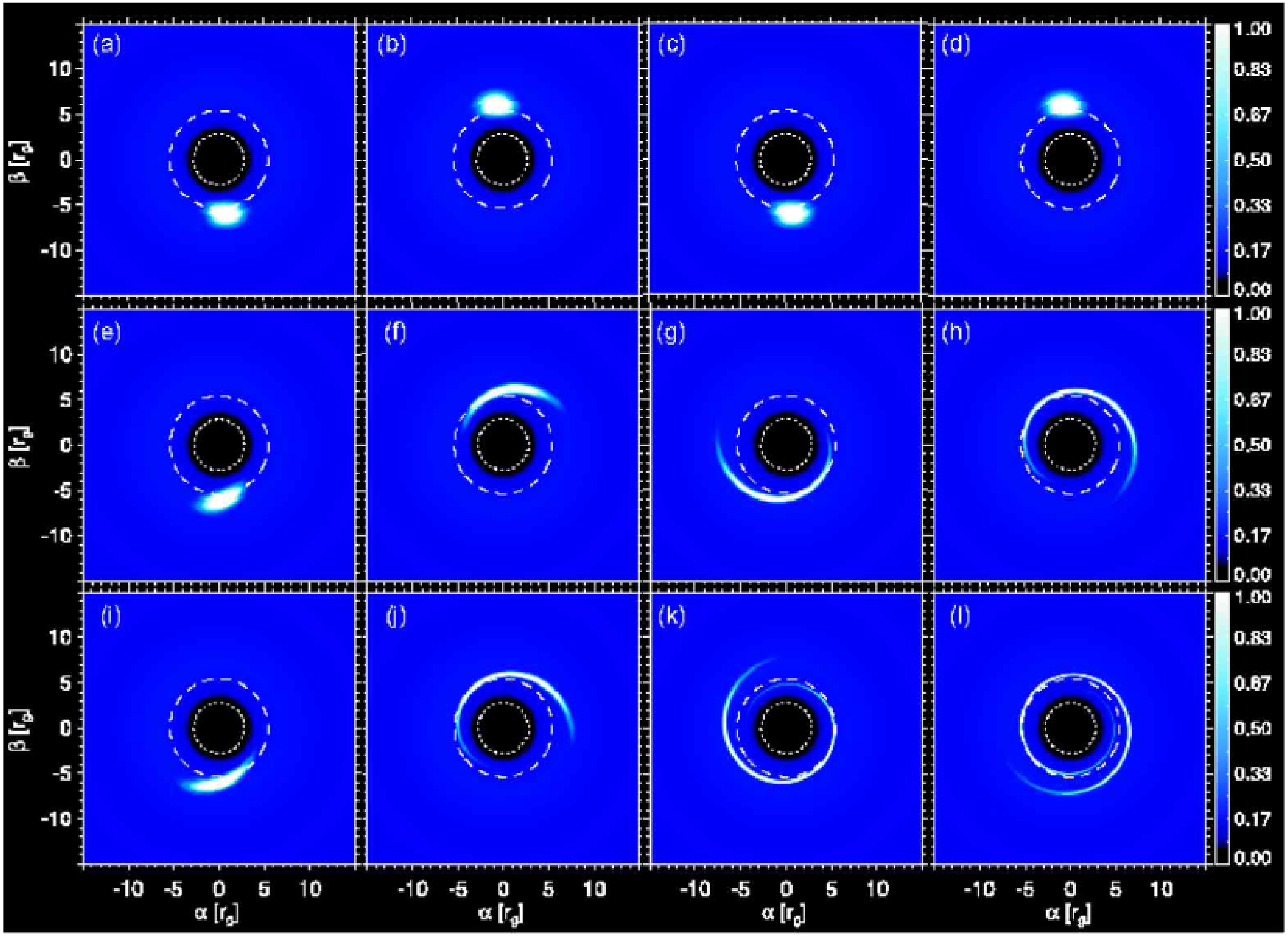

Zamaninasab et al. 2009

NIR Polarized Flux Density from SgrA*

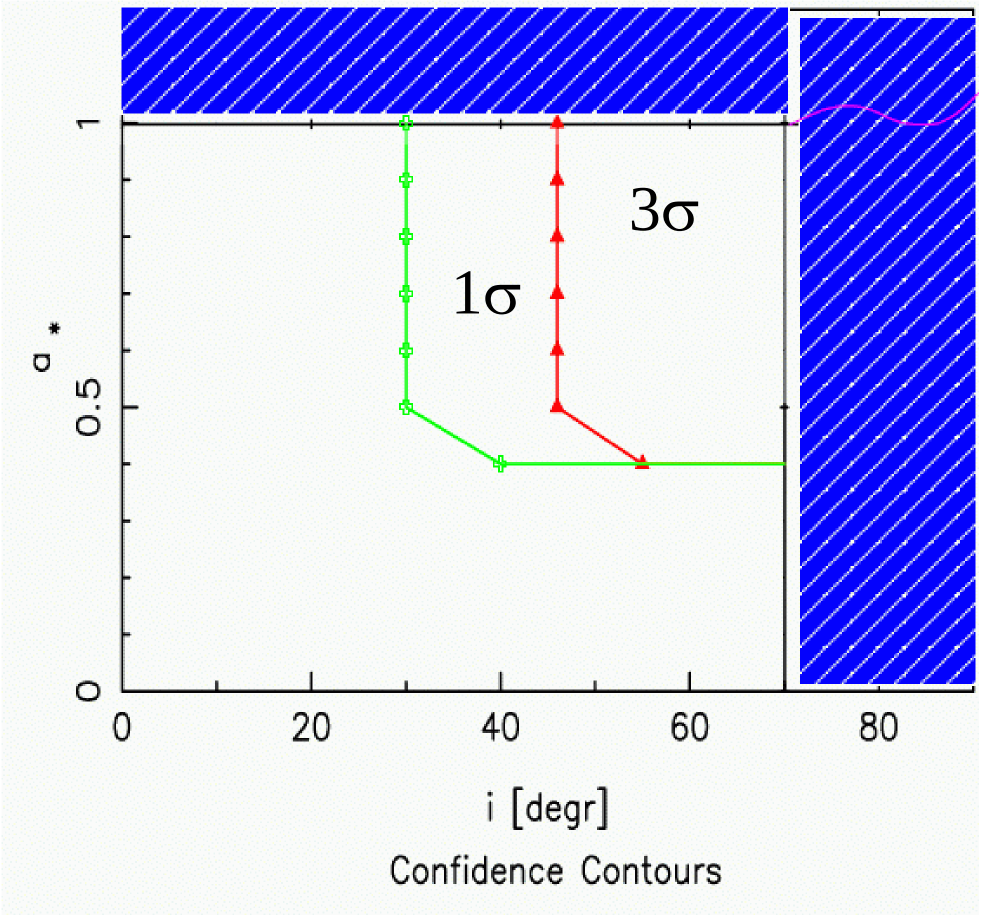

χ^2 analysis indicates
a= 0.4-1
i=50^{o}-70^{o}

Meyer, Eckart, Schödel, Duschl, Muzic, Dovciak, Karas 2006a
Meyer, Schödel, Eckart, Karas, Dovciak, Duschl 2006b
Eckart, Schödel, Meyer, Ott, Trippe, Genzel 2006

Spin determination for SgrA*

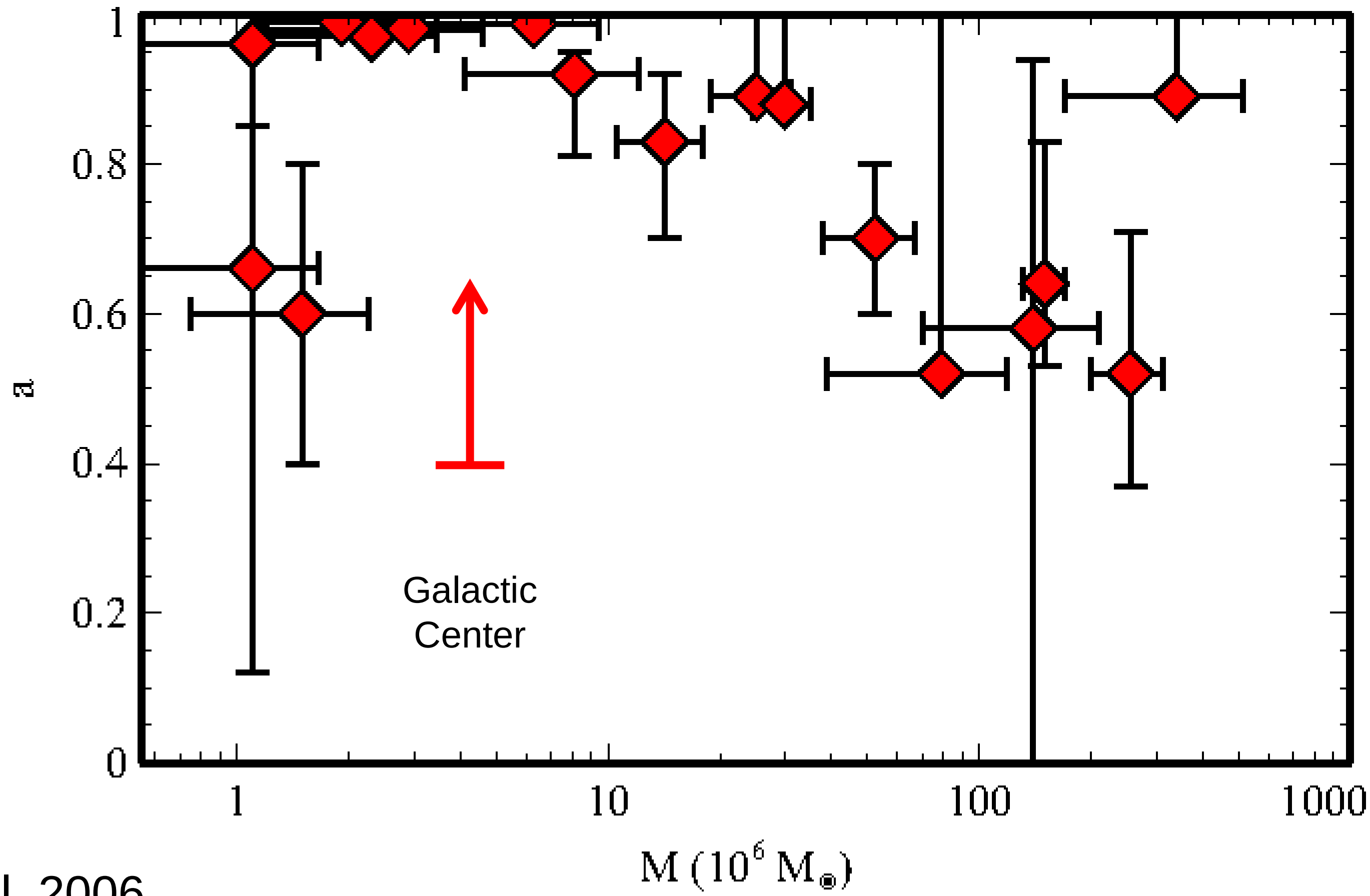

Eckart et al. 2006
Meyer et al. 2008
Zamaninasab et al. 2009/10

Reynolds et al. 2013

Current / upcomming events

A Dusty S-cluster Object is Approaching SgrA*

A dusty object that can be identified with a star or a pure dust cloud
Is approaching the Black Hole SgrA* at the
Center of the Milky Way (Gillessen et al. 2012, Eckart et al. 2012).
Periapse will probably be reached in ***September 2013 to May 2014***.

An enhanced accretion activity is expected. Brighter flares may also help to gain information of the particel acceleration processes.

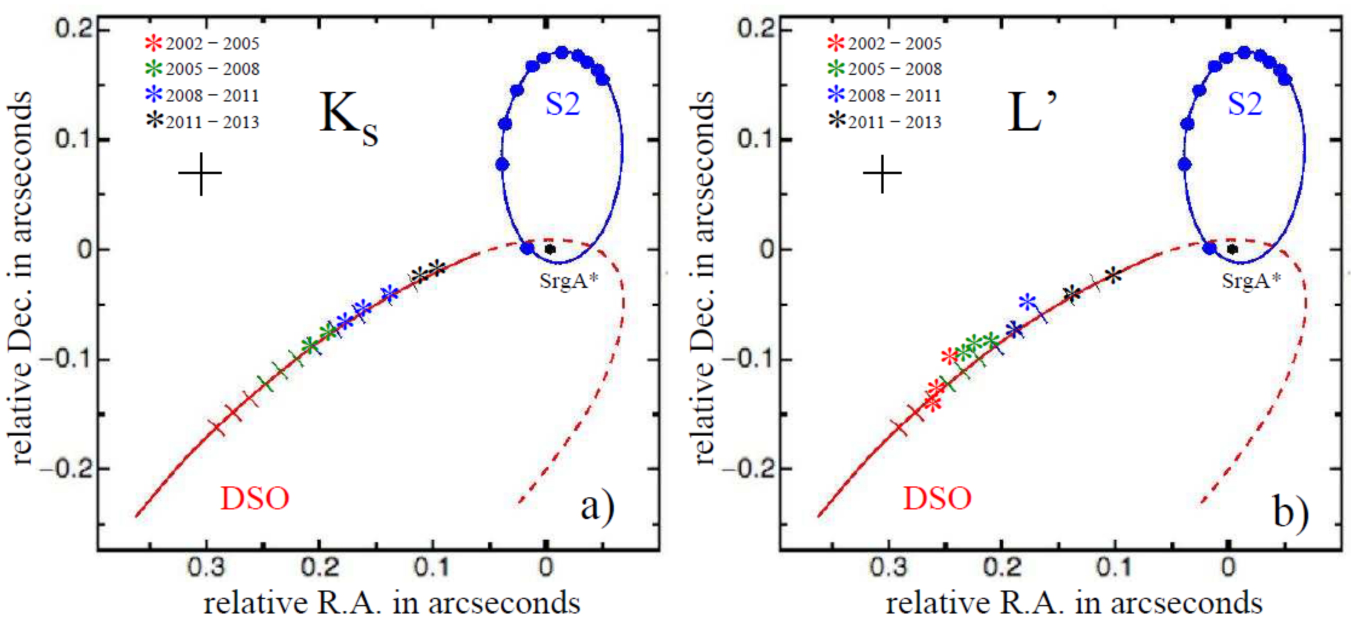

Gillessen+, Burkert+,
Murray-Clay & Loeb,
Ecakrt+
und andere

Eckart et al. 2012

DSO/G2 closing in

See low proper motion of
the DSO/G2 ‚tail' component ?

Gillessen et al. 2013

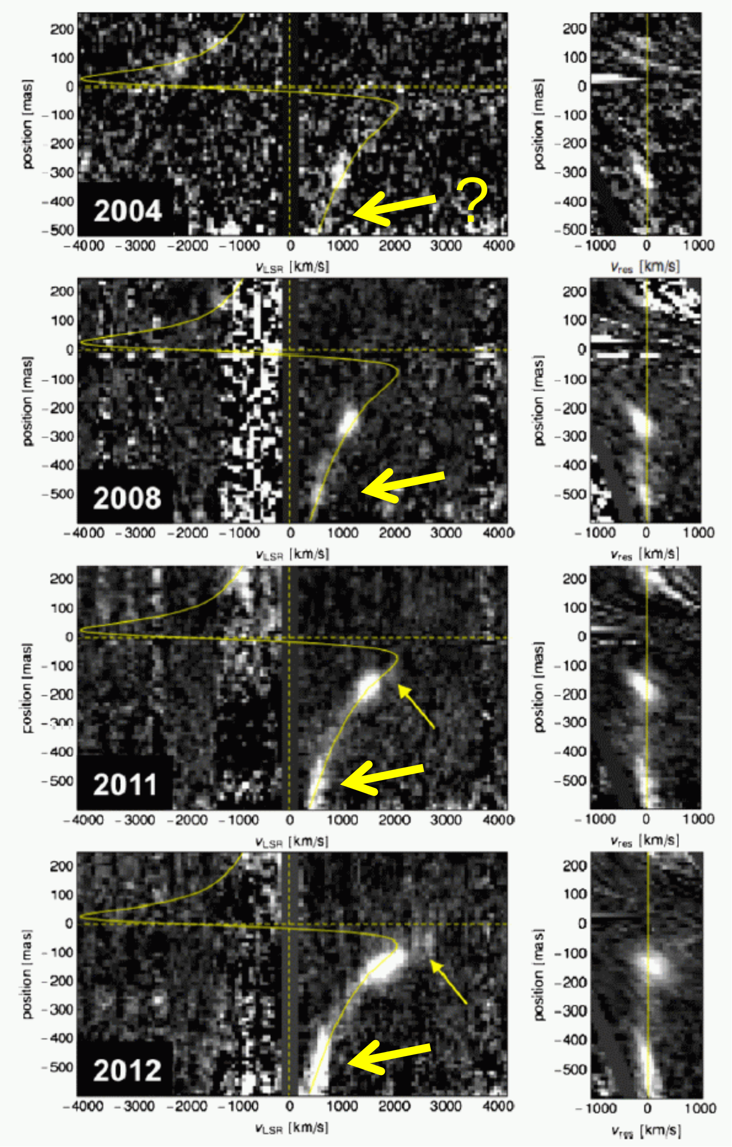

Comparison of trajectories published for DSO/G2

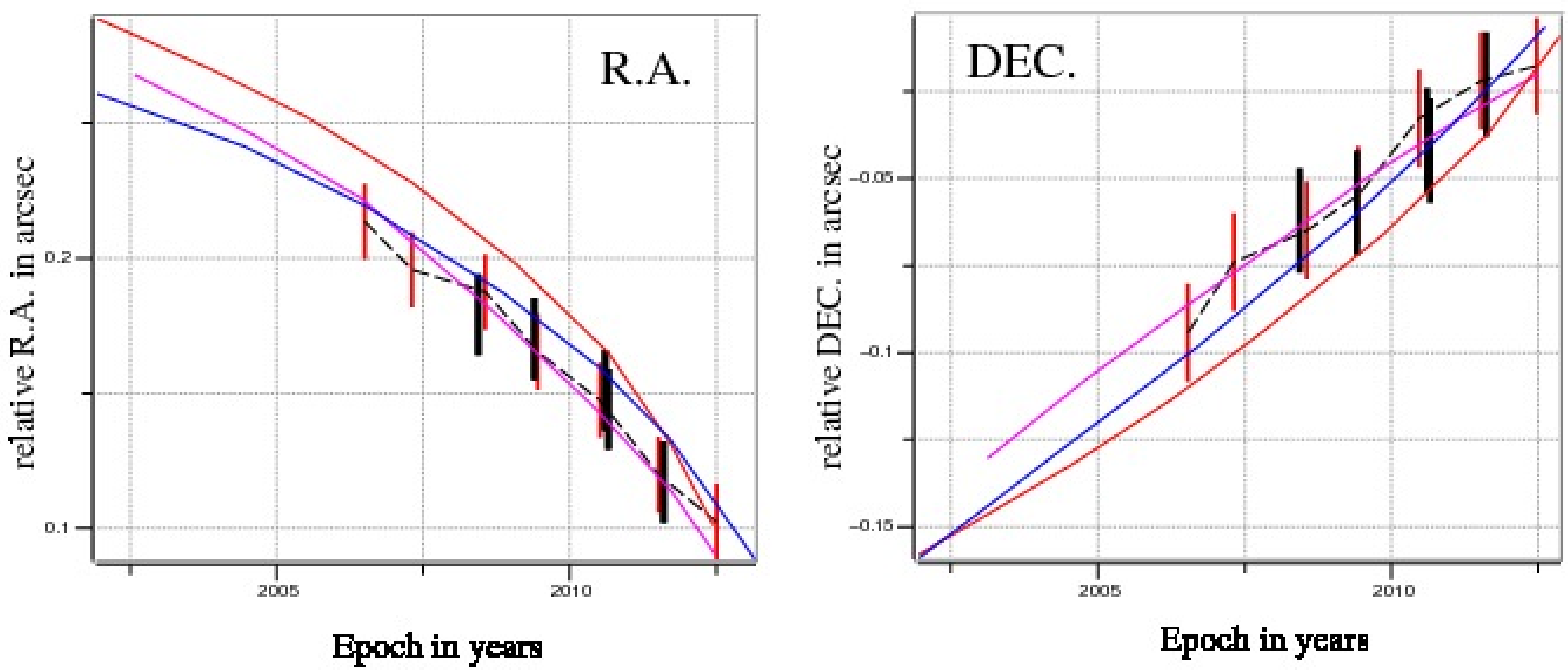

A comparison between the L'-band tracks of the DSO used by Gillessen et al. (2013) (magenta line; L'-band), Phifer et al. (2013) (blue (K'-band Brγ) and red (L'-band) lines). We also show the coordinates obtained from the Ks-band identification by Eckart et al. (2013) using VLT NACO data (data points with red error bars connected by a black dashed line). Data point with thick black error bars represent the K'-band identification based on Keck NIRC2 data.

DSO identified in public Keck data

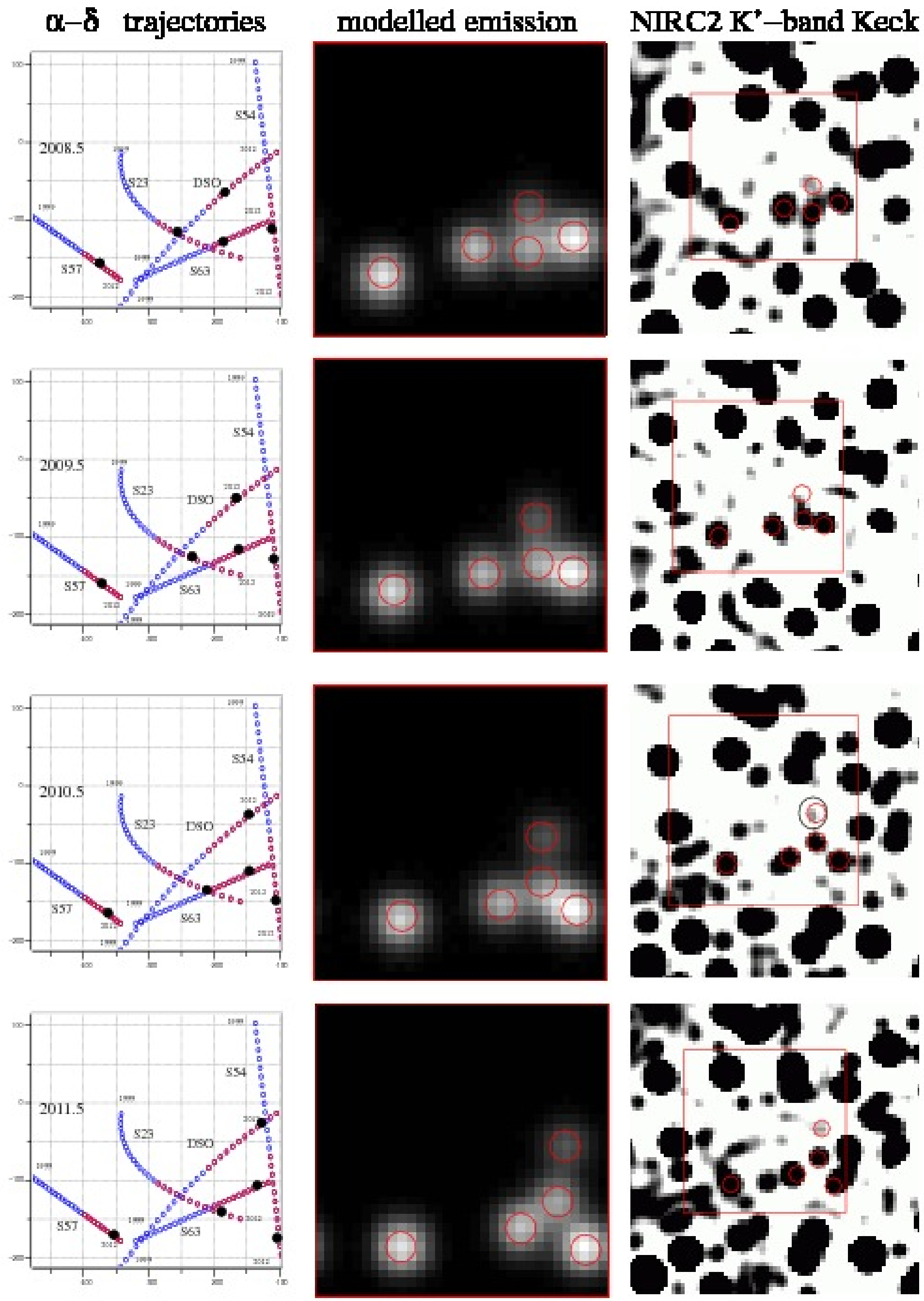

Improved 2011/2012 DSO identification in VLT

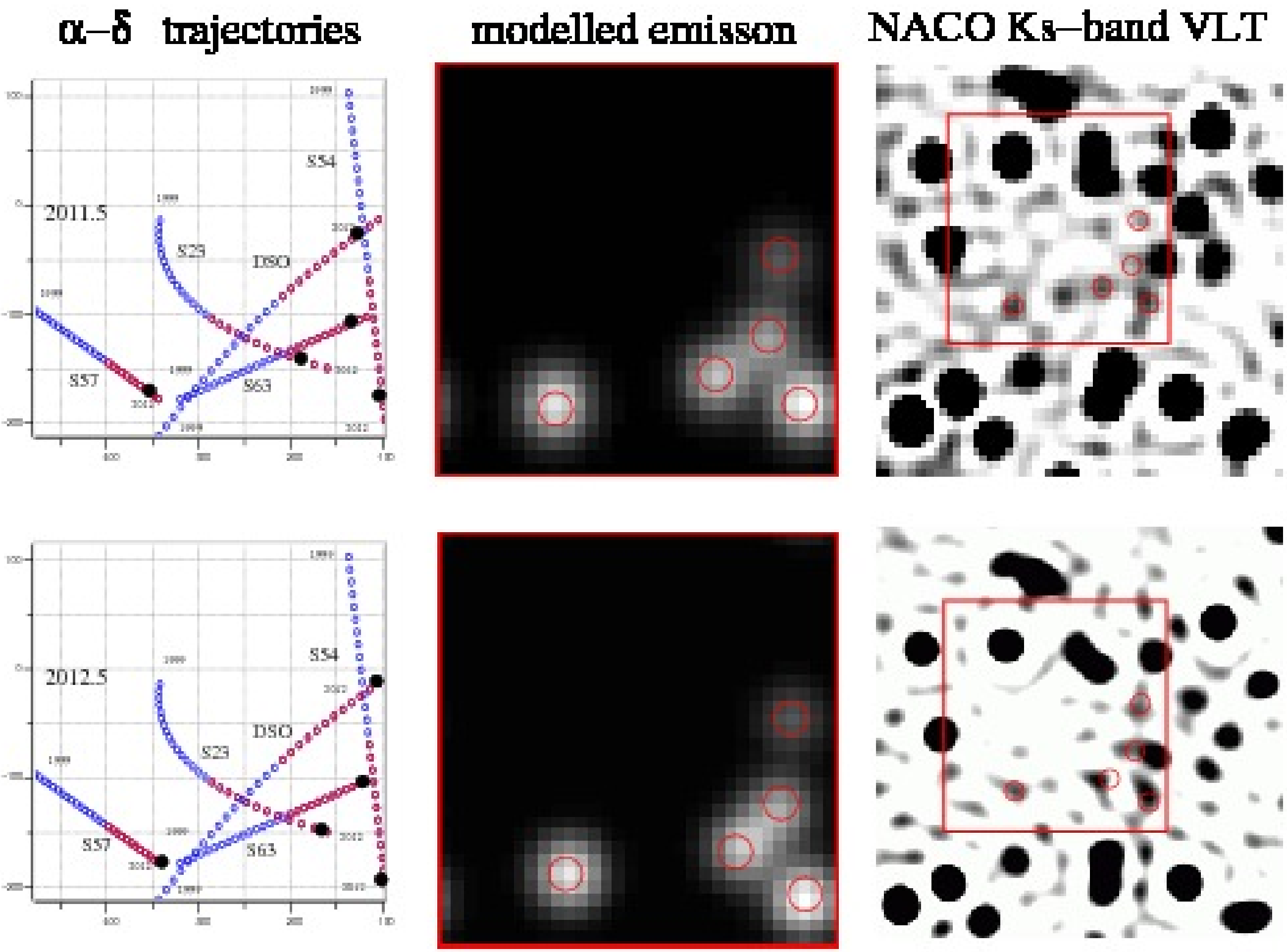

Comparison of trajectories published for DSO/G2

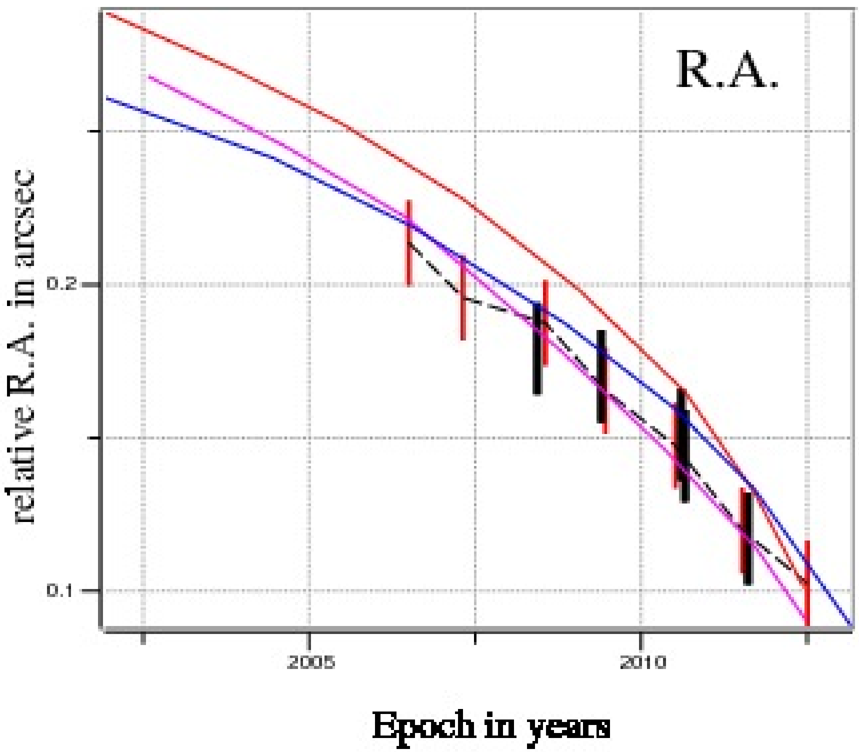

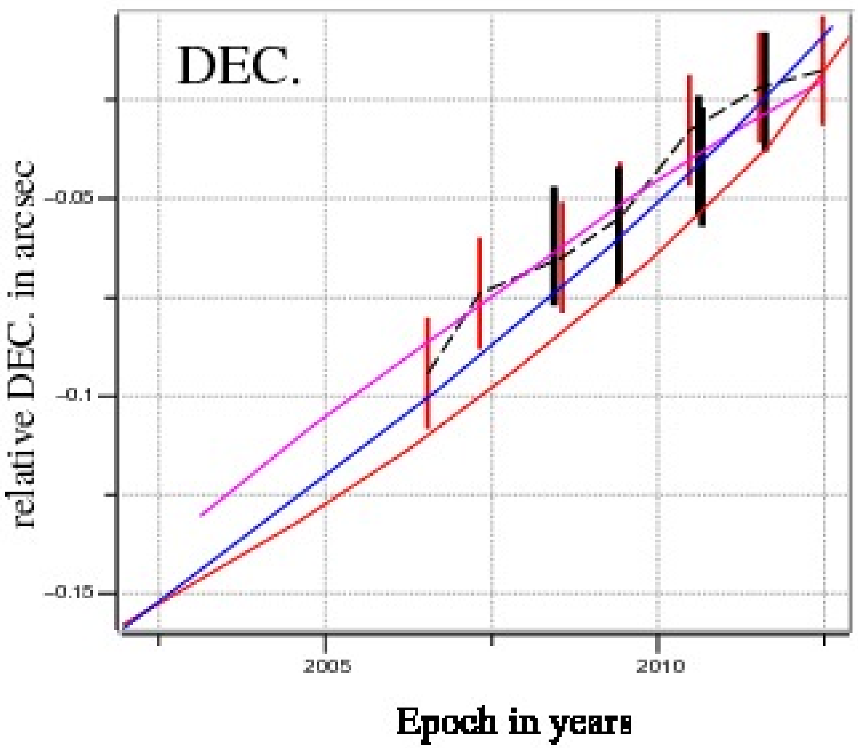

A comparison between the L'-band tracks of the DSO used by Gillessen et al. (2013) (magenta line; L'-band), Phifer et al. (2013) (blue (K'-band Brγ) and red (L'-band) lines). We also show the coordinates obtained from the Ks-band identification by Eckart et al. (2013) using VLT NACO data (data points with red error bars connected by a black dashed line). Data point with thick black error bars represent the K'-band identification based on Keck NIRC2 data.

K-band identification of the DSO

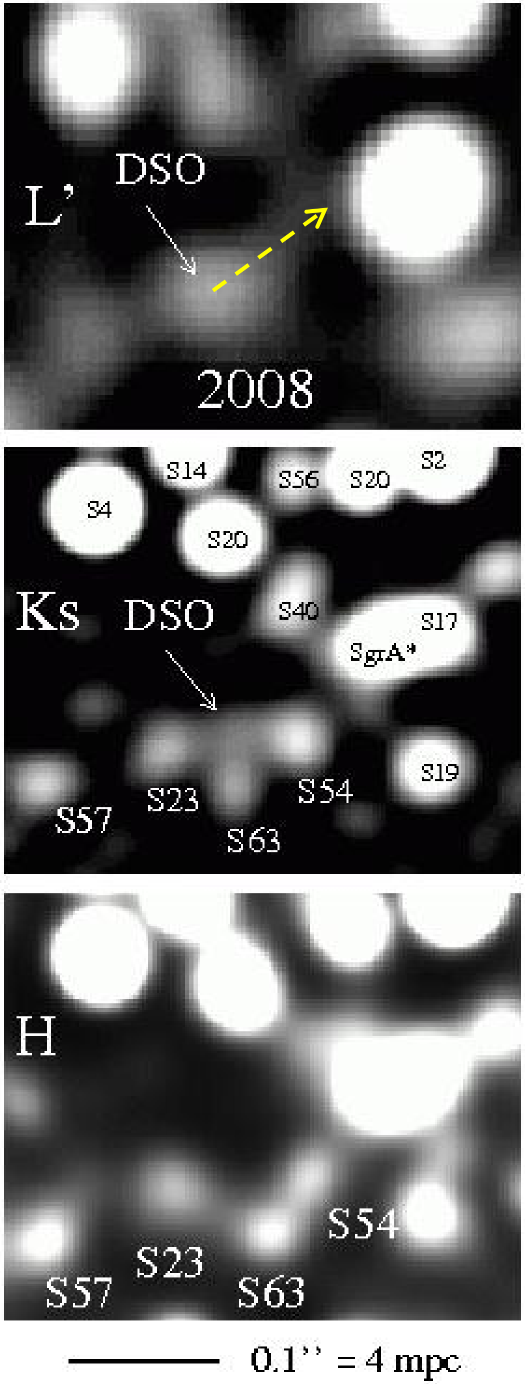

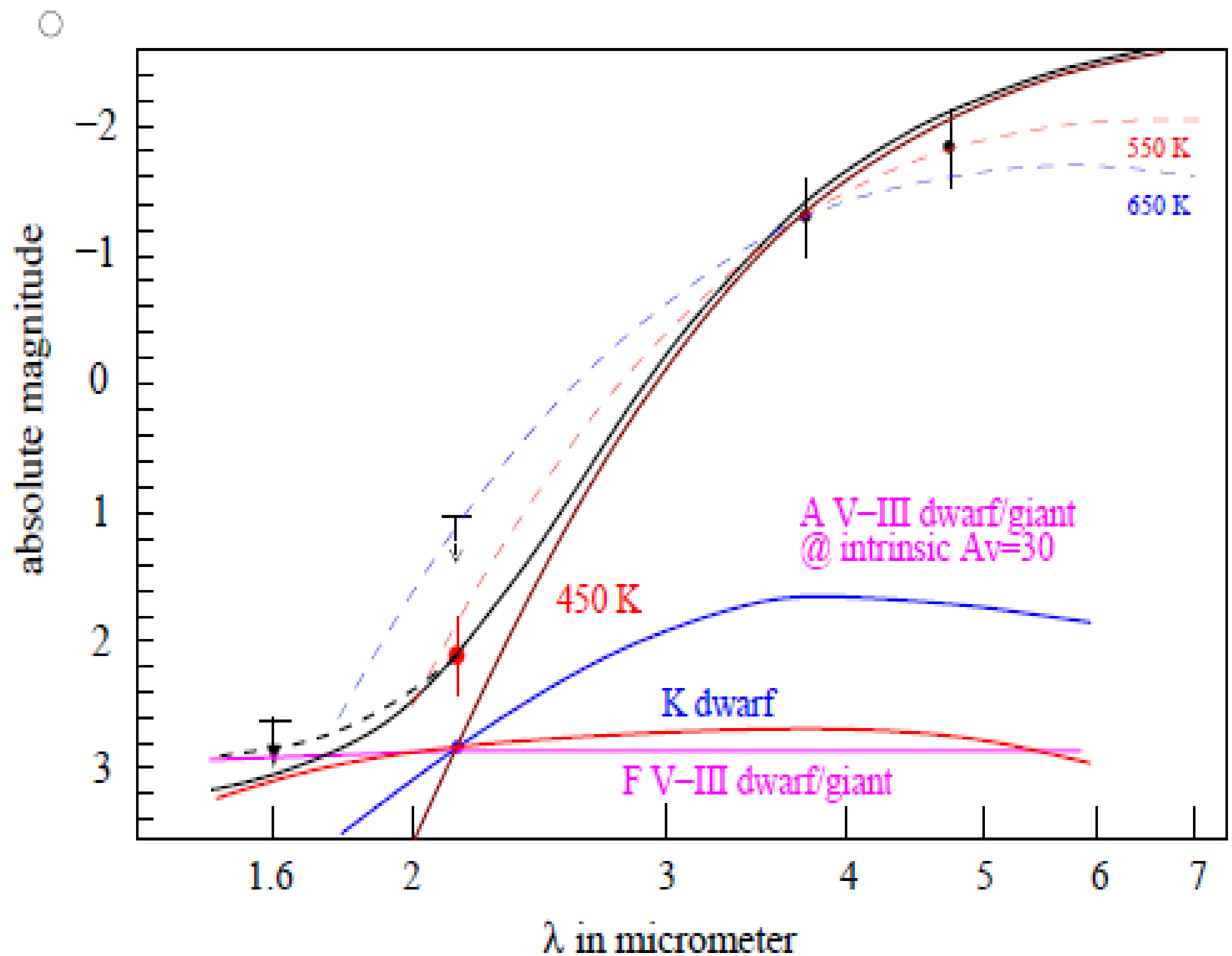

Eckart et al. 2012

NIR Colors of the DSO

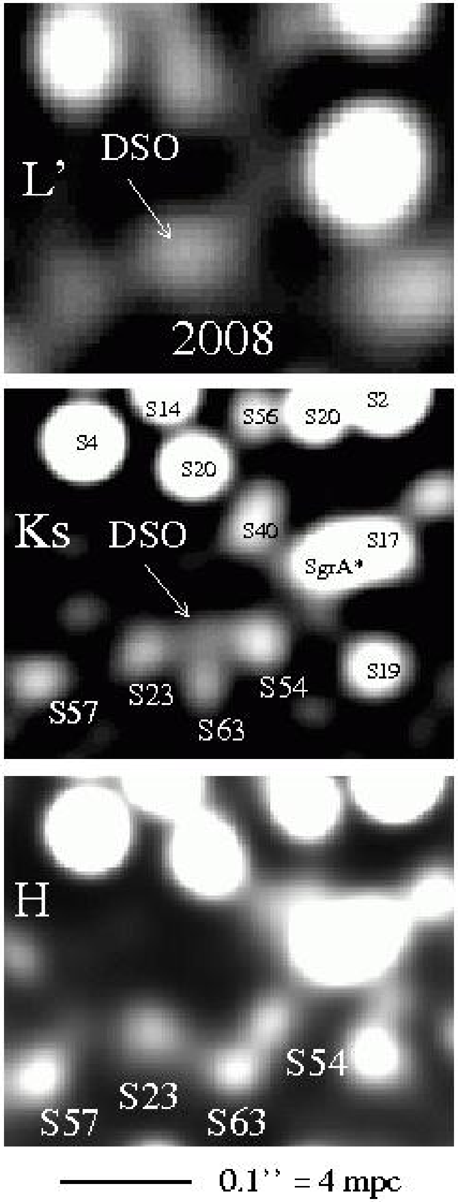

Eckart et al. 2012

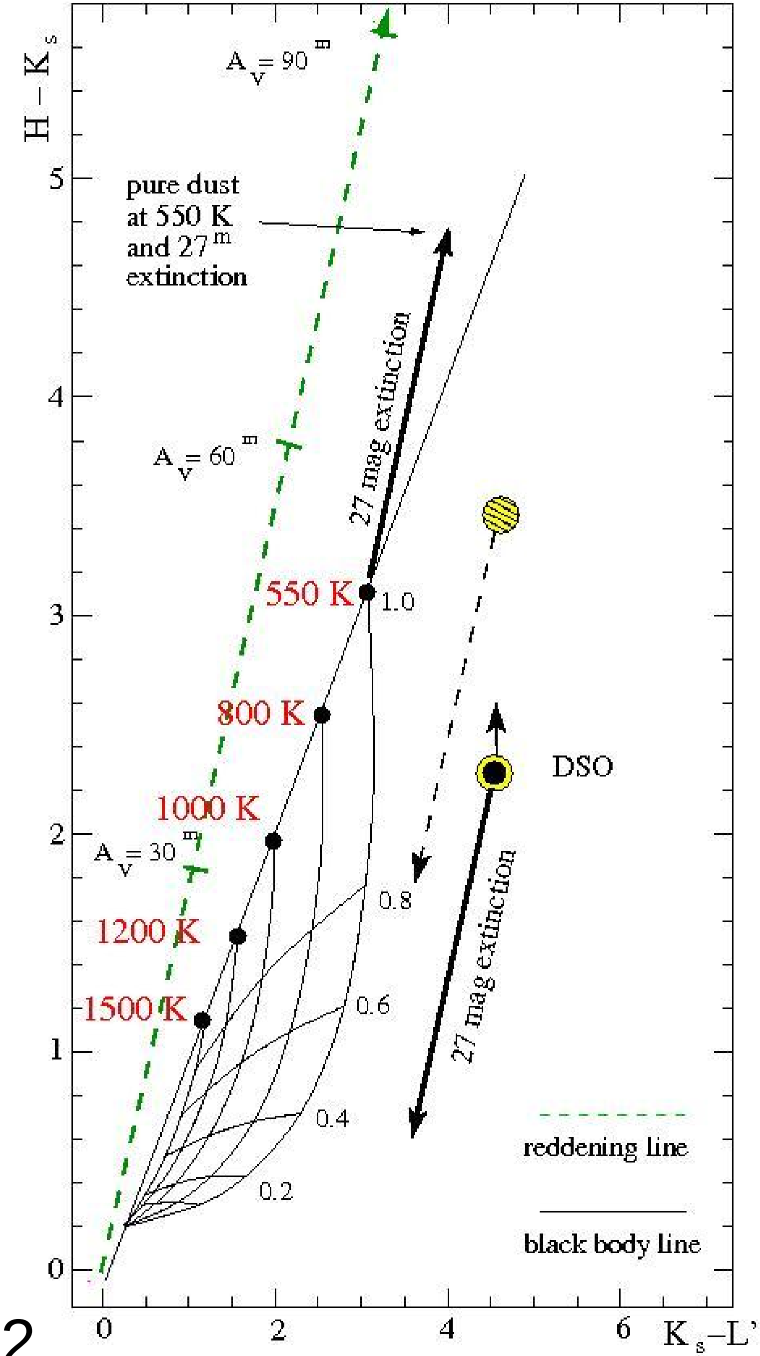

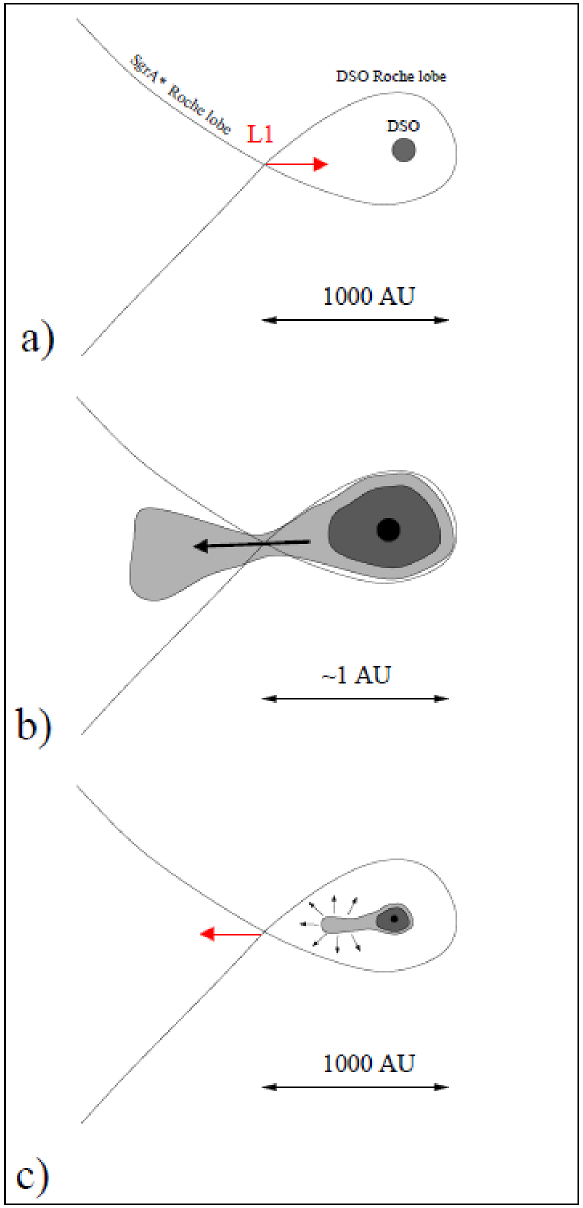

Fig. 16. Sketch of the relative position and motion of the Lagrange point L1 and the DSO.

Eckart et al. 2012

DSO Accretion in 2013/14 ?

The presence of a star may have a influence on the accretion activity.

(Schartmann + 2012; Burkert + 2012)

The MIR continuum emission
Is due to a compact object
(<0.1“), while the
Brγ line flux is extended over 0.2“
ist (Gillessen + 2012)

DSO/G2 as a pure gas and dust source?

Burkert et al. 2012,
Schartmann et al. 2012

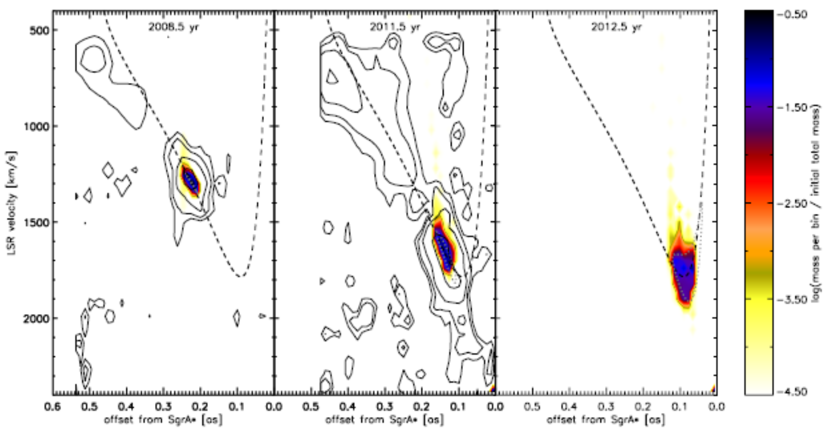

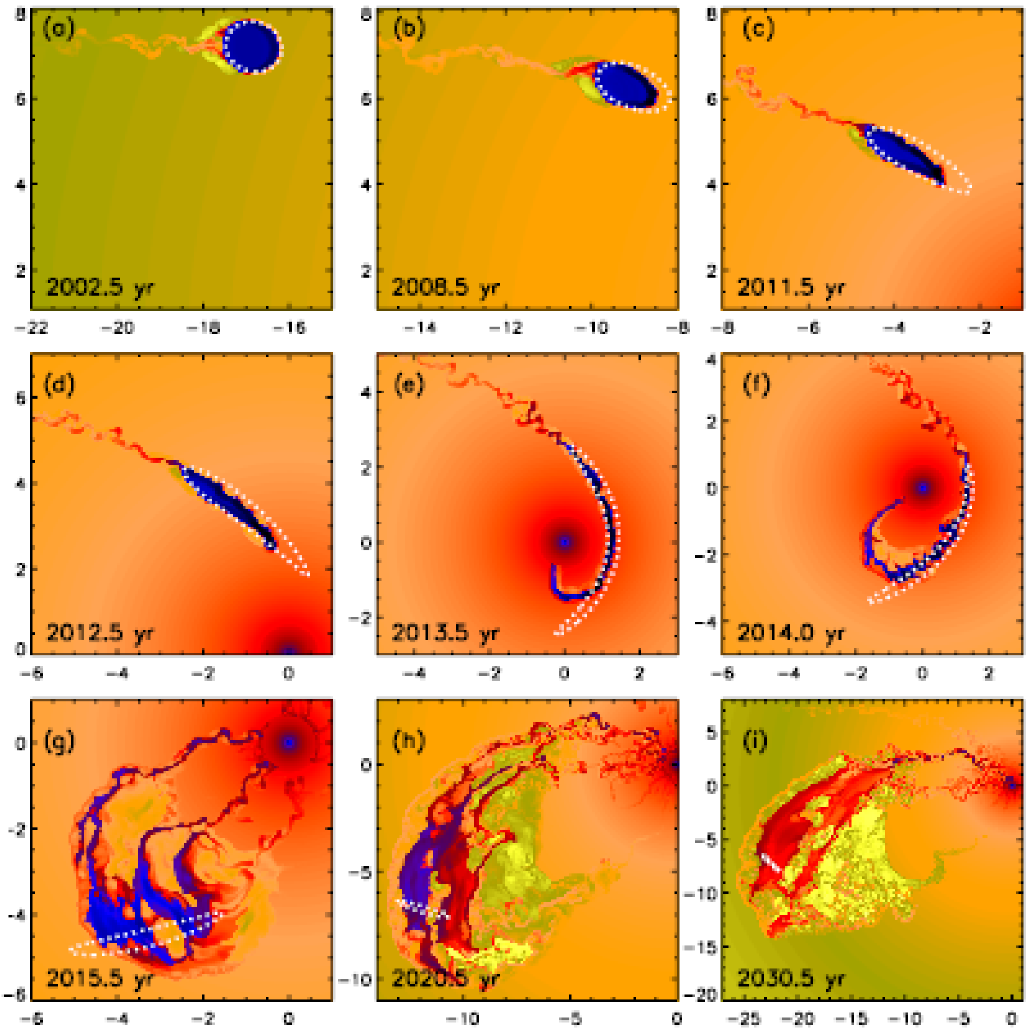

Cometary Sources: Shaped by a wind from SgrA*?

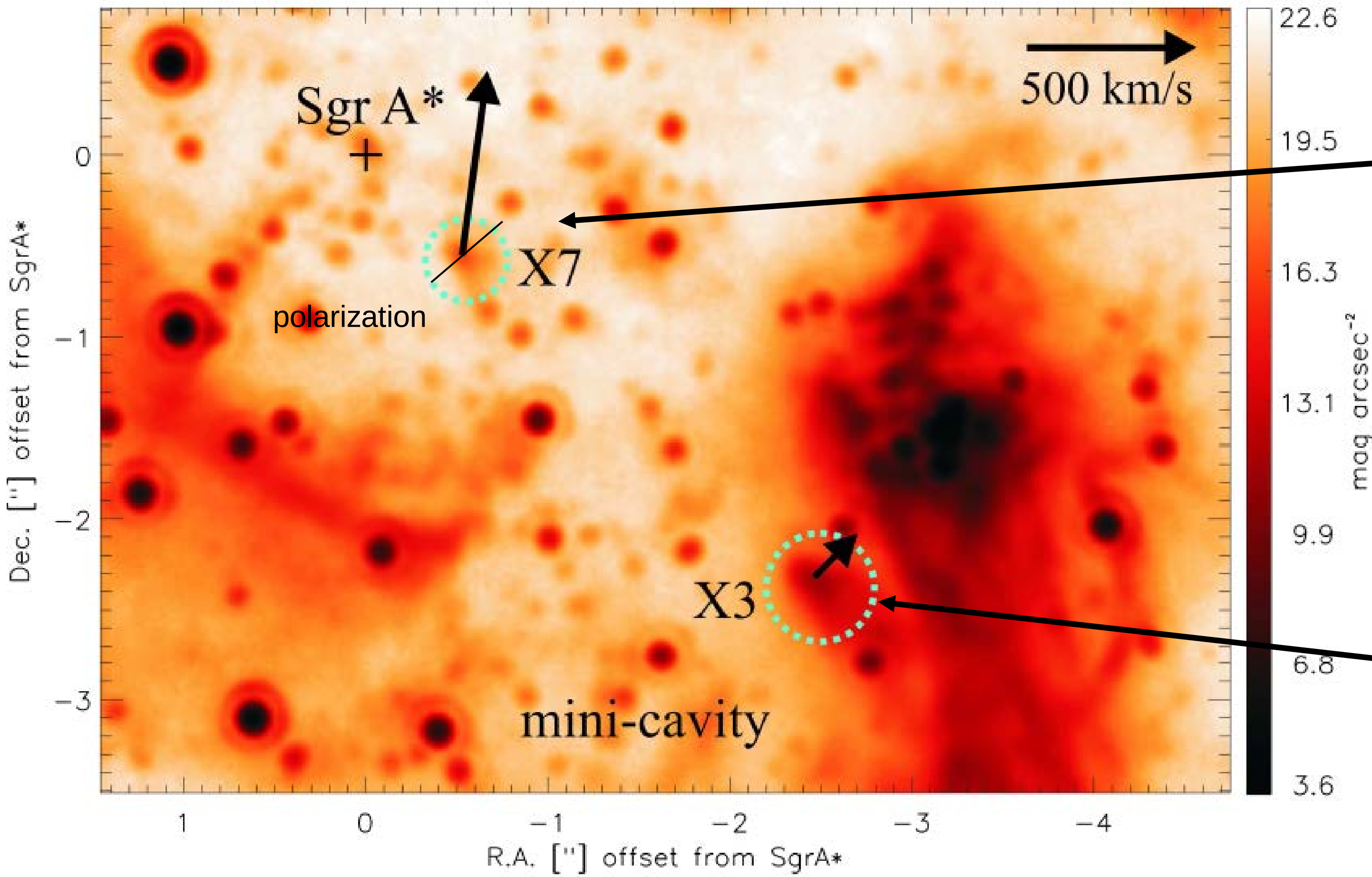

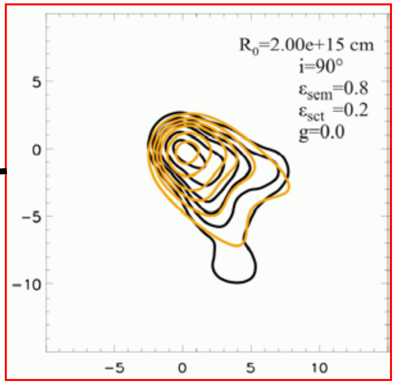

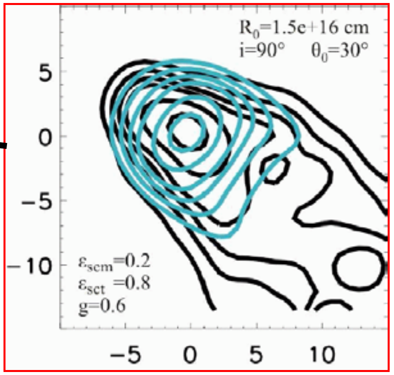

X7 polarized with 30% at PA -34+-10
Mie → bow-shock symmetry along PA 56+-10
includes direction towards SgrA*

Besides the Mini-Cavity – the strongest indication for a fast wind from SgrA*!

Muzic, Eckart, Schödel et al. 2007, 2010

Accretion onto SgrA*

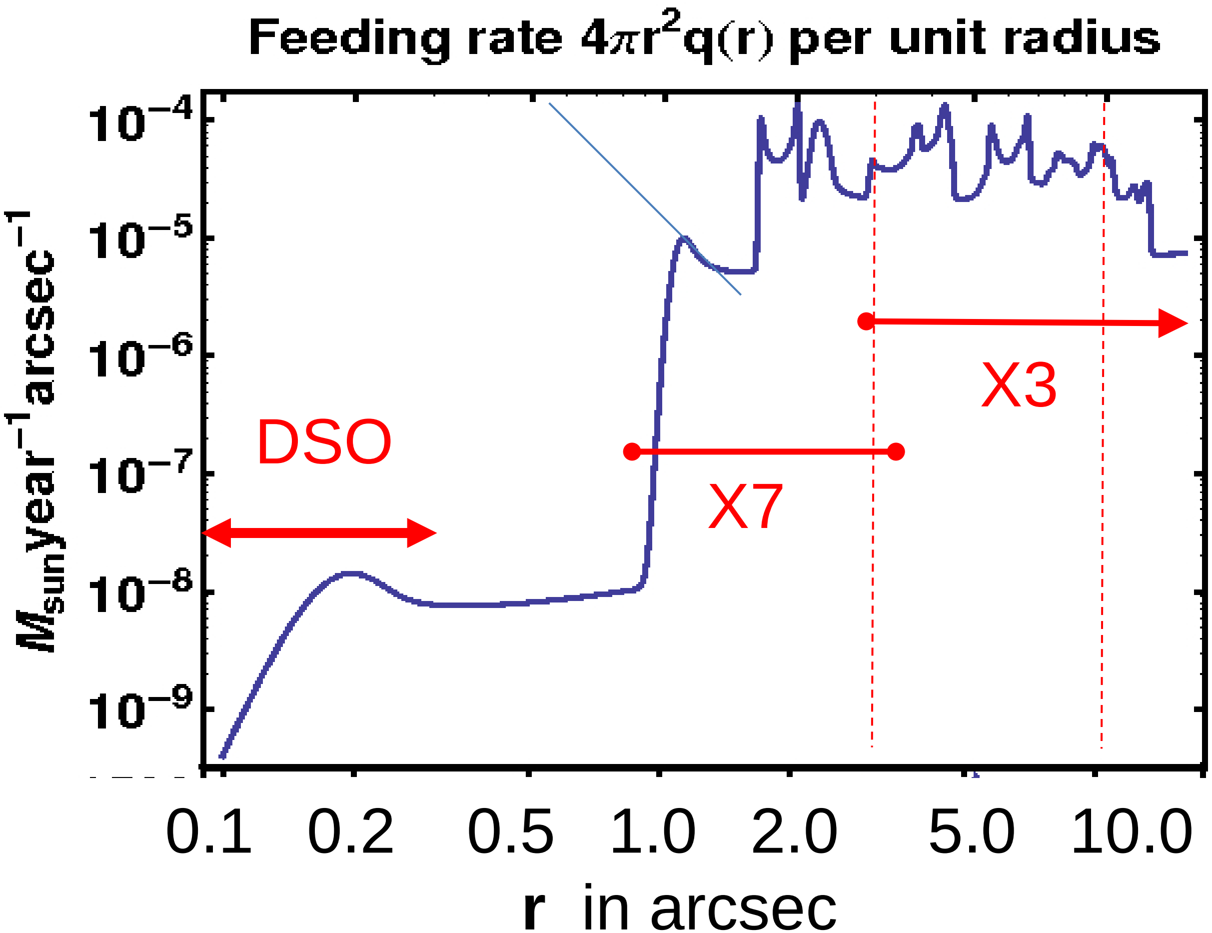

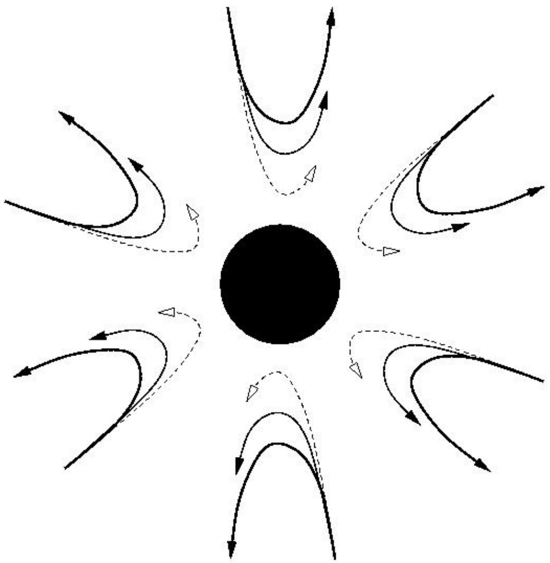

radius dependent accretion

Mass input into the feeding region around the BH on the upper panel. Square averaged wind velocity vw on the lower panel. Feeding is averaged over stellar orbits. Each wiggle represents a turning point of a single orbit. Only the star S02 and the DSO may feed matter within 0.8".

Shcherbakov & Baganoff ApJ, 2010

Observing the DSO Flyby 2013/2014

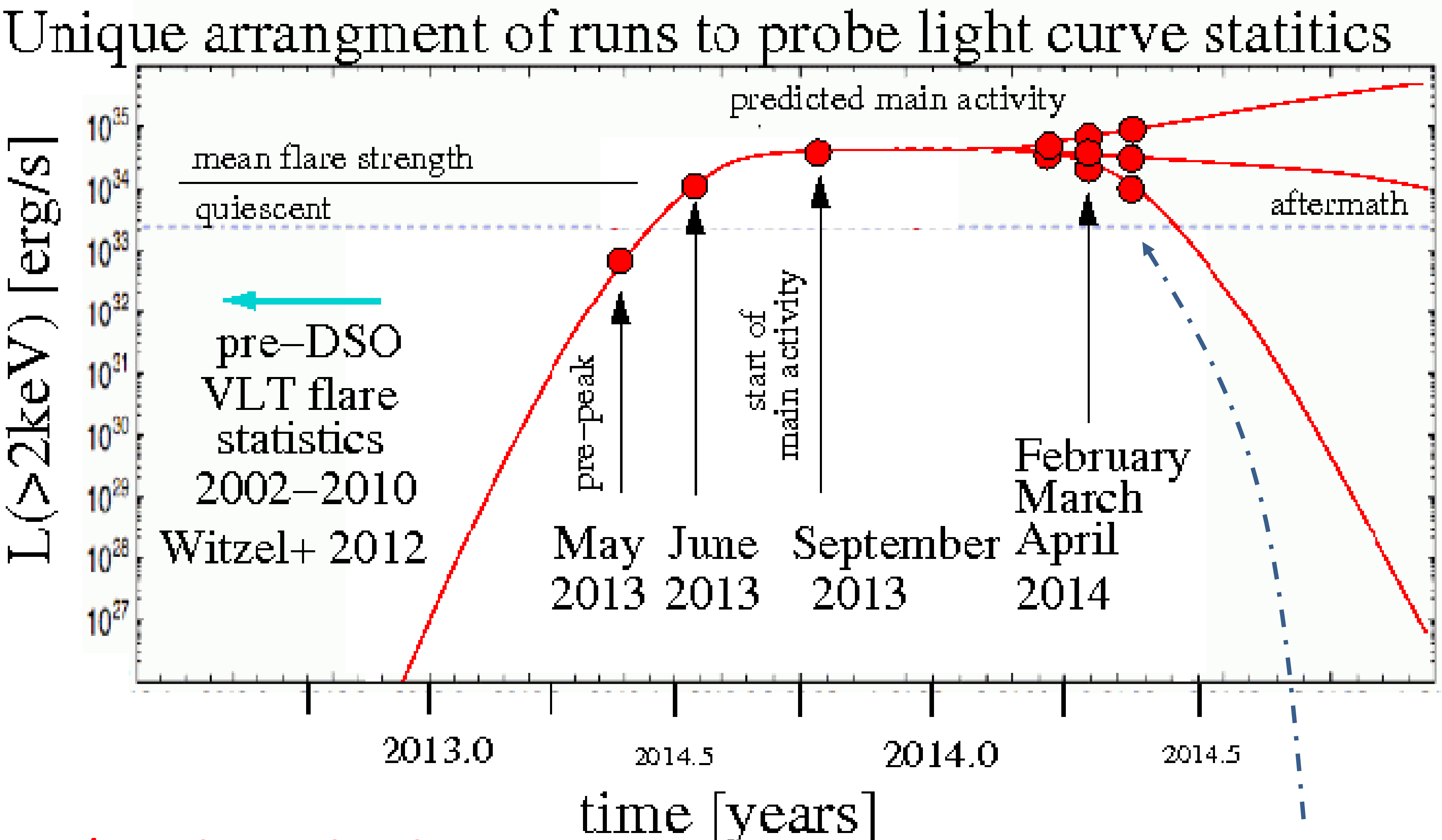

2013/14 multi-wavelength run (Eckart+)

predictions: Gillessen+ Phifer+ 13

$$\boxed{L = \frac{GM\dot{M}}{2r} = 2\pi r^2 \sigma T^4}$$

XMM
N. Grosso,
D. Porquet et al.

The LLAGN in the Center of the Galaxy

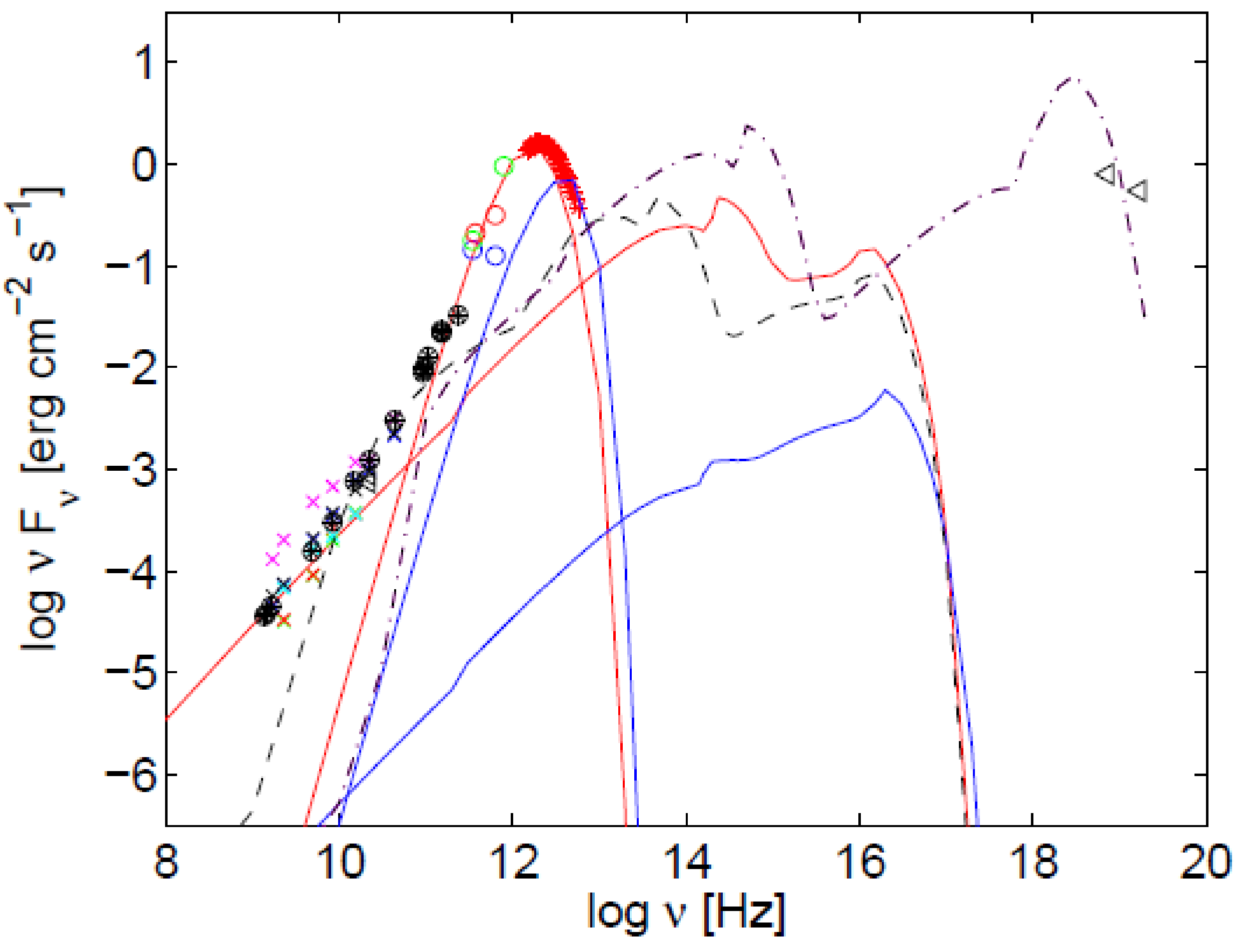

Comparison of continuum and emission line properties of the GC and bonified LLAGNs by **Contini 2011**, MNRAS 418, 1935; in „**The LLAGN in the centre of the Galaxy**“; black X : NGC 3147; cyan X : NGC 4579; blue X : NGC 4203; red X : NGC 4168; green X : NGC 4235; magenta X : NGC 4450.

SgrA* as an extreme LLAGN Nucleus

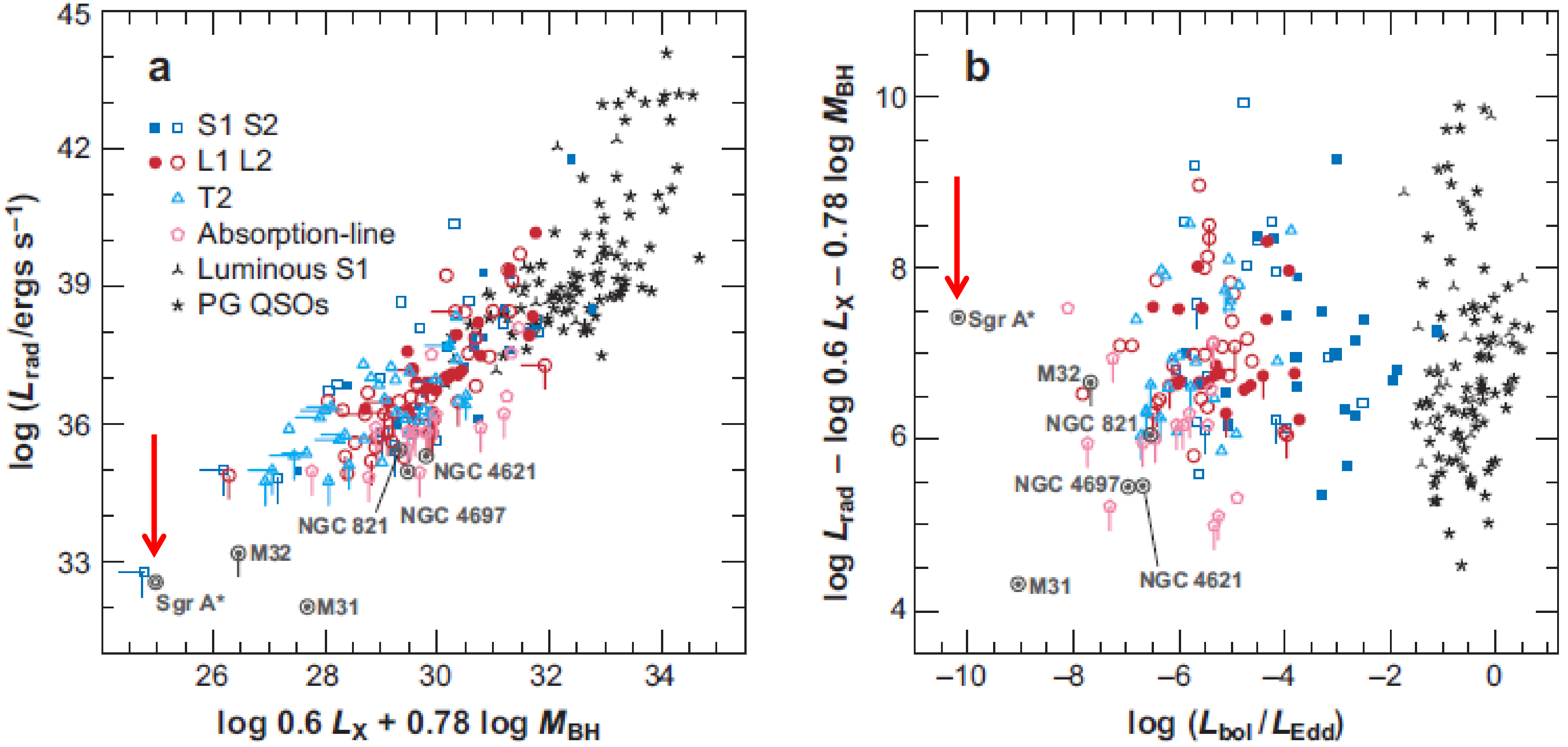

Ho 2008: Fundamental plane correlation among core radio luminosity, X-ray
(a) luminosity, and BH mass. (*b*) Deviations from the fundamental
plane as a function of Eddington ratio.

DSO and consequences for a general LLAGN model

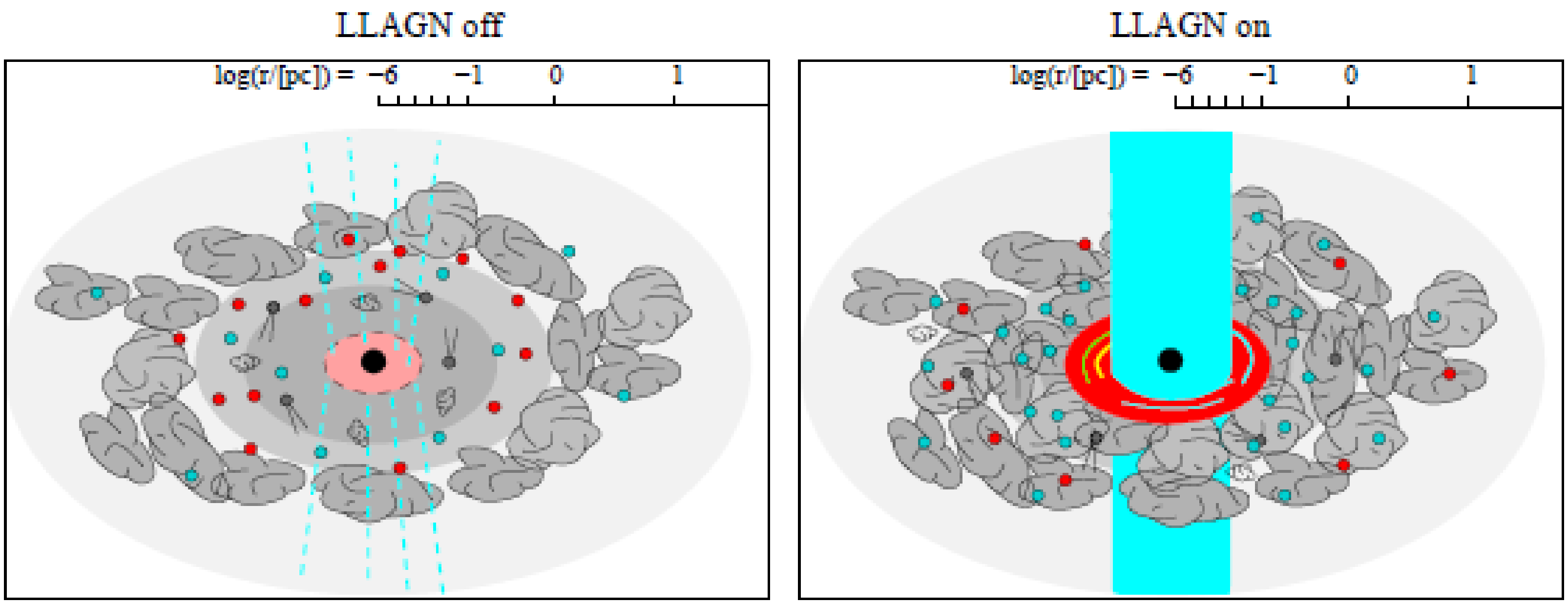

Inclined view on an LLAGN in its 'off' and 'on' state. A logarithmic scale along the semi-major axis is given. The molecular and atomic gas reservoir is indicated by dark clouds. The stellar cusp is indicated by the grey background. A temporary or truncated disk and a more substantial accretion disk are depicted by the pink and red disks surrounding the central black hole.
The cyan lines and tube-like structure represent the not necessarily collimated wind or outflow off-state and a possible jet in the on-state.
Red giants and blue young stars are shown as filled red and blue circles.
In the off state the activity is dominated by rare and sporadic accretion events linked to dusty DSO-like objects (grey circles with commentary tails) and to smaller cloudlets that are clearly visible in the off-state image.

The GC2013 COST conference in Granada, Spain
19-22, November 2013

http://www.astro.uni-koeln.de/gc2013

Impressum

Universität zu Köln
Mathematisch-Naturwissenschaftliche Fakultät
Fachgruppe Physik
I. Physikalisches Institut

Teaching | Research | Instrumentation | Modelling | Jobs | CDMS | SFB 956

Search this site | Search

- News
  - Events
    - GC2013
      - Contact
      - Program
      - Venue
    - Seyfert 2012
    - LabAstrophysics
  - Conferences
- Research
- Workgroups
- Teaching
- Publications
- Personnel
- Institute

Home » News » Events

GC2013

The Galactic Center Black Hole Laboratory

November 19 - 22, 2013

Granada, Spain

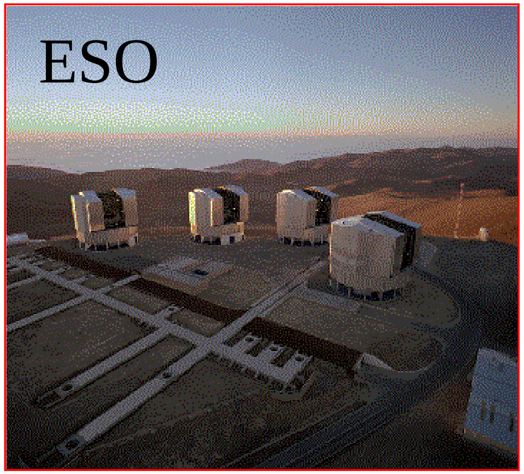

NL leads Euro-Team
University of Cologne
studies for
METIS @ E-ELT

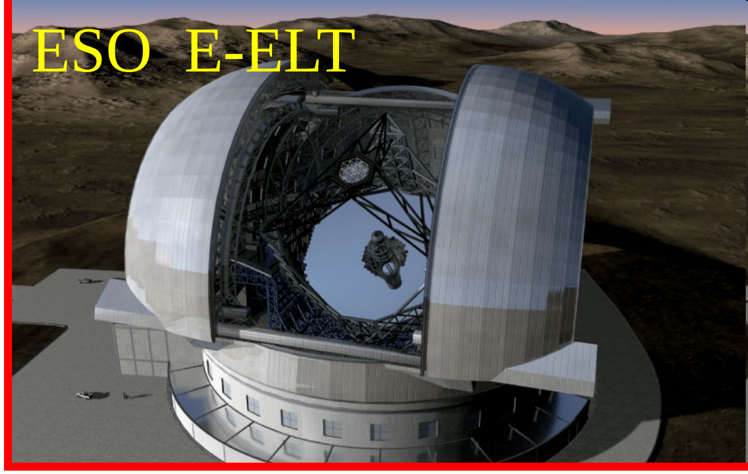

MPE, MPIA, Paris, SIM
Universitity of Cologne
participation
GRAVITY @ VLTI

The Galactic Center is a unique laboratory in which one can study signatures of strong gravity with GRAVITY

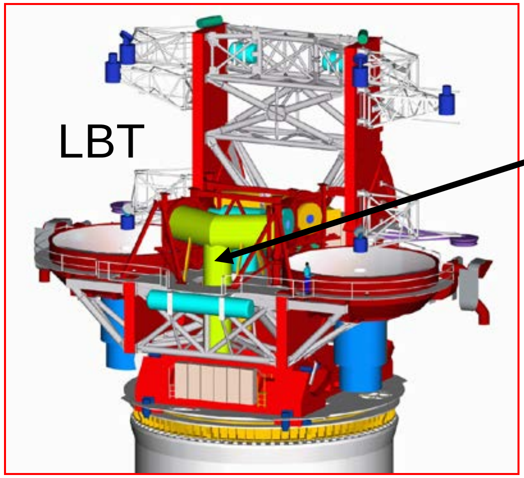

NIR Beam Combiner:
Universitity of Cologne
MPIA, Heidelberg
Osservatorio Astrofisico di Arcetri
MPIfR Bonn

Cologne
contribution to
MIRI on JWST

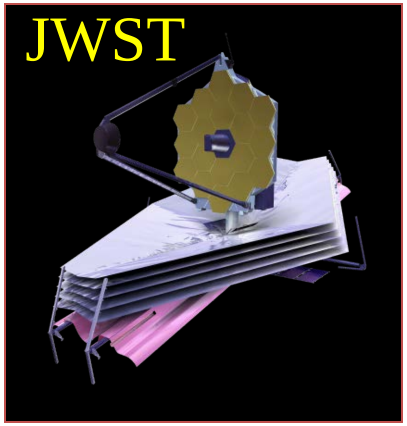

END